CHAPTER 5

RESULTS AND DISCUSSION

This chapter presents results and discussion on numerical modeling and experimental of performance PEMFCS. The analysis flow gas characteristics based on velocity and pressure distribution within flow channels, fuel gas consumption capability in flow filed, and PEMFC experimental on test station will be shown in the following section.

5.1 Numerical Analysis Results

Gas flow was studied in proton exchange membrane fuel cell by varies number of channel length, channel curvature, inlet manifold and dimension of channel and there are analyze relationship with pressure drop, velocity distribution.

Channel length and channel curvature of flow field was developed from the result of multi-serpentine flow fields. The channel curvature has 4 curves which shown in figure 5.1. The channel length has 6 cases studied, which based on varied 1 to 6 channels on multi serpentine flow field. Number of channel was independent with channel length, which increases number of channel made channel length must be shorter. Characteristics of depths channel are change 0.8, 1 and 1.2 mm. Inlet manifolds are change ratio number of channel and shape of manifolds that are help for gas flow distribution in inlet and water management in outlet.

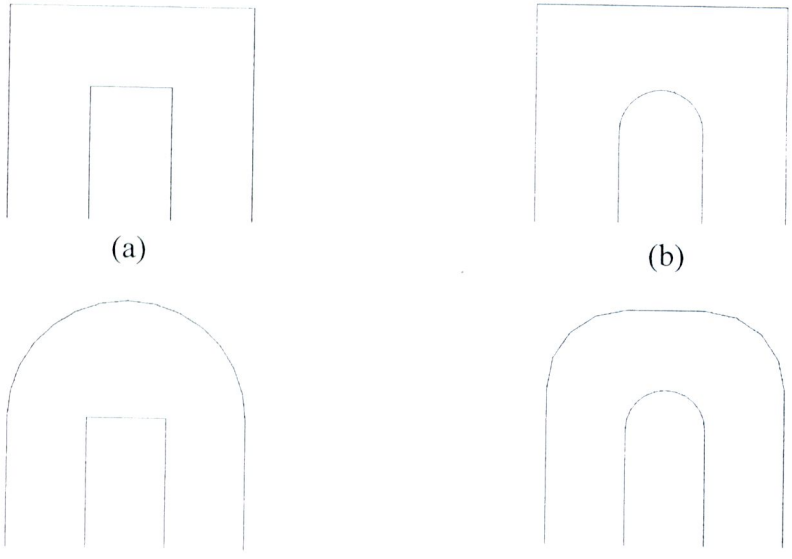

Figure 5.1 Channel curvatures (a) non-fillet curve (Type 1) (b) inside fillet curve (Type 2) (c) outside fillet curve (Type 3) (d) fillet curve (Type 4)

5.1.1 Effect of Channel Curvature on Flow Field

Effect of channel curvature has 4 curves of this study. There are non-fillet curve, inside fillet curve, outside fillet curve and fillet curve. All geometries based on serpentine flow field patterns model shown in figure 5.2. The solutions from model will be shown and analyzed for these curve configurations. The results of flow and pressure distribution are effect of curvatures at depth channel 0.5 mm. were show in figure 5.3-5.11.

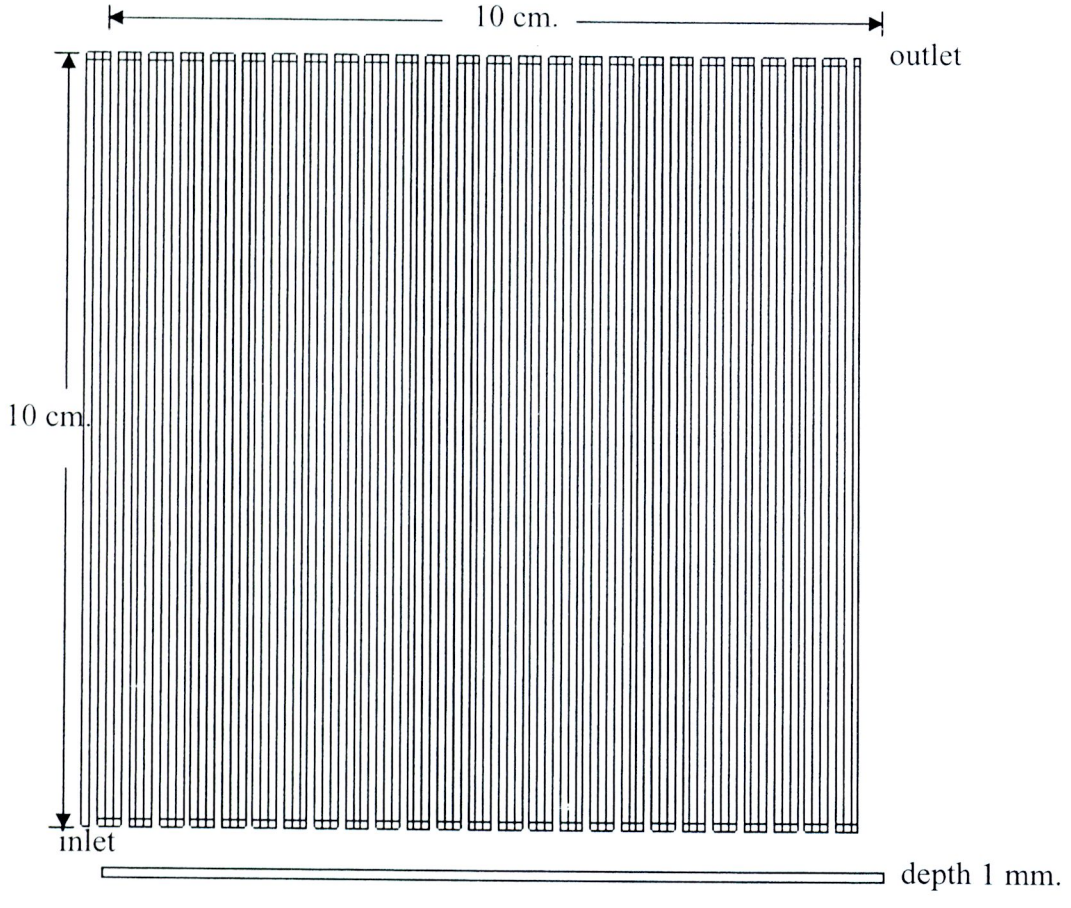

Figure 5.2 Serpentine flow filed pattern modeling

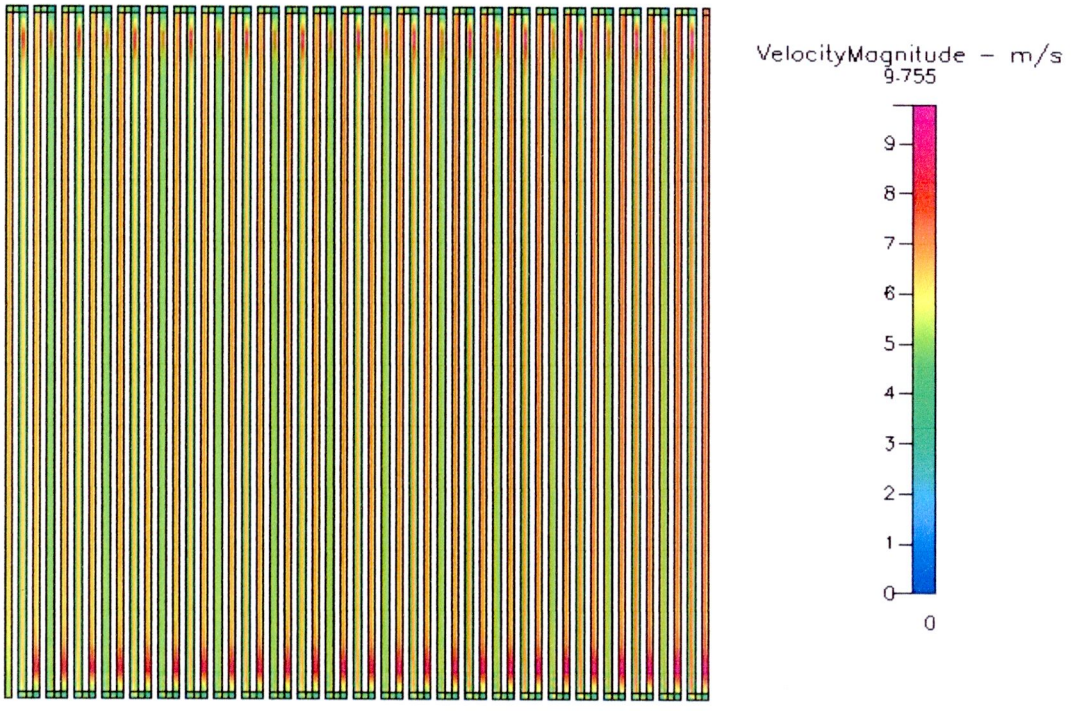

Figure 5.3 Velocity distribution at 300 cm^3/min of non-fillet curve

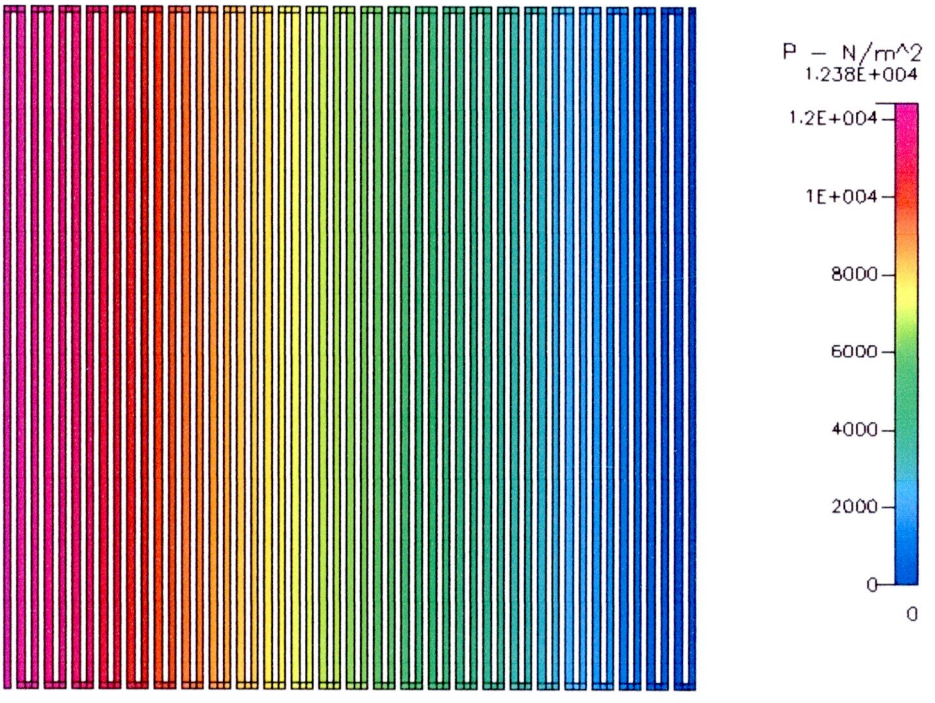

Figure 5.4 Pressure distribution at 300 cm^3/min of non-fillet curve

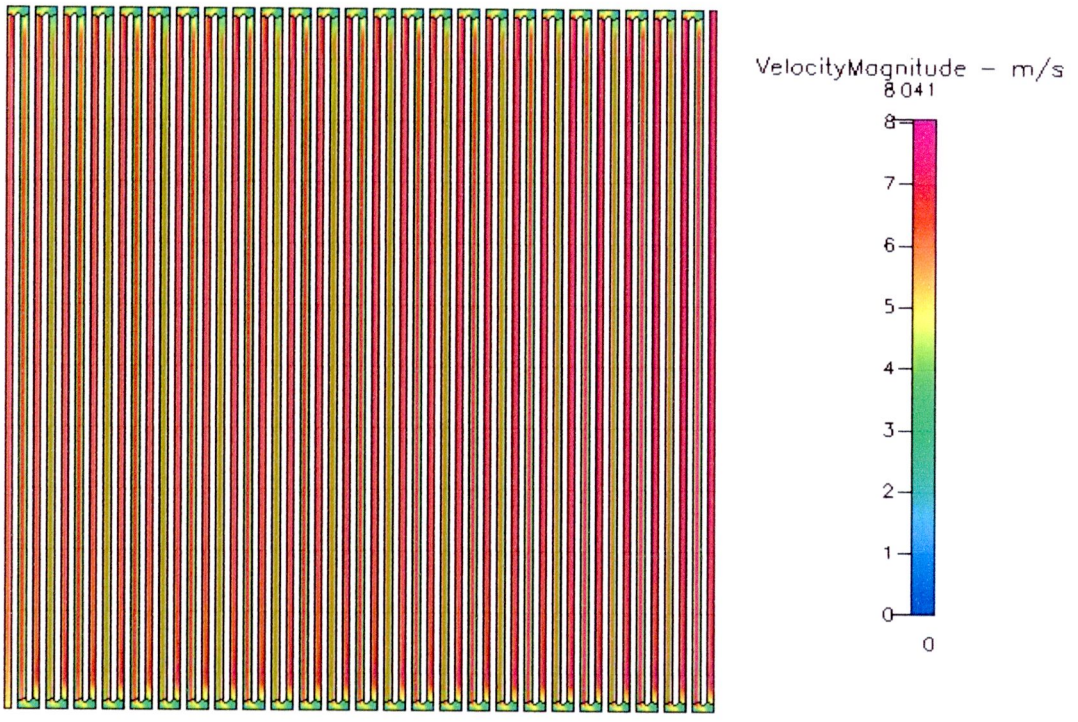

Figure 5.5 Velocity distribution at 300 cm^3/min of inside fillet curve

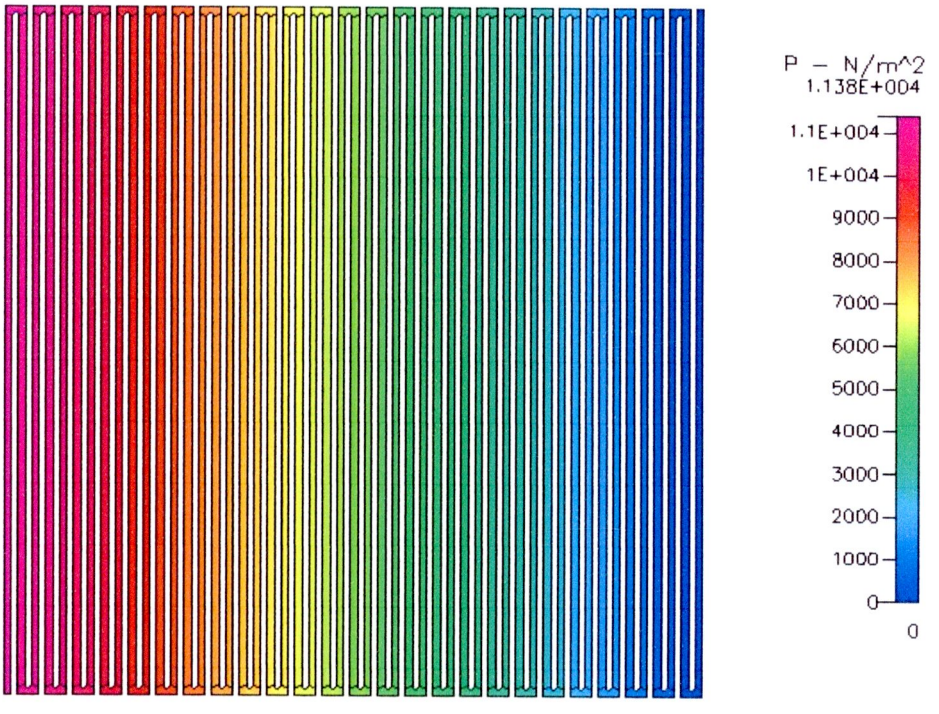

Figure 5.6 Pressure distribution at 300 cm^3/min of inside fillet curve

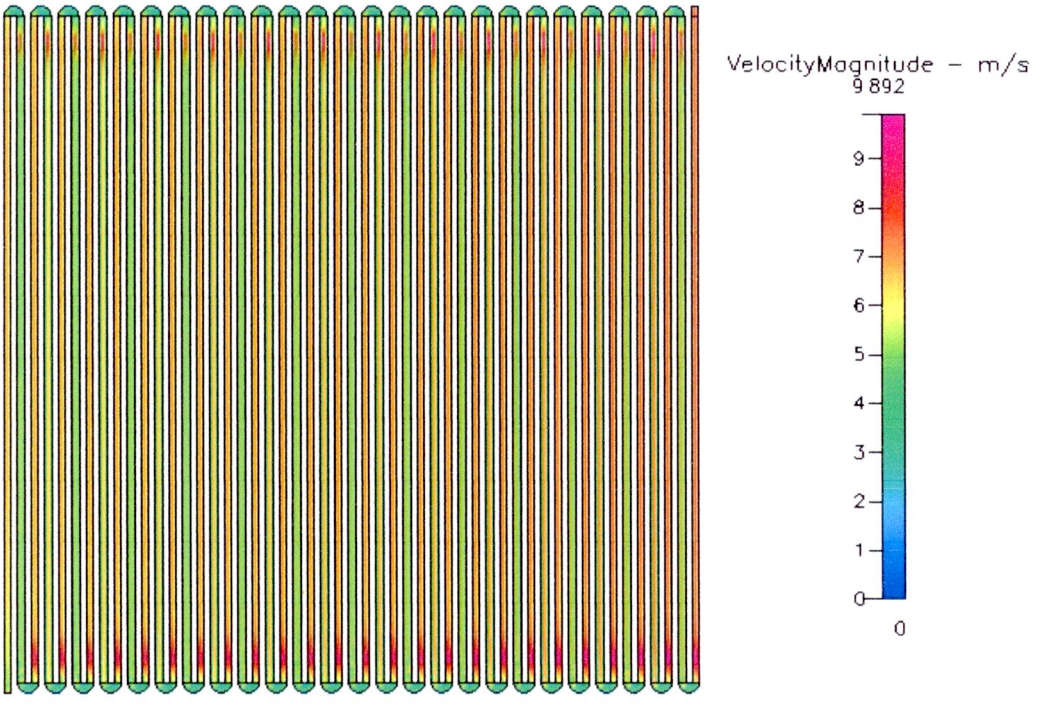

Figure 5.7 Velocity distribution at 300 cm^3/min of outside fillet curve

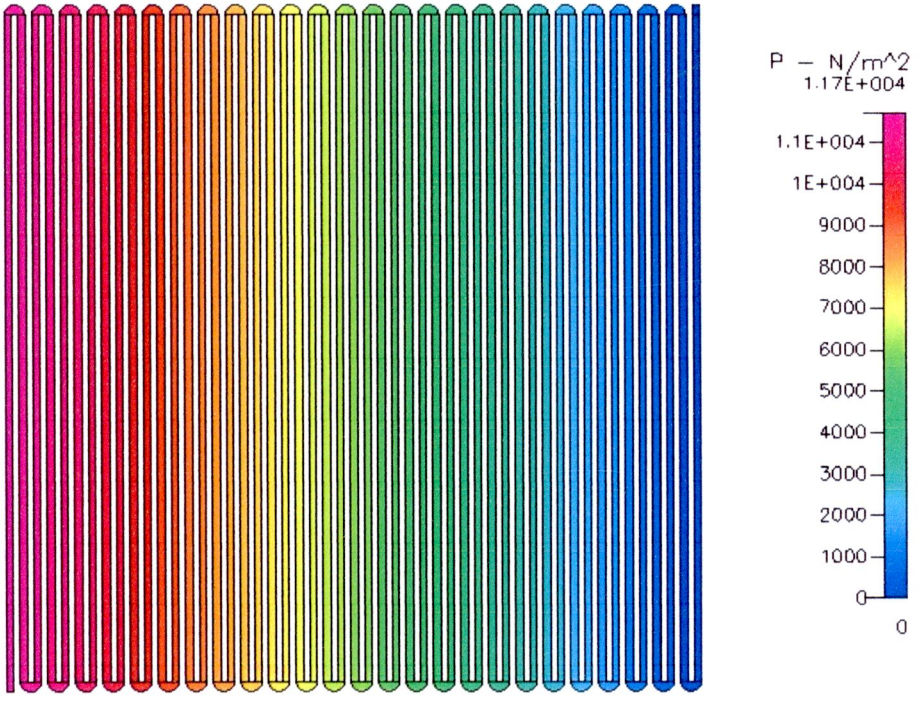

Figure 5.8 Pressure distribution at 300 cm^3/min of outside fillet curve

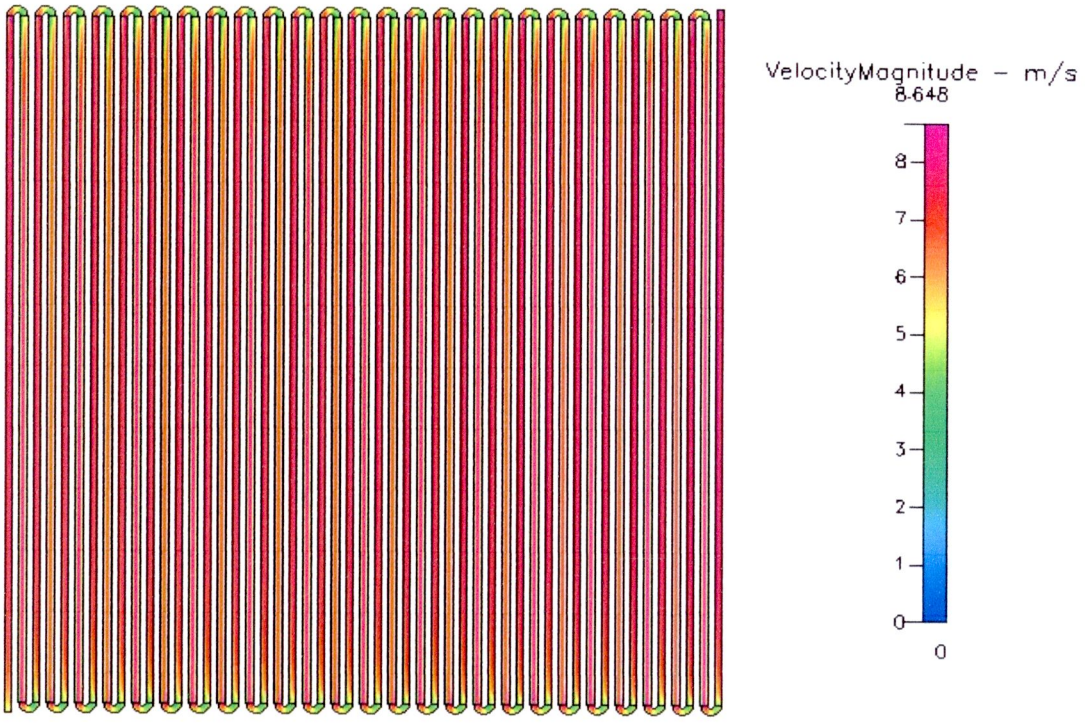

Figure 5.9 Velocity distribution at 300 cm^3/min of fillet curve

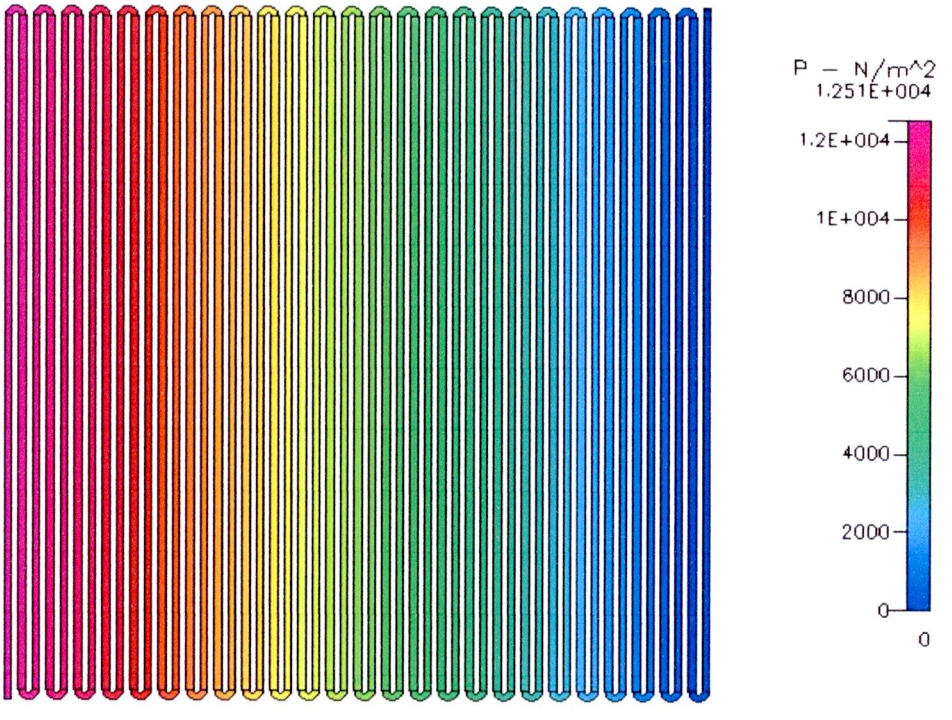

Figure 5.10 Pressure distribution at 300 cm^3/min of fillet curve

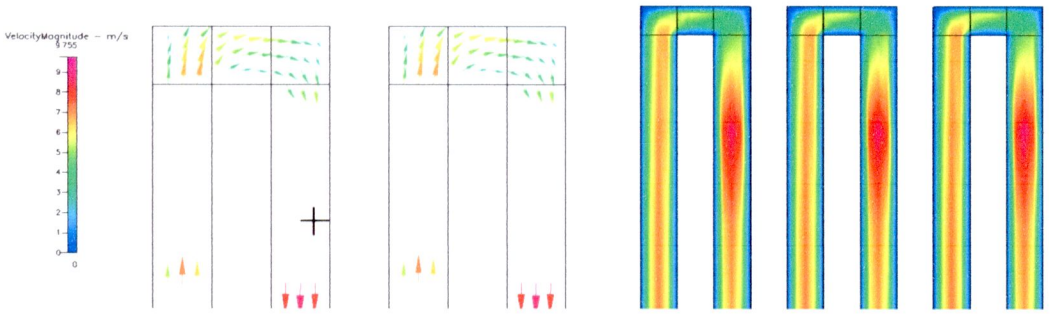

(a)

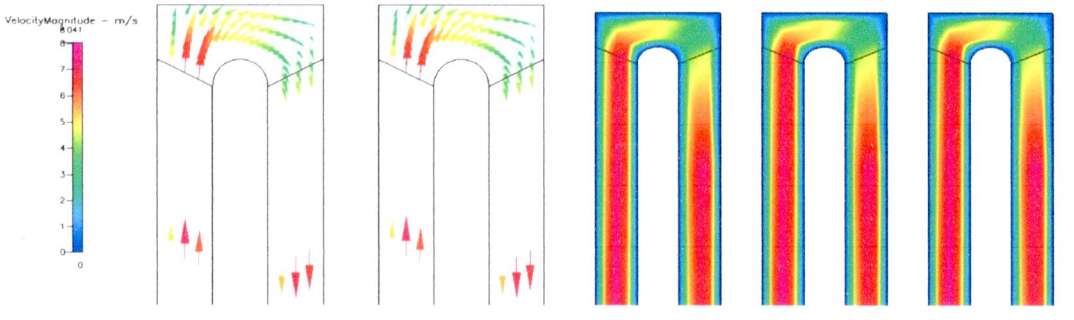

(b)

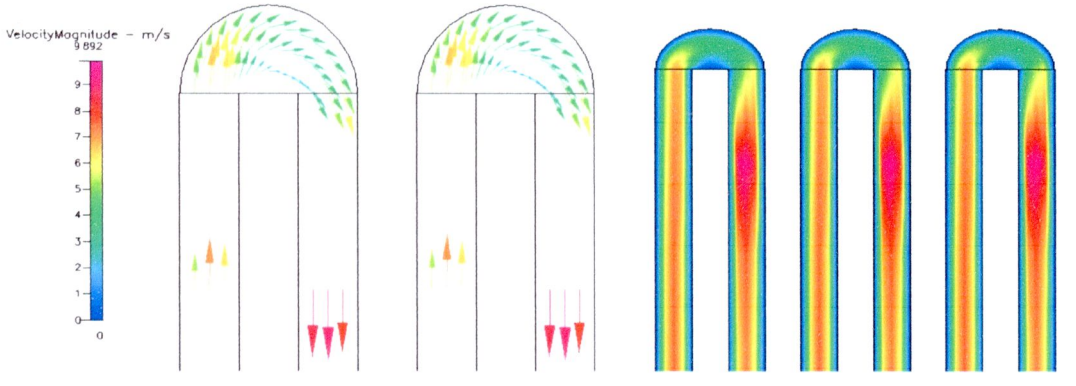

(c)

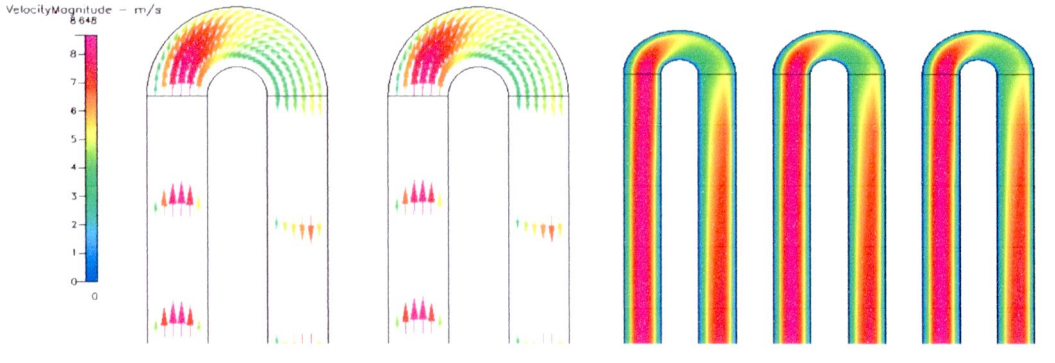

(d)

Figure 5.11 Characteristics of flow distribution at 300 cm^3/min
(a) non-fillet curve (b) inside fillet curve (c) outside fillet curve (d) fillet curve

In figures 5.3 and 5.4, there are type 1 curve serpentine flow field. Gas high velocity at begin inlet gas channel until constant before inlet curve area which has high velocity at inner wall channel. Velocity at depth 0.5 mm. has about 7.6 m/s in flow straight channel. Characteristics of gas distribution in straight channel have high flow rate in channel and it rather constant flow at middle flow field. Gas is distributes full channel in same direction and it has no clash of gas flow. In curve area, velocity decreased from straight channel until outlet curve area. Outlet curve area, it has high velocity at middle channel and increased from curve area. Figure 5.11a display non-uniform velocity distribution. Gas high distribution appears at upper curve and low gas distribution at bottom curve and it has avoided area at bottom center. Gas flow rate is decrease when gas into curvature and change direction flow (it has occurred secondary flow shown in figure 5.13). Flow rate was increased when gas went to straight part channel and secondary flow was appeared. Pressure in this flow field has highest at inlet area and decreased along with length flow channel until to outlet has zero. Pressure drop has about 1.24×10^4 N/m^2 and each flow channel was found linear pressure loss about 190 N/m^2 in all straight channels.

In figure 5.5-5.10 was shown type 2, 3 and 4 curves have velocity about 6, 4.3 and 4 m/s in flow straight channel at depth 0.5 mm., respectively and pressure drop has about 1.14×10^4 N/m^2, 1.17×10^4 N/m^2 and 1.25×10^4 N/m^2, respectively. Figure 5.11(b) displays non-uniform velocity distribution on type 2 curve. Gas was constant distributed in straight channel before into curve more than type 1. In curve area has high velocity into curve and it start decreased at middle curve area until outlet curve area. Gas high distribution appears at upper curve and low gas distribution at bottom curve, its have avoid area at bottom center. Outlet curve area, it has high velocity at middle channel and constant along with bottom channel before to next curve. Figure 5.11(c) shows uniform velocity distribution on type 3 curve. Gas was distributed similar with type 1 curve. Gas high distribution and smooth flow appears at upper curve and low gas distribution still occurs at bottom curve, its have avoid area at center bottom curve. Outlet curve area has high velocity at outer gas channel and constant along with bottom channel before to next curve. Figure 5.11(d) is type 4 curve, it has gas distributed into inlet curve area similar type 2 curve and gas distributed at outlet curve area similar type 3 curve. There is provides uniform velocity distribution and gas distributes overall through the turn.

The results of different inside fillet curve and outside fillet curve have influence on gas distribution in inlet curve and outlet curve, respectively.

In figure 5.12 was shown locations of secondary flow cross-section area which its have 7 locations in cross-section curve area of all curves. Locations 1-7 were shown cross-section areas at 0.5 mm. before inlet curve, inlet curve, 0.5 mm. before middle curve, middle curve, 0.5 mm. after middle curve, outlet curve and 0.5 mm. after outlet curve. Secondary flow has important for gas distribution into MEAs for the increasing electro-chemical reaction in fuel cell. The secondary flow in all curve shown in figures 5.13-5.16.

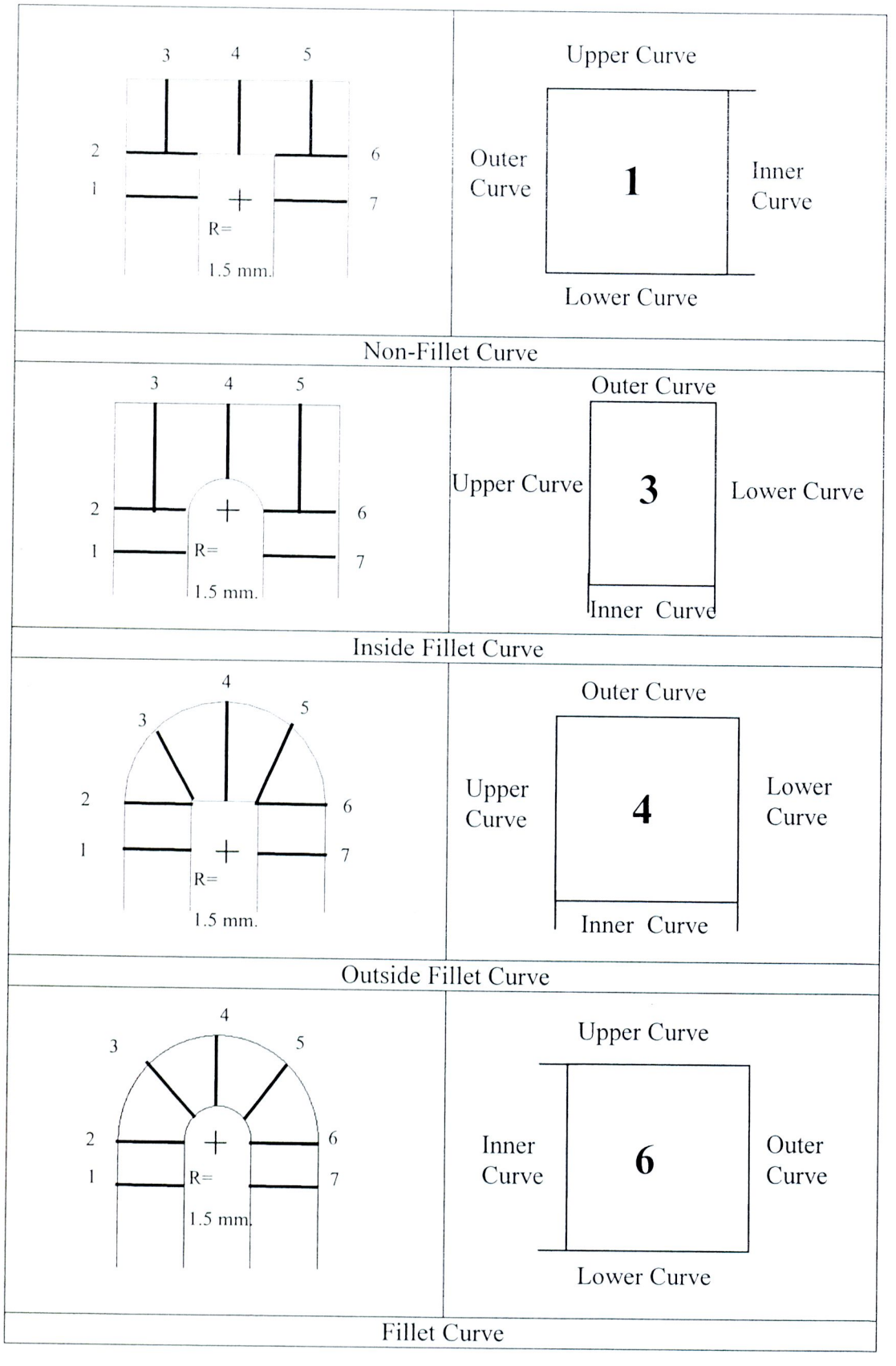

Figure 5.12 Location of cross-section in secondary flow view

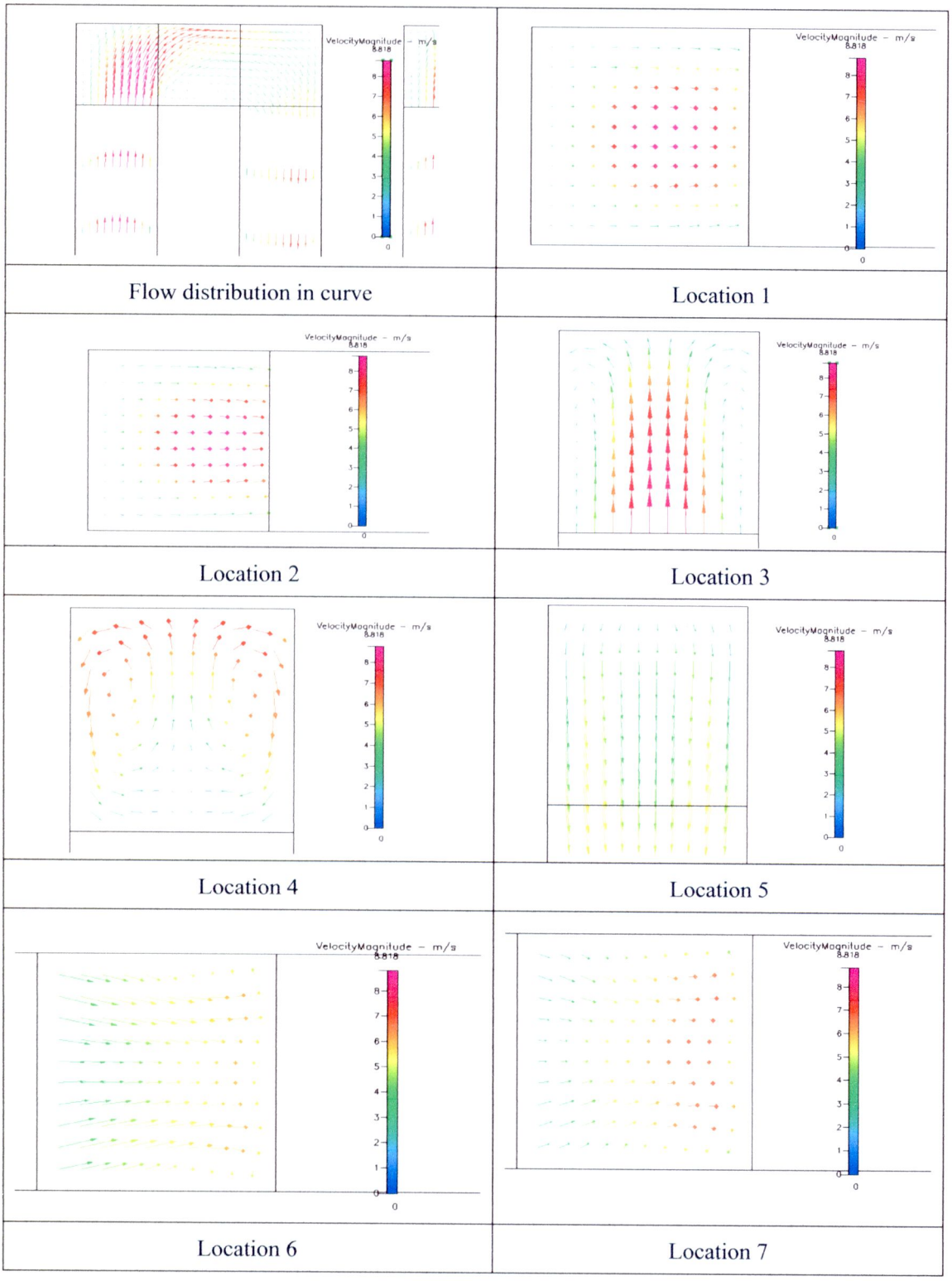

Figure 5.13 Secondary flow in Non-fillet curve

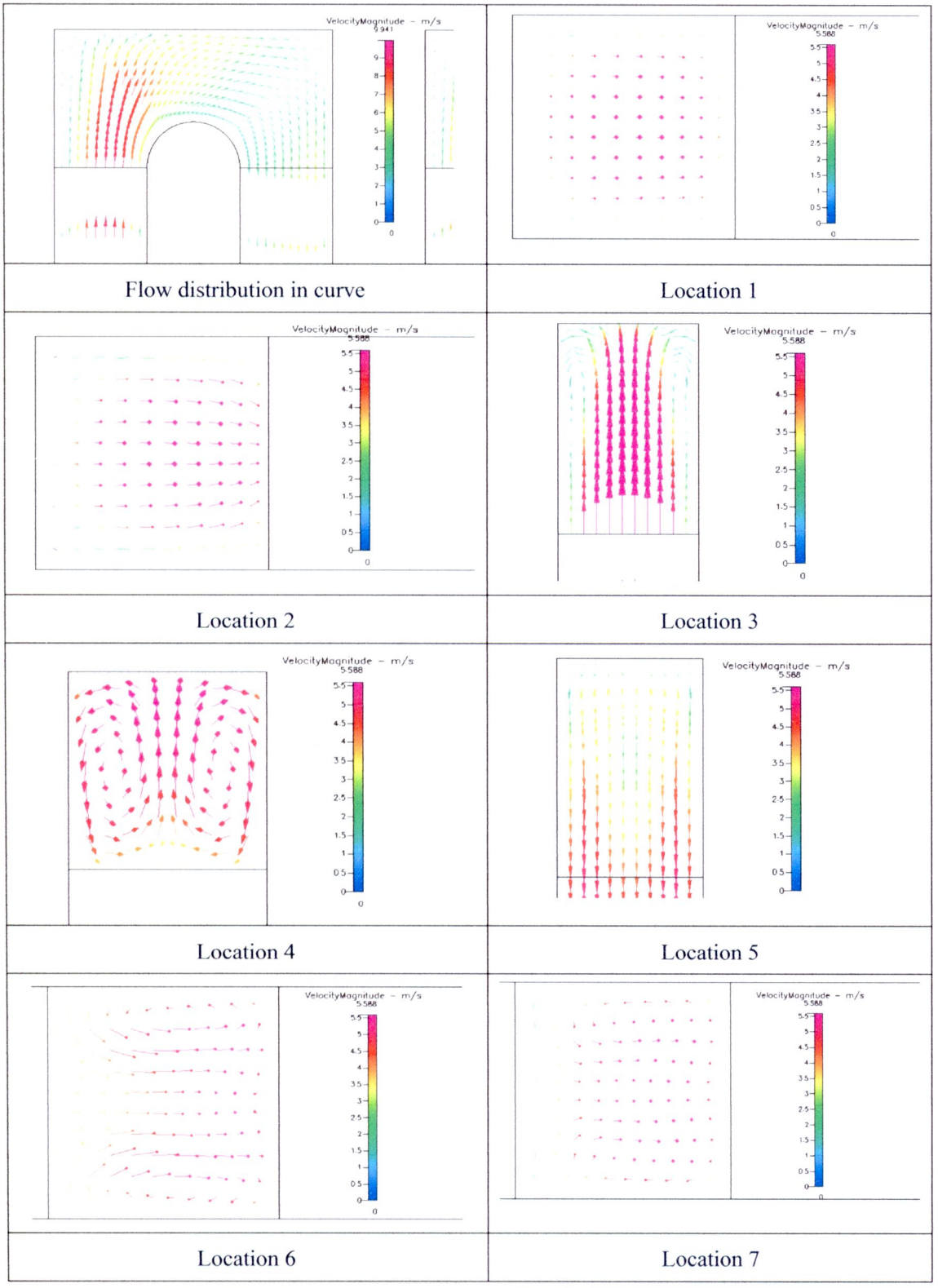

Flow distribution in curve | Location 1

Location 2 | Location 3

Location 4 | Location 5

Location 6 | Location 7

Figure 5.14 Secondary flow in Inside-fillet curve

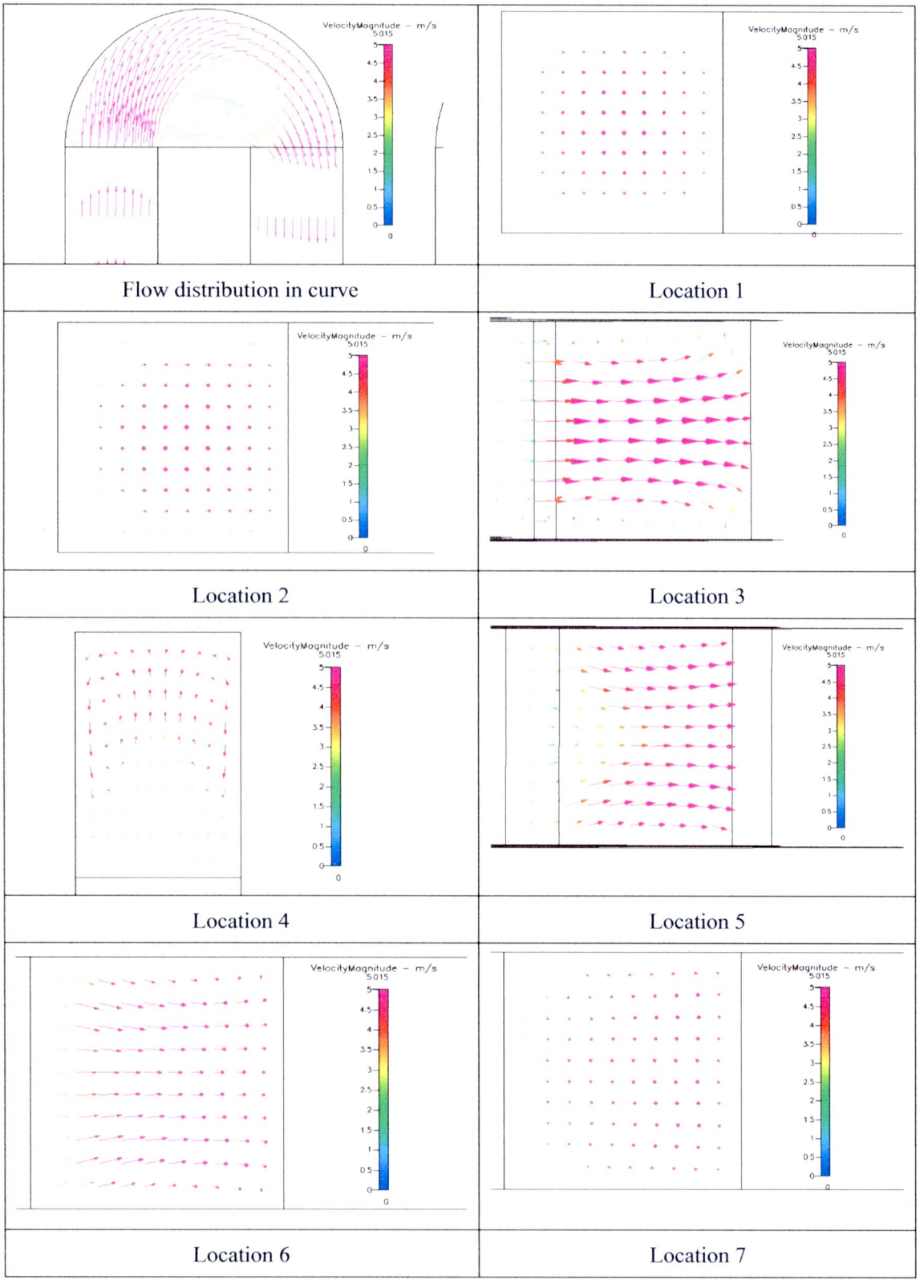

Figure 5.15 Secondary flow in Outside-fillet curve

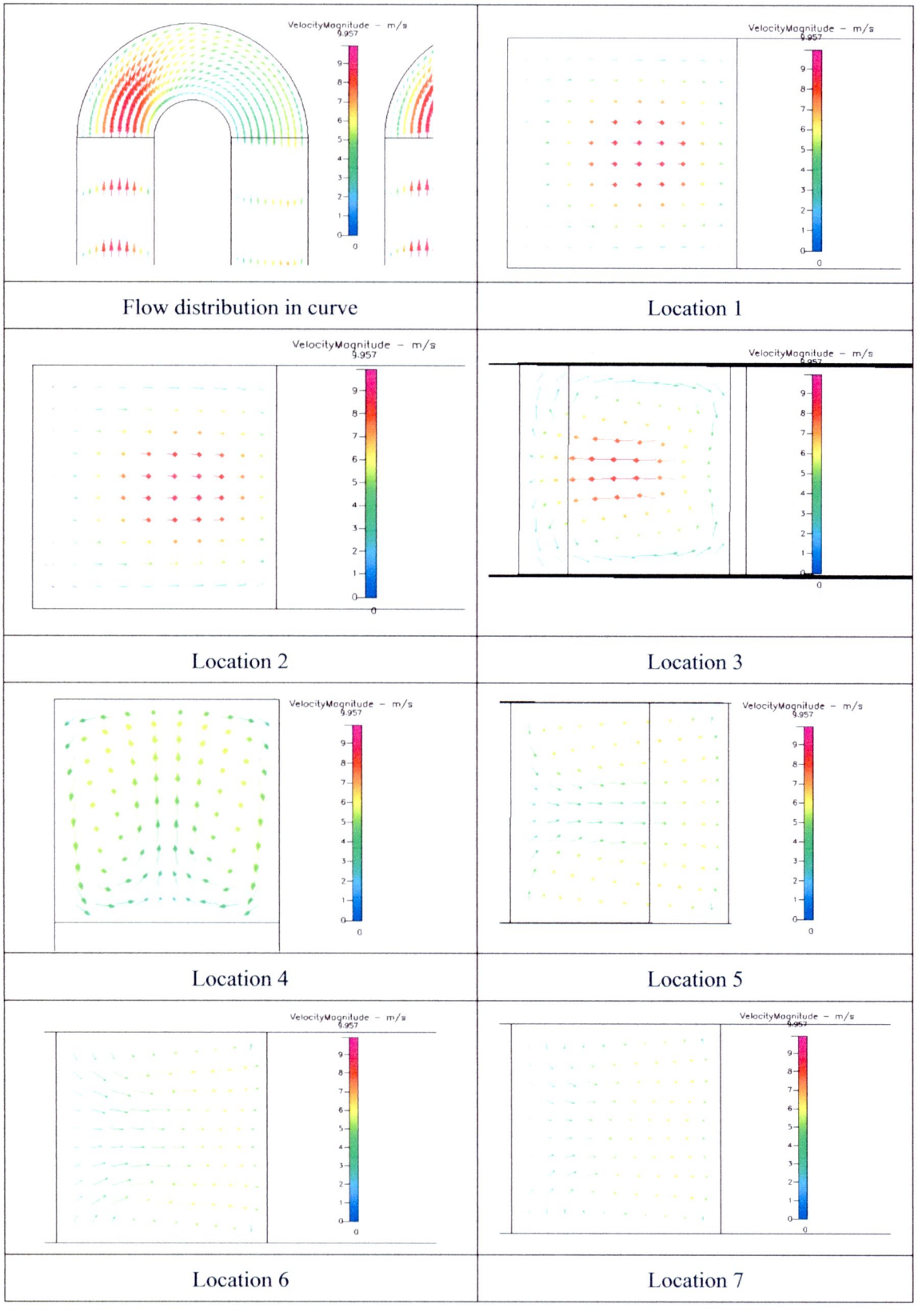

Figure 5.16 Secondary flow in fillet curve

Figure 5.13 shown secondary flows in non-fillet flow. At location 1 and 2, its have not secondary flow and gas flow goes to inside curvature which highest velocity occurred at middle cross-section area of channel. Location 3 has start secondary flow at outer curve which highest velocity occurred at outer cross-section area of channel, direction of flow clash to outer curvature and it appeared the secondary flow in corner. Location 4 has occurred secondary flow overall cross-section area. The highest velocity appeared at outer curve and lower at inner curve. Location 5 show gas direction goes out curve and velocity is nearby value. Location 6, it appears secondary flow but the velocity is less than location 4. Location 7, at upper and lower of cross-section have a little secondary flow and middle cross-section was start into the primary flow. Distance of secondary flow was 34 mm. which it analysis from difference pressure at curve and characteristics of flow distribution from graphic.

Figure 5.14 was show secondary flows in Inside-fillet curve. Location 1 was straight flow in channel straight line and gas flow into curve a little. Location 2, gas direction turn into the curve and gas was deviated in the middle inner curve. Location 3 has start secondary flow same type 1 curve but gas was constant velocity at the middle cross-section. The secondary flow occurred at outer curve and gas was clashing this area. Location 4 was occurred secondary flow overall cross-section area. The velocity is nearby at all cross-section area. Location 5, gas goes out curve and high velocity at outlet curve. It appears secondary flow at location 6 and 7 in all cross-section area and distance of secondary flow was 34 mm. form inlet curve.

Figure 5.15 shown secondary flows in outside-fillet curve. At location 1 and 2, there were not secondary flow and gas flow in straight line direction. The velocity was quite the same all cross-section area. Location 3 has start secondary flow and location 4 was occurred secondary flow same type 1 and 2 curve but secondary flow at upper and lower curve area was a less more than others. Location 5 and 6 were show gas was a little secondary flow. Gas changed to the primary flow showing location 7. Distance of secondary flow was 30 mm.

In figure 5.16 was shown the secondary flow in fillet curve. Locations 1 and 2 have not secondary flow and direction of gas was goes in the curve. Locations 3, 4 and 5 have occurred secondary flow but in location 3 has high velocity in middle cross-section area and location 4 has a rather constant velocity in all area. At location 5 has a little secondary flow. Location 6 has a secondary flow at upper and lower cross-section area and middle this area, gas goes to outer curve. In location 7, gas has less secondary flow because gas was developing to primary flow but it has high secondary more than others. Secondary flow occur 37 mm. from inlet curve.

The results of secondary flow in all curves found type 4 has a more secondary flow than others curve. Distance of secondary flow was type 4 curve has a highest and type 3 has a lowest.

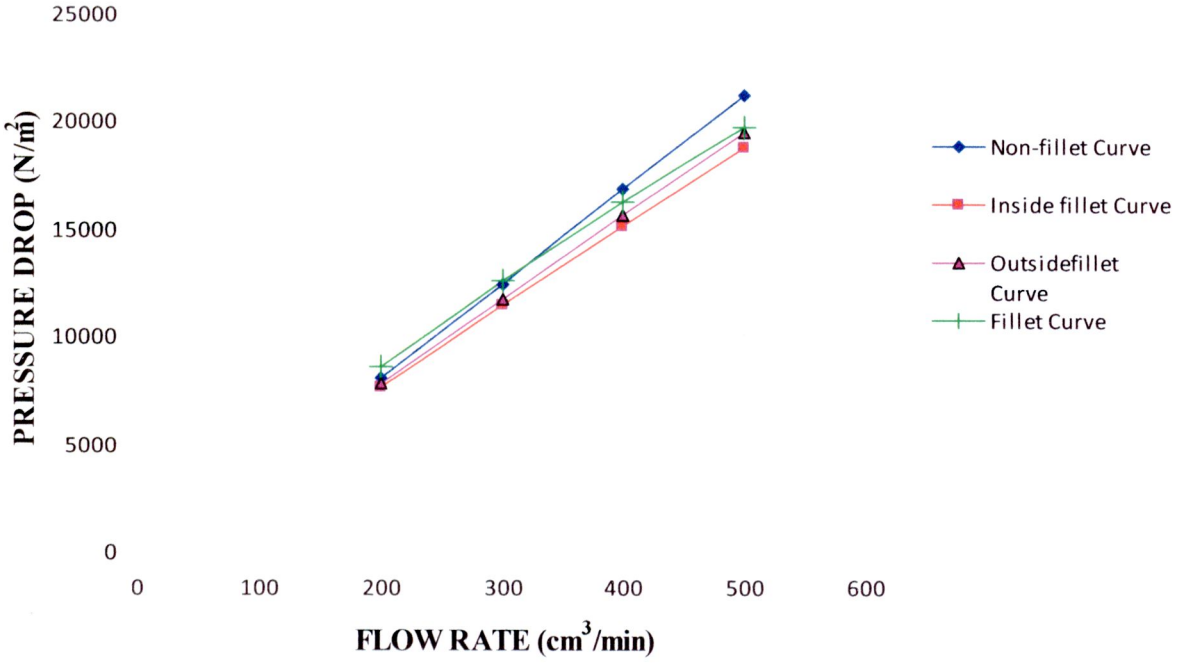

Figure5.17 Pressure drop and flow rate in different channel curve

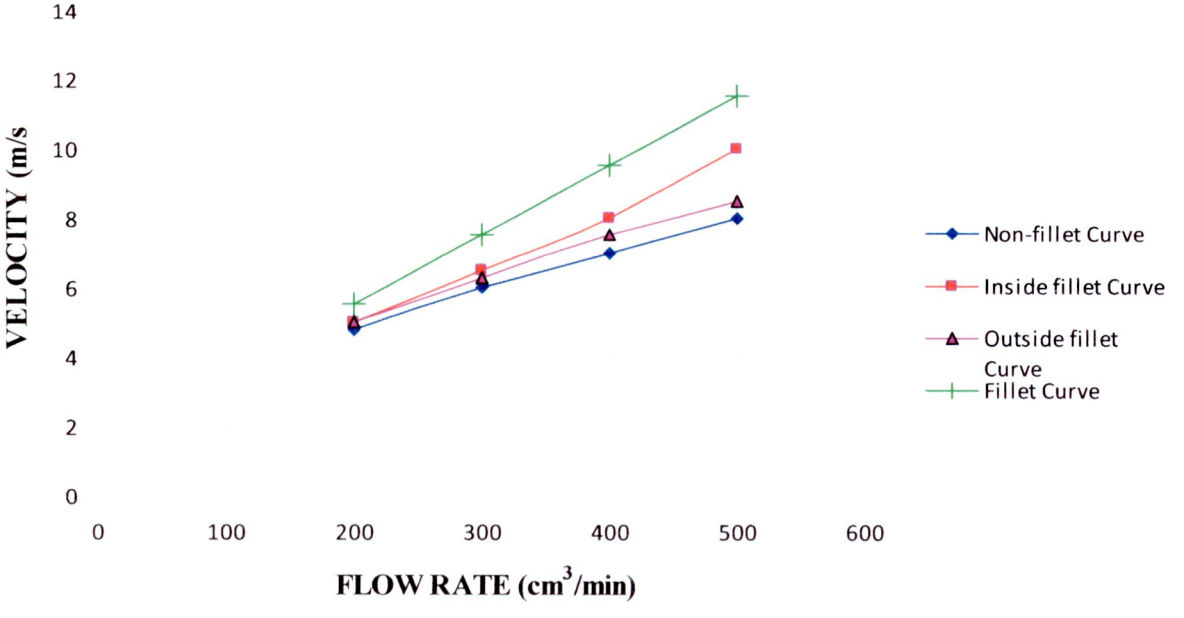

Figure 5.18 Velocity at 0.5 depth and flow rate in different channel curve

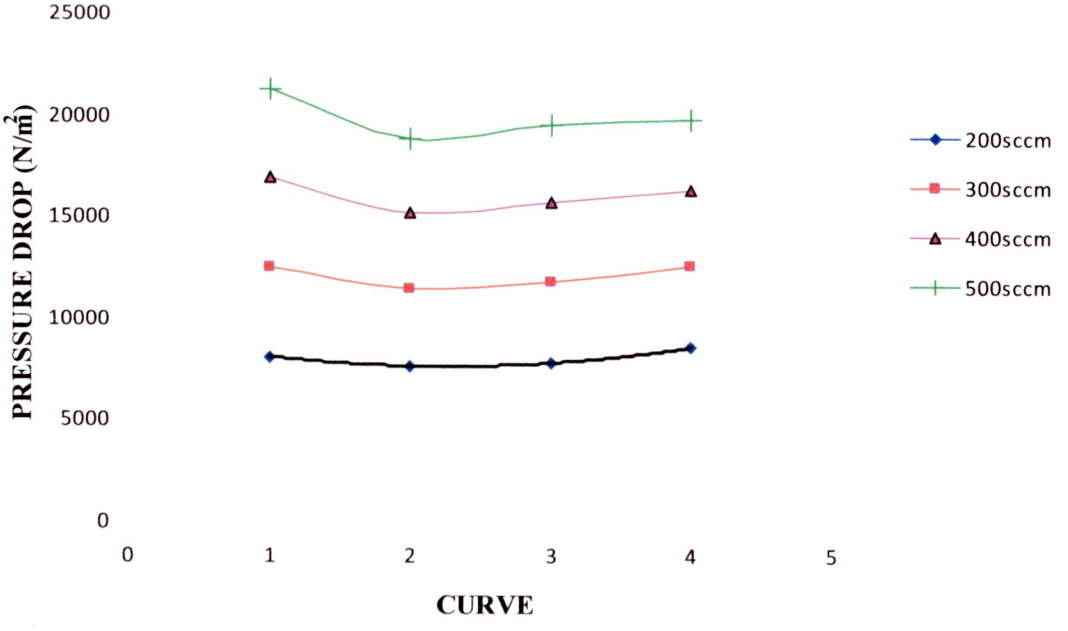

Figure 5.19 Curve type and pressure drop

When vary flow rate between 200-500 cm^3/min then type 1 curve has a highest pressure and subordinate is type 4 curve, type 3 curve and type 2 curve, respectively are show in figure 5.17. The type 4 curve has highest velocity and type 2 curve, type 3 curve and type 1 curve is latter are shown in figure 5.18. The type 1 curve is highest pressure drop but it has lowest velocity and type 4 curve is high velocity. Curve type and pressure drop show in figure 5.19 which describe to trend pressure drop line and characteristic of curve from each flow rate.

The results of different channel curve that inside curve and outside curve have influence on gas distribution in inlet curve and outlet curve, respectively. From studies, the non-fillet curve and fillet curve is also confirm the good configuration because it has non-uniform flow distribution and high pressure drop. Fillet curve has a highest distance for secondary flow and non-fillet curve has a highest a curve area. Those results are good for the high electro chemical reaction in MEAs and water management. From results, there are can be used for design flow field to improve performance.

5.1.2 Effect of Channel Length on Flow Field

Effect of channel length will focus on the 6 different 100 cm^2 flow field patterns. There are 1-channel serpentine, 2-channels serpentine, 3-channels serpentine, 4-channels serpentine, 5-channels serpentine and 6- channels serpentine which increase number of channel get channel length is shorter. Length of channel is shown in Table 5.1. All geometries have similar patterns, but different gas path lengths. The solutions from the model will be shown and analyzed for these different flow-field configurations. The pattern of this distributed network and the effect on pressure drop will be studied and generic design principles will be developed. The results of flow and pressure drop are effect of length show in figures. 5.20-5.32.

Table 5.1 Length of channel flow

Number of channel	1	2	3	4	5	6
Length (mm.)	5150	2535.5	1748.5	1312	1009	908

In design of flow field length for the build flow field is nearby 100 cm. which it is analysis axis x for design channel, it can be consider relationship from;

1 turn: Distance of axis x = 2R
2 turn: Distance of axis x = 4R-w
3 turn: Distance of axis x = 6R-w

Therefore, it can be build relationship of number flow channel can be used in equation 5.1

$$x = 2nR-(n-1)w \tag{5.1}$$

Where R = Radius of curve (measurement at center of radius to outer wall)
w = Channel Width
n = number of turn in serpentine channel

And design of multi serpentine flow field length has many curves is similar single serpentine but it used in 2 radiuses are inner radius curve and outer radius curve. It can describe from equation 5.2

In multi-serpentine channel

1 turn: Distance of axis x = 2R
2 turn: Distance of axis x = 3R-[r-w]
3 turn: Distance of axis x = 4R-2[r-w]

Therefore, distance of axis x in multi-serpentine can use in equation 5.2

$$x= (n+1)R + (n-1)(r-w) \tag{5.2}$$

Where R = Radius of outer radius curve (measurement at center of radius to outer wall curve of last channel)
r = Radius of inner radius curve (measurement at center of radius to outer wall curve of first channel)

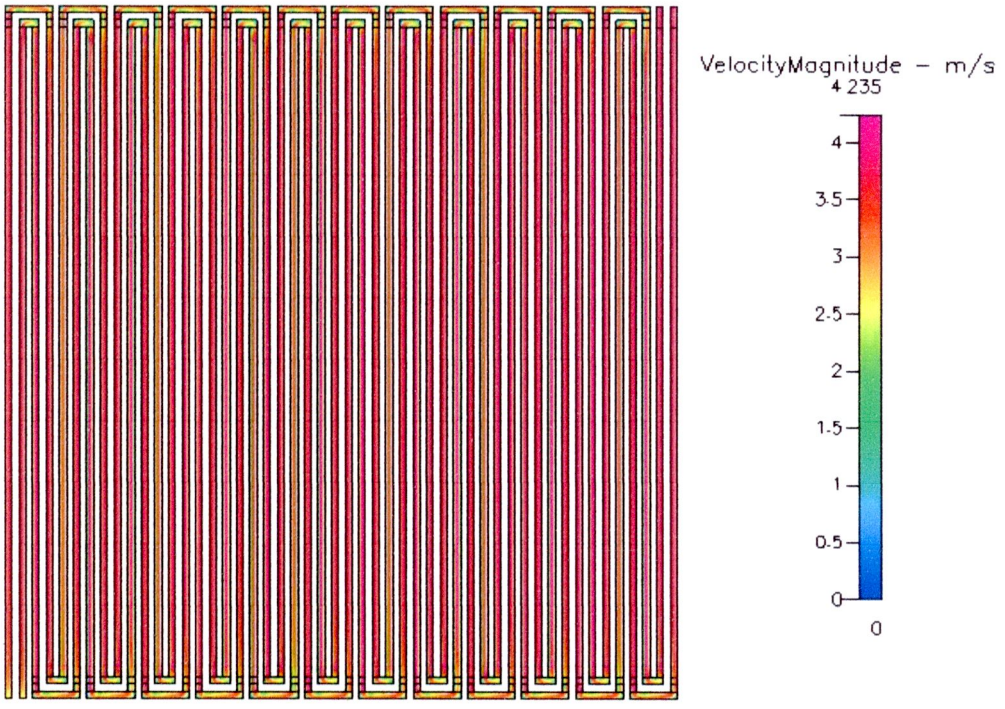

Figure 5.20 Velocity distribution at 300 cm^3/min of 2 channels

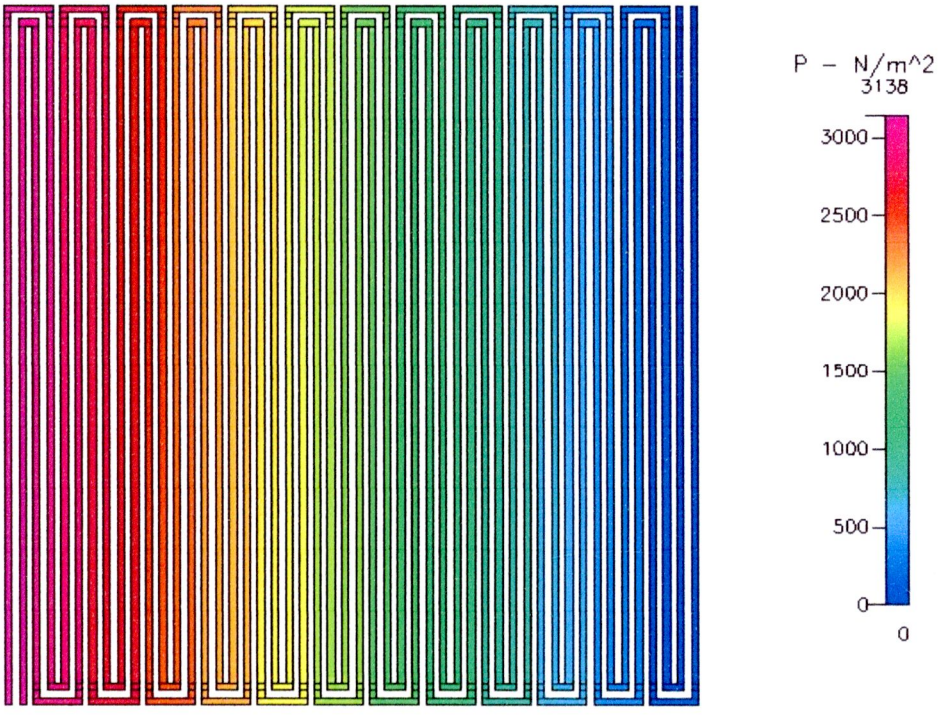

Figure 5.21 Pressure distribution at 300 cm^3/min of 2 channels

Figure 5.22 Velocity distribution at 300 cm^3/min of 3 channels

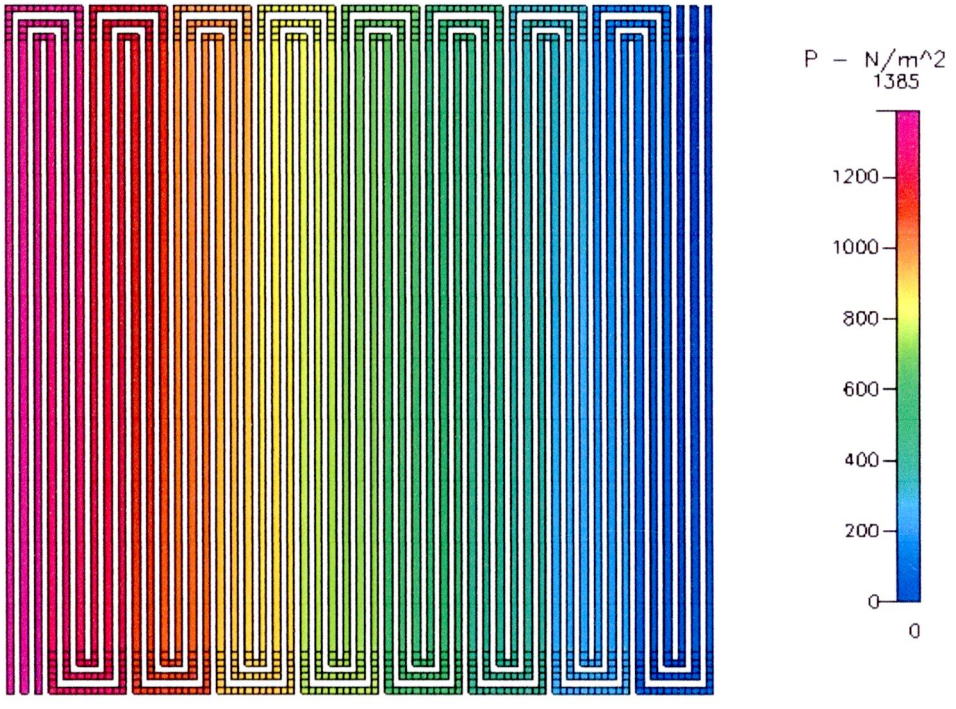

Figure 5.23 Pressure distribution at 300 cm^3/min of 3 channels

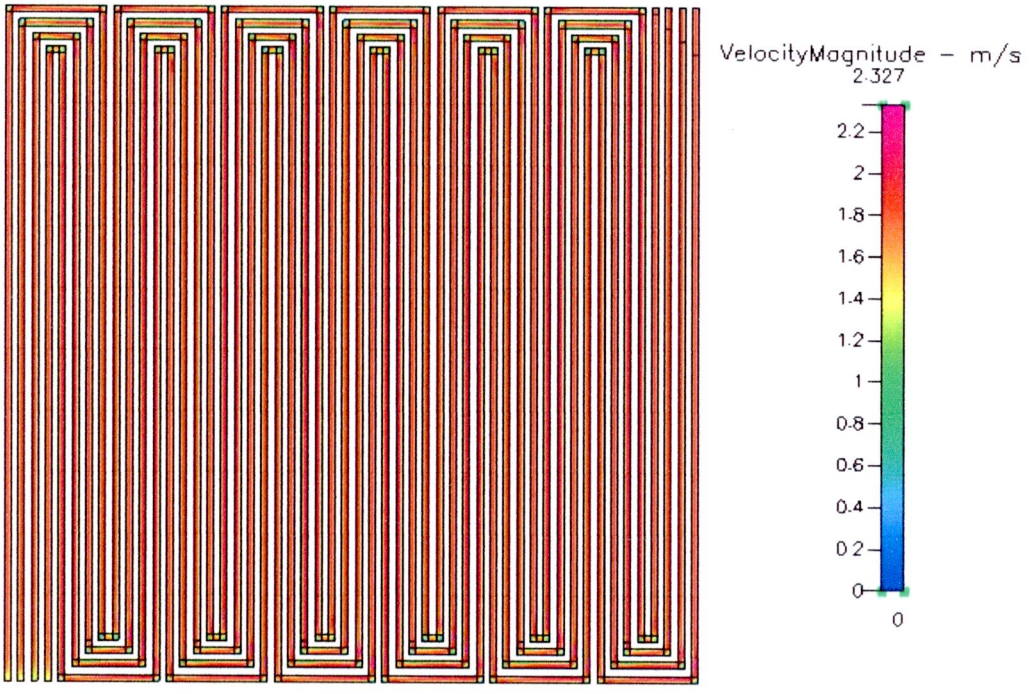

Figure 5.24 Velocity distribution at 300 cm^3/min of 4 channels

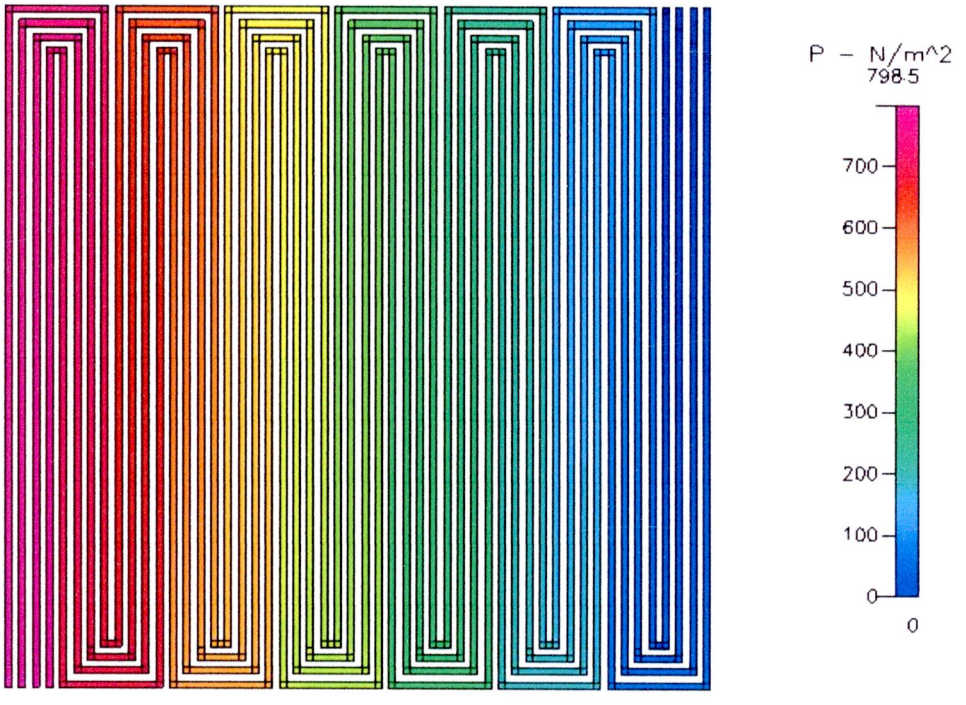

Figure 5.25 Pressure distribution at 300 cm^3/min of 4 channels

Figure 5.26 Velocity distribution at 300 cm^3/min of 5 channels

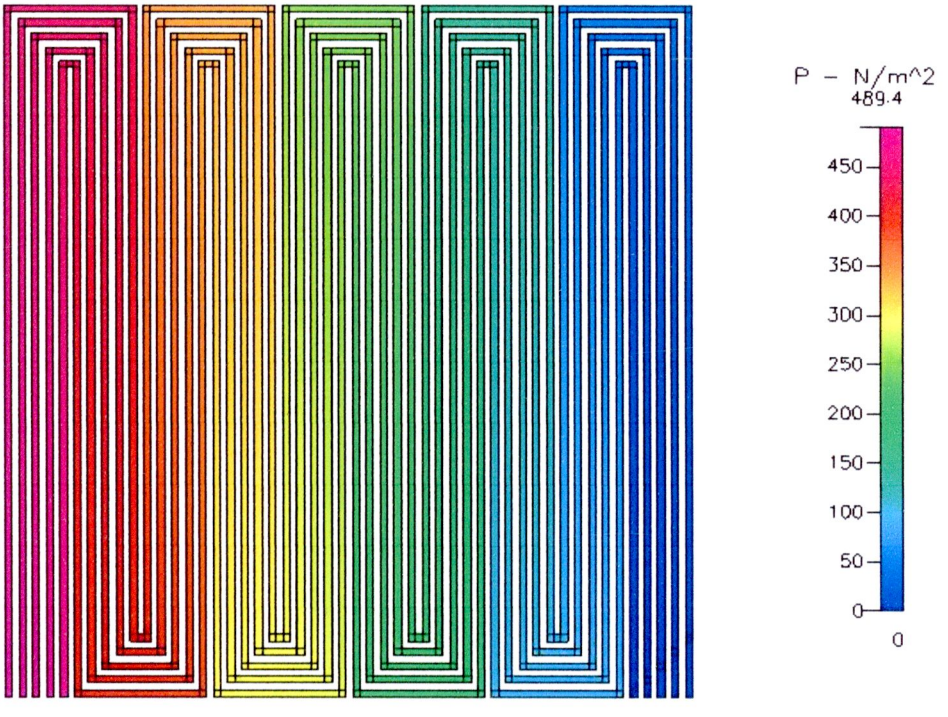

Figure 5.27 Pressure distribution at 300 cm^3/min of 5 channels

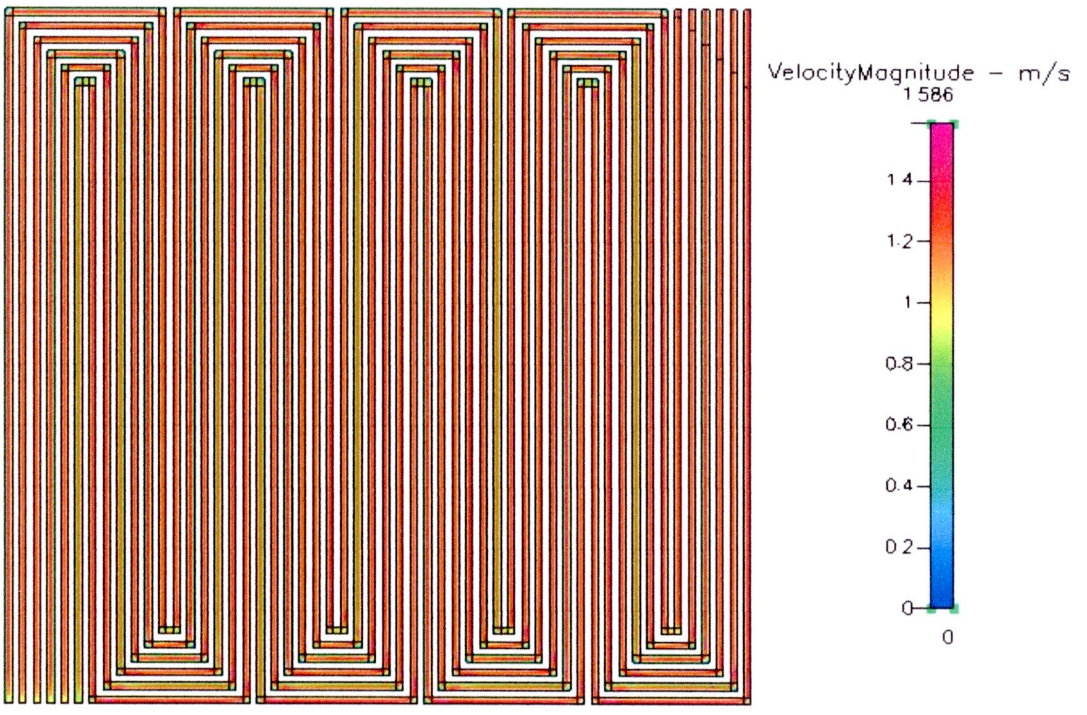

Figure 5.28 Velocity distribution at 300 cm^3/min of 6 channels

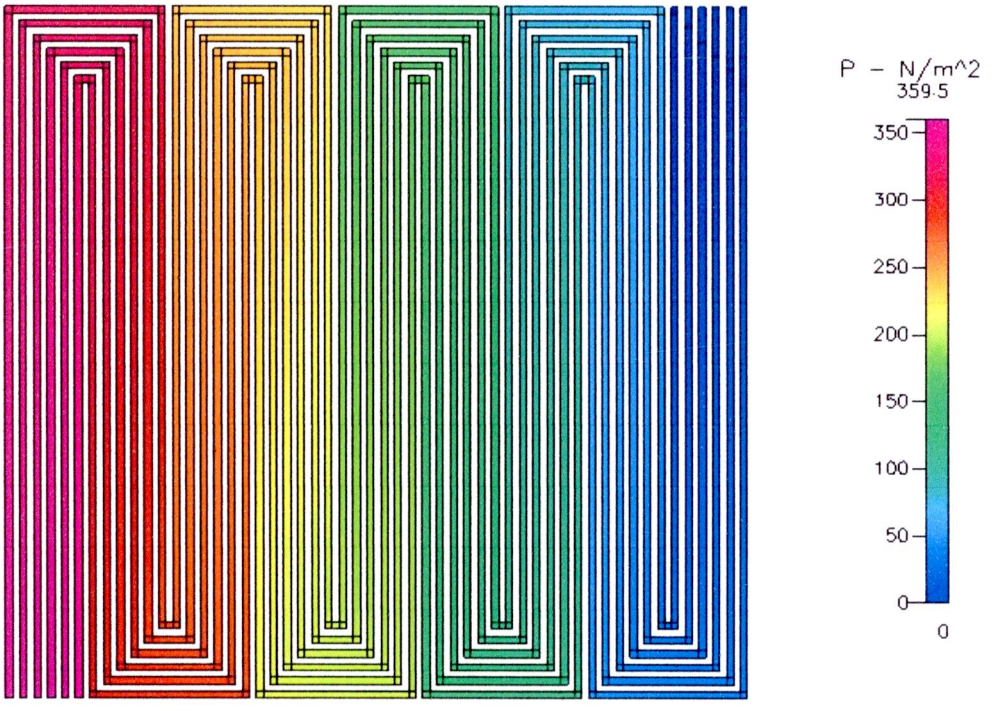

Figure 5.29 Pressure distribution at 300 cm^3/min of 6 channels

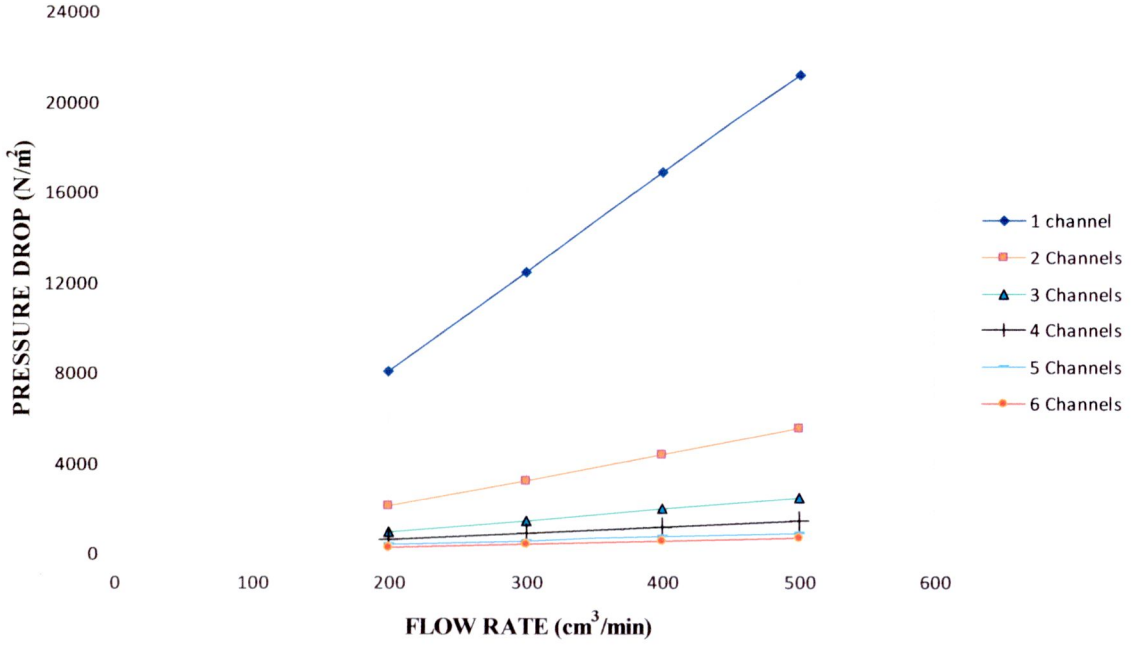

Figure 5.30 Pressure drop and flow rate in different channel length

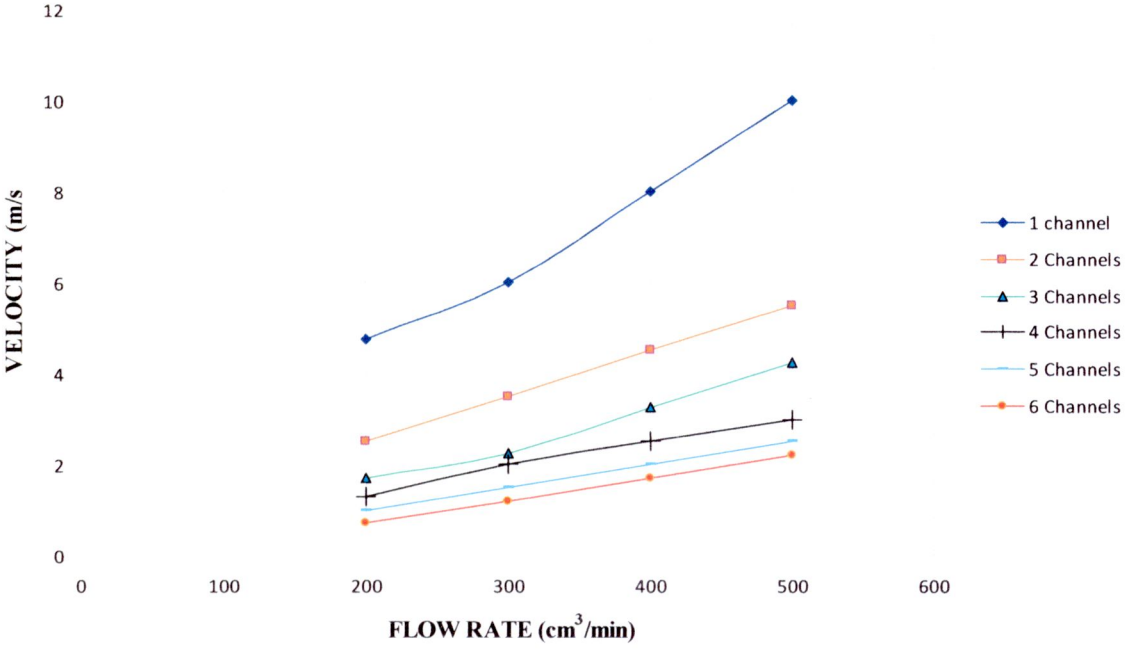

Figure 5.31 Velocity at depth 0.5 mm. and flow rate in different channel length

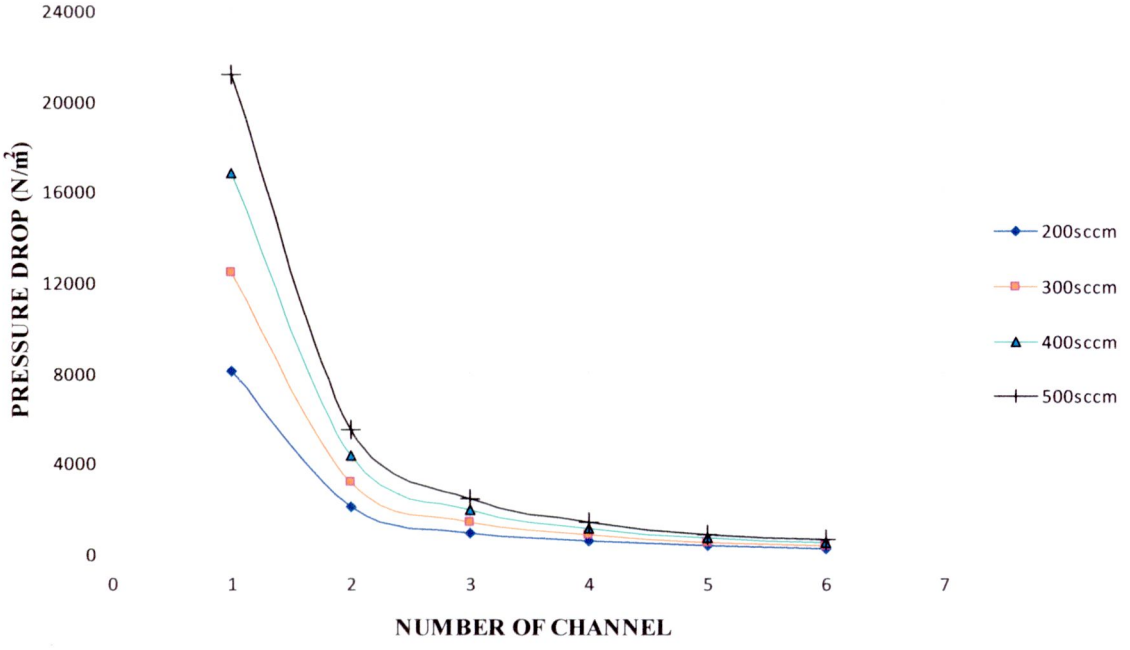

Figure 5.32 Number of channel and pressure drop

This figure 5.20-5.29 shows 2 channel to 6 channels serpentine flow field that pressure drop increase with the increase of path length. The pressure drop decrease as the number of flow channels increase because there are more parallel paths that the flow can take. The velocities and pressure drop distribution in 1, 2, 3, 4, 5 and 6 serpentine channels at 300 cm^3/min was 1 channel has average velocity about 4 m/s and pressure drop is 1.24×10^4 N/m^2. Gas distribution has uniform in serpentine pattern. Lower velocities distribution appears at channel curvatures and high velocities distribution at downstream of channel. The pressure drop has decreases along length channel. In 2, 3, 4, 5 and 6 channels have velocity about 3.5, 2.25, 2, 1.5 and 1.2 m/s at depth 0.5 mm., and pressure drop is 3,138, 1,385, 798.5, 489.4 and 359.5 N/m^2, respectively. When vary flow rate between 200-500 cm^3/min then 1 channel has a highest pressure and highest velocity, 2 channels to 6 channels has lower pressure and velocity, respectively are show in figures 5.30-5.31. In 4, 5 and 6 channels have nearby pressure drop. Number of channel and pressure drop show in figure 5.32 which describe to trend pressure drop line and number of channel from each flow rate.

The result of effect flow-field path length was studied the velocity and pressure drop. It can be concluded that changing flow-field configuration by varying path length of PEMFC by changing the number of parallel channels affect, its performance and uniformity. The longer path length gives more pressure drop. Therefore, the path length of a PEMFC flow-field is one of the major variables for optimizing the performance, efficiency, and durability of PEMFC.

5.1.3 Effect of Channel Shape on Flow Field

a) channel depth

Effect of channel depth has 3 depths of serpentine pattern in this study. There are 0.8, 1.0 and 1.2 mm.. It is changing depth channel depend on cross section area is

change. The solutions of these depths will be shown and analyzed of velocity distribution and pressure drop are effect of depth was shown in figure 5.33-5.39.

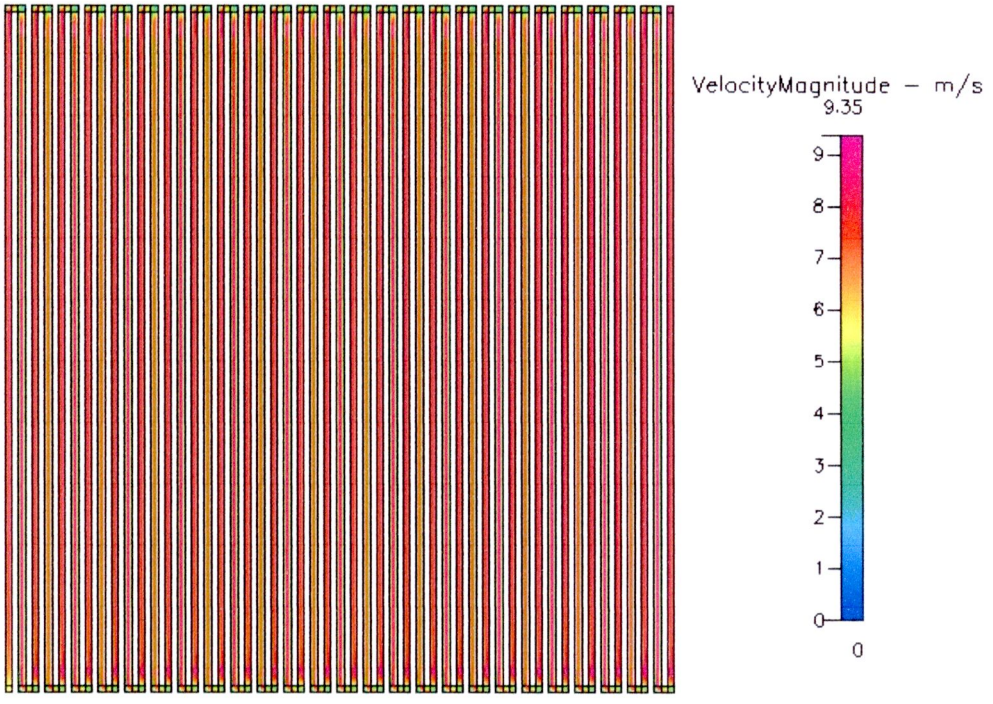

Figure 5.33 Velocity distribution at 300 cm^3/min of 0.8 mm. depth

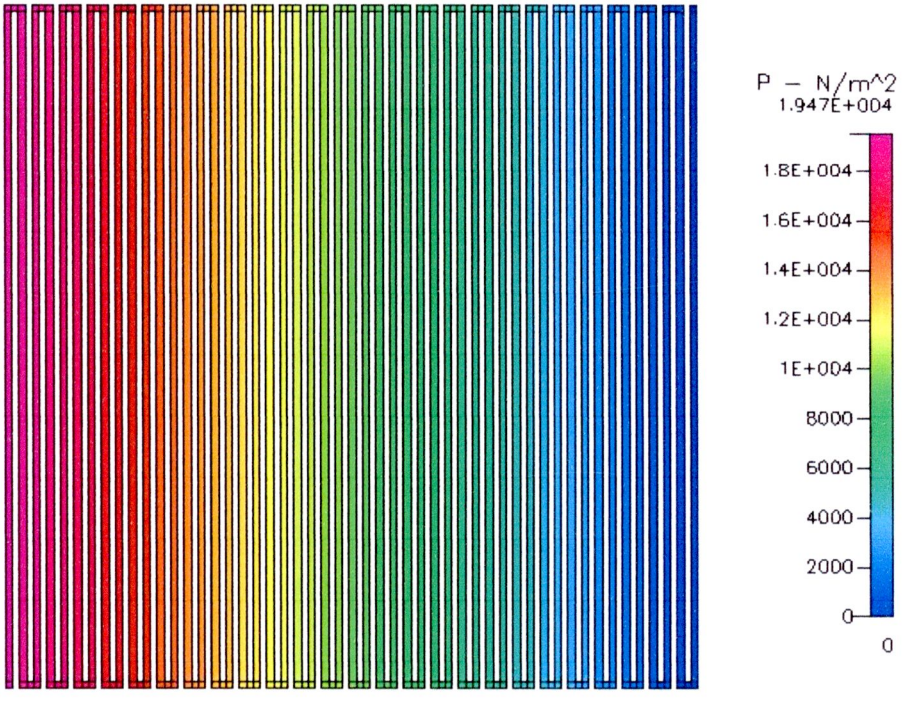

Figure 5.34 Pressure distribution at 300 cm^3/min of 0.8 mm. depth

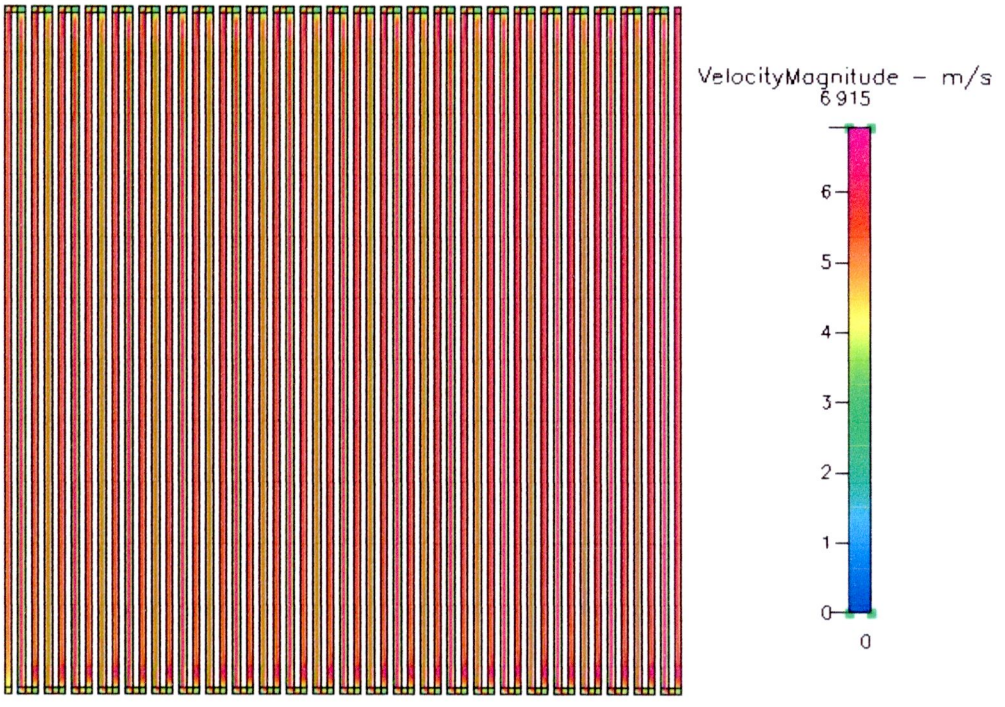

Figure 5.35 Velocity distribution at 300 cm^3/min of 1.2 mm. depth

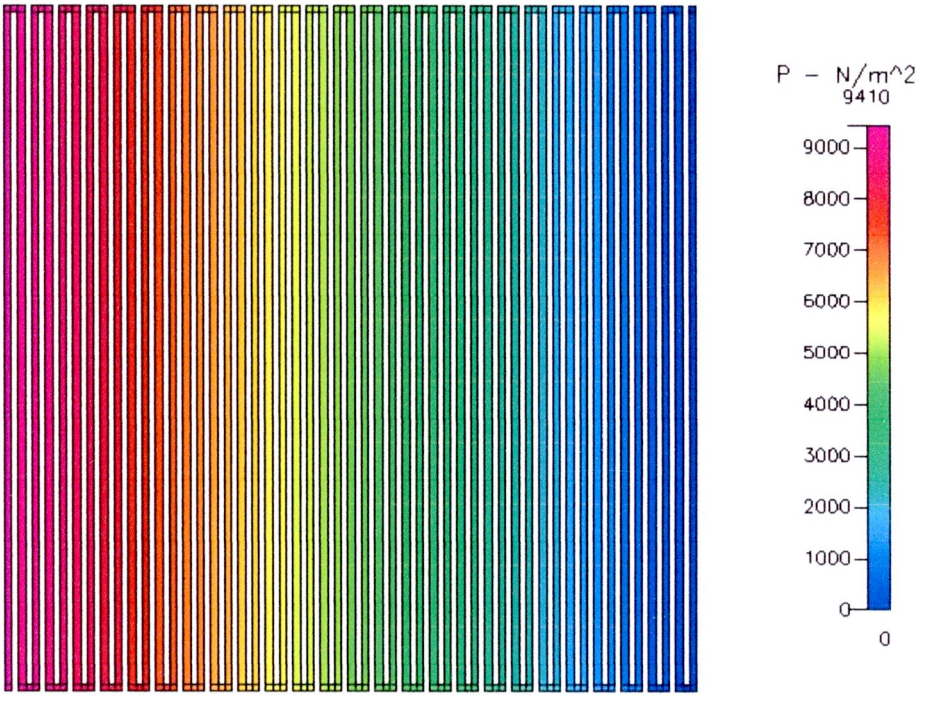

Figure 5.36 Pressure distribution at 300 cm^3/min of 1.2 mm. depth

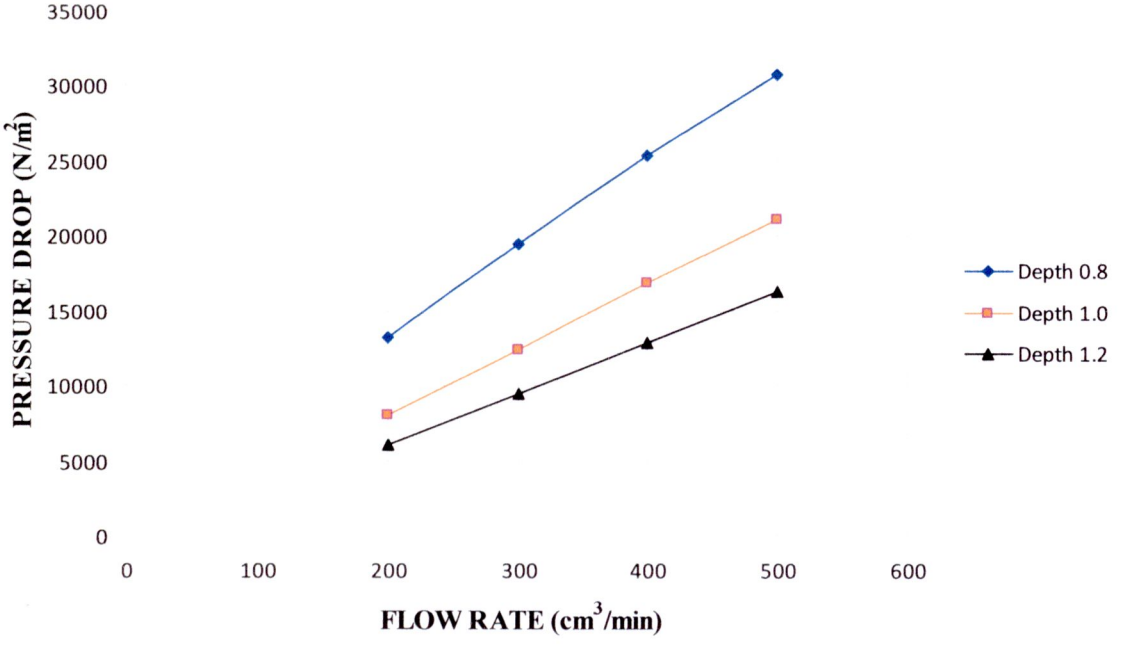

Figure 5.37 Pressure drop and flow rate in different channel depth

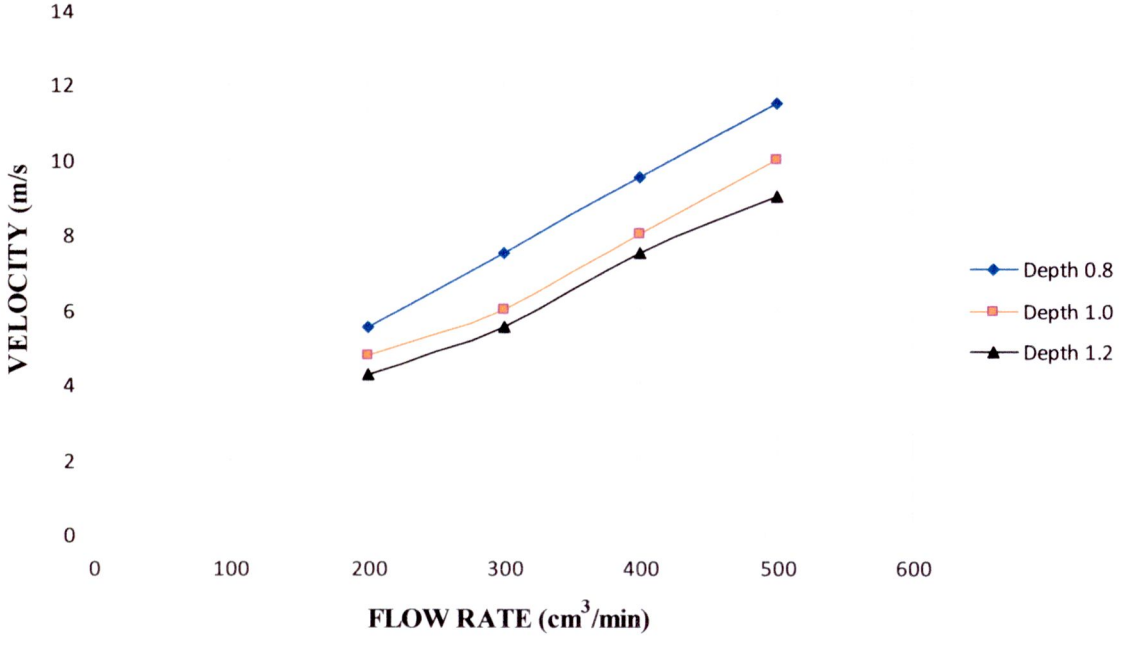

Figure 5.38 Velocity at depth 0.5 mm and flow rate in different channel depth

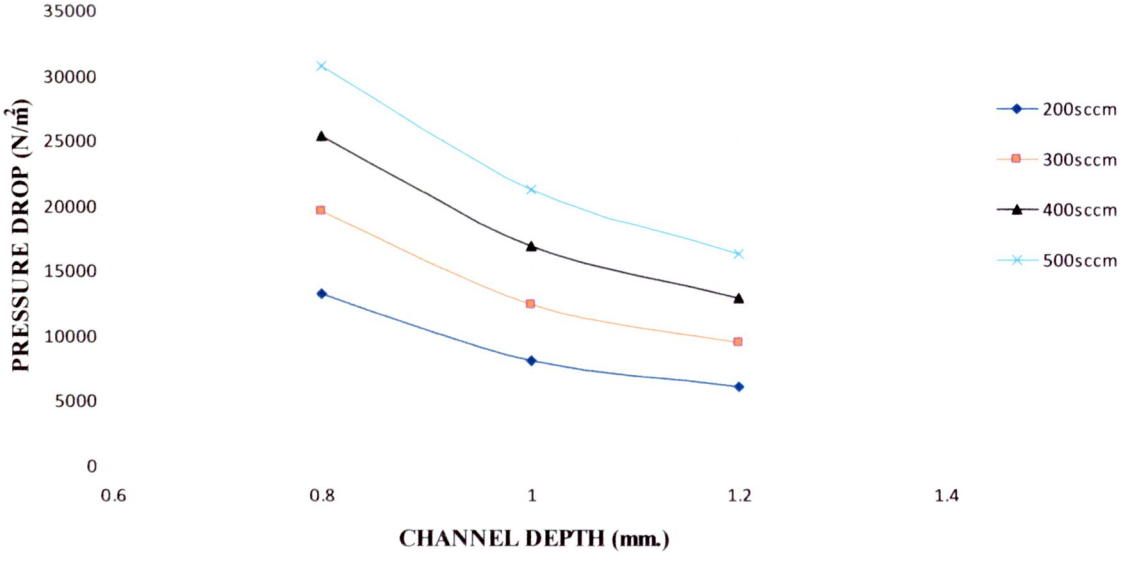

Figure 5.39 Channel depth and pressure drop

This figure 5.33-5.36 shows 0.8 and 1.2 depth serpentine flow field that pressure drop increase with the decrease of depth channel. The pressure drop decreased as the cross section area increase because there is low velocity. The velocities and pressure drop distribution in 0.8, 1 and 1.2 depth at 300 cm^3/min was 0.8 mm. has velocity about 8 m/s and pressure drop is 1.95×10^4 N/m^2. Gas distribution has uniform in serpentine pattern. Lower velocities distribution appears at channel curvatures and high velocities distribution at straight channel. The pressure drop has decreases along with length channel. In 1 and 1.2 depth channels have velocity about 7 and 6 m/s, and pressure drop is 1.24×10^4 and 9400 N/m^2, respectively. When vary flow rate between 200-500 cm^3/min then 0.8 depth channel has a highest pressure drop and velocity, 1 and 1.2 depth channels has lower than pressure and velocity, respectively are show in figures 5.37-5.38. Channel depth and pressure drop show in figure 5.39 which describe to trend pressure drop line and channel depth from each flow rate.

The result of effect flow-field depth was show the velocity and pressure drop, which it is depend to changing depth channel flow-field configuration by changing the cross section area of channels can affect its velocity and mass flow rate. The lower cross section area gives higher than velocity and pressure drop. Therefore, the flow-field depth of a PEMFC flow-field is one of the major variables for optimizing the performance of PEMFC.

b) channel width

Various channel widths were used to see the flow field effect in velocity distribution and pressure drop. The flow field dimension based on serpentine flow field and its have 3 widths in this study. Channel width has 0.8 mm. and rib 1.2 mm. which has a longer curve, 1 mm. and 1.2 mm. and rib 0.8 mm. which has a shorter curve and common depth in 1.0 mm.. The results of these widths will be shown of velocity distribution and pressure drop are effect of width was shown in figure 5.40-5.46.

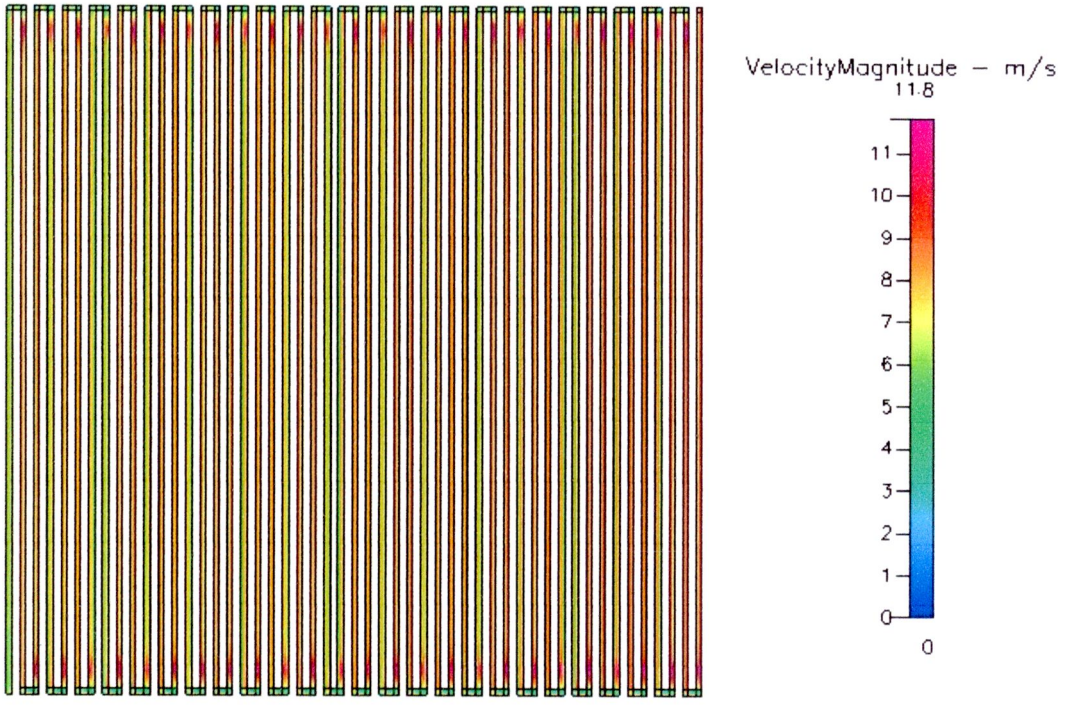

Figure 5.40 Velocity distribution at 300 cm^3/min of 0.8 mm. width

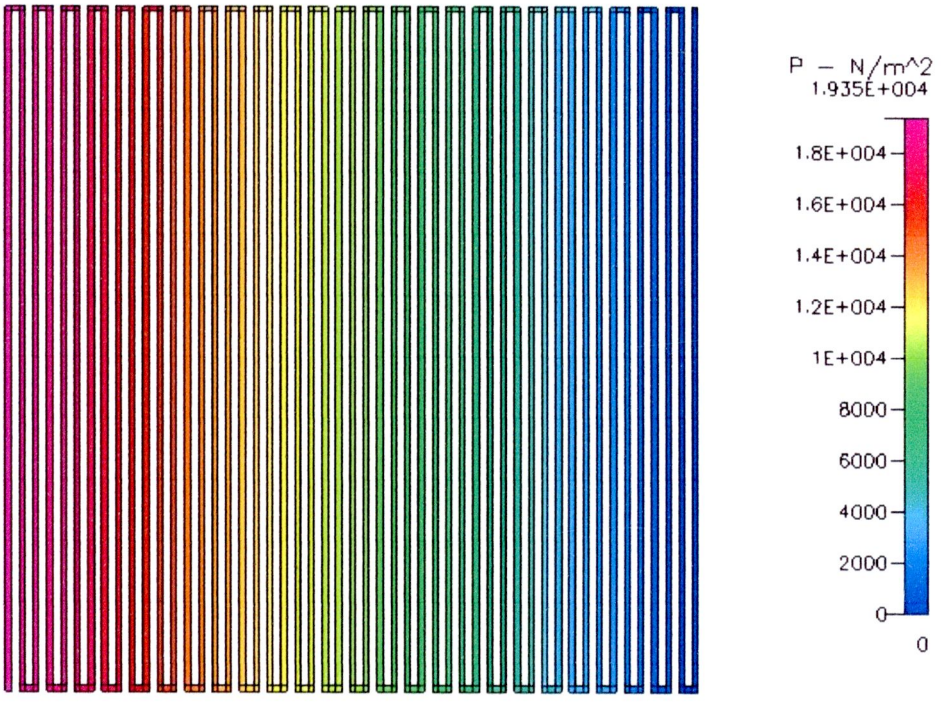

Figure 5.41 Pressure distribution at 300 cm^3/min of 0.8 mm. width

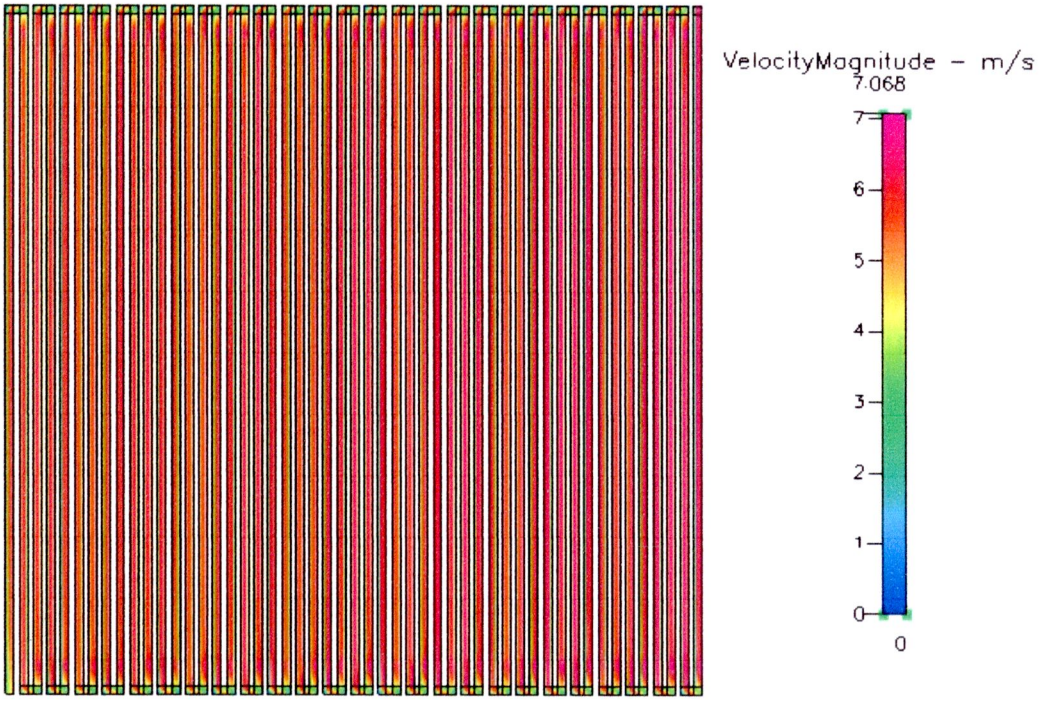

Figure 5.42 Velocity distribution at 300 cm^3/min of 1.2 mm. width

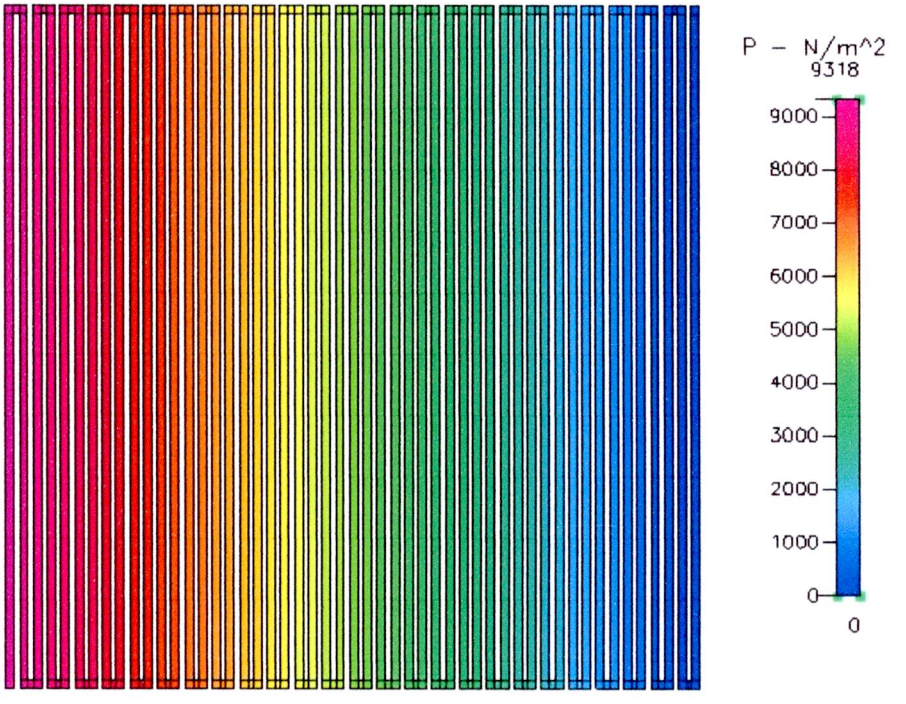

Figure 5.43 Pressure distribution at 300 cm^3/min of 1.2 mm. width

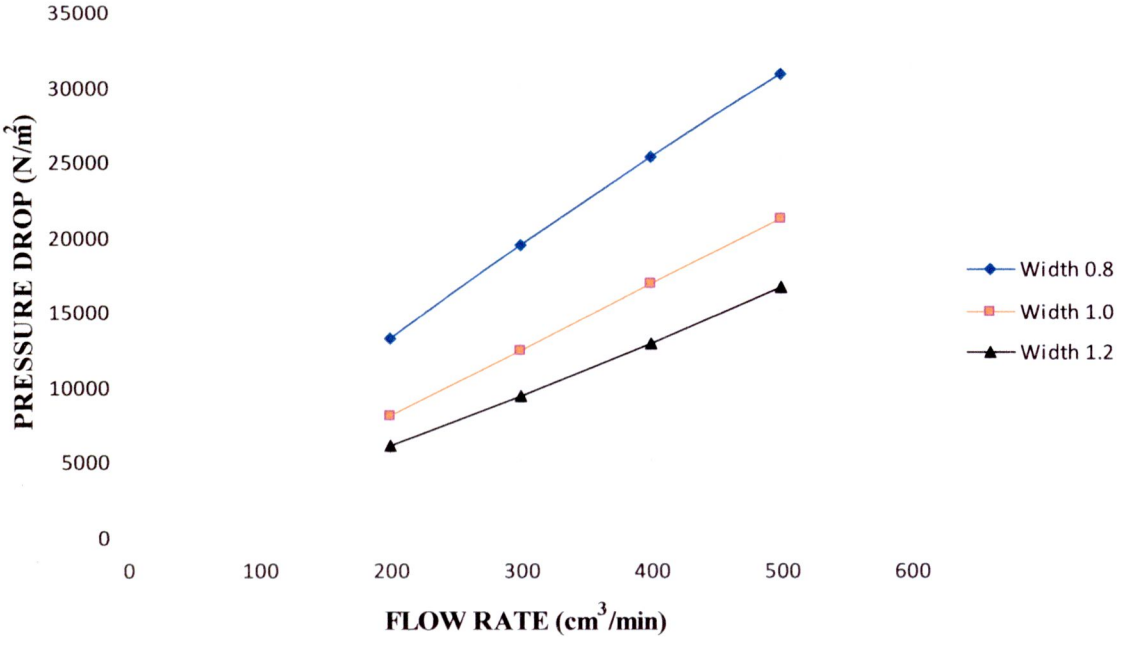

Figure 5.44 Pressure drop and flow rate in different channel width

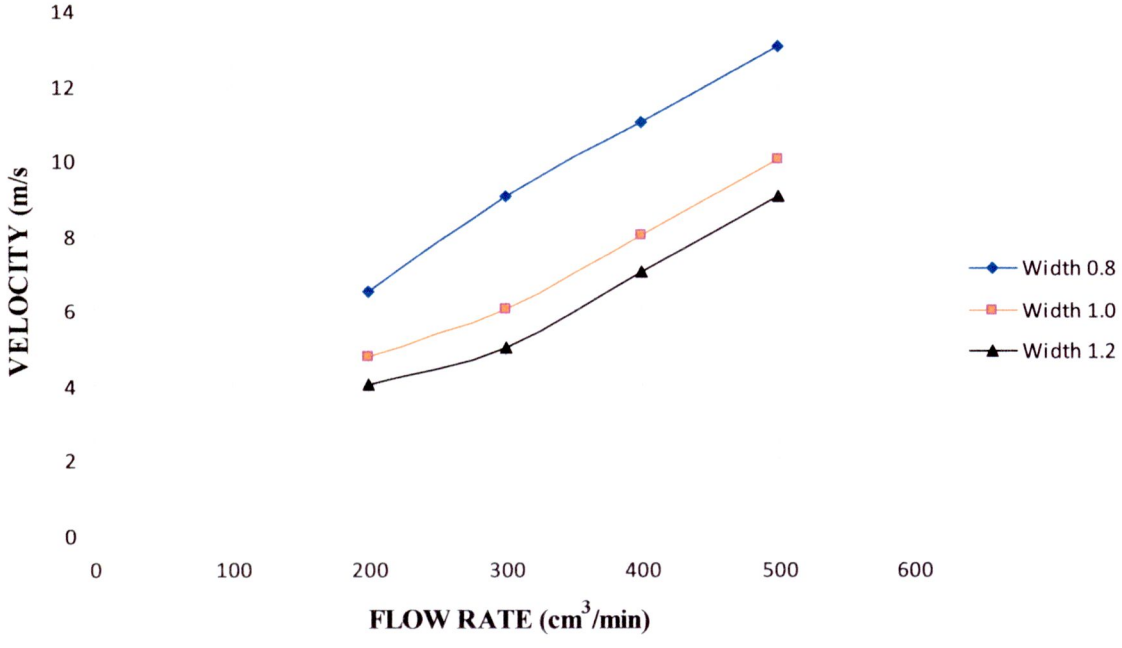

Figure 5.45 Velocity at depth 0.5 mm and flow rate in different channel width

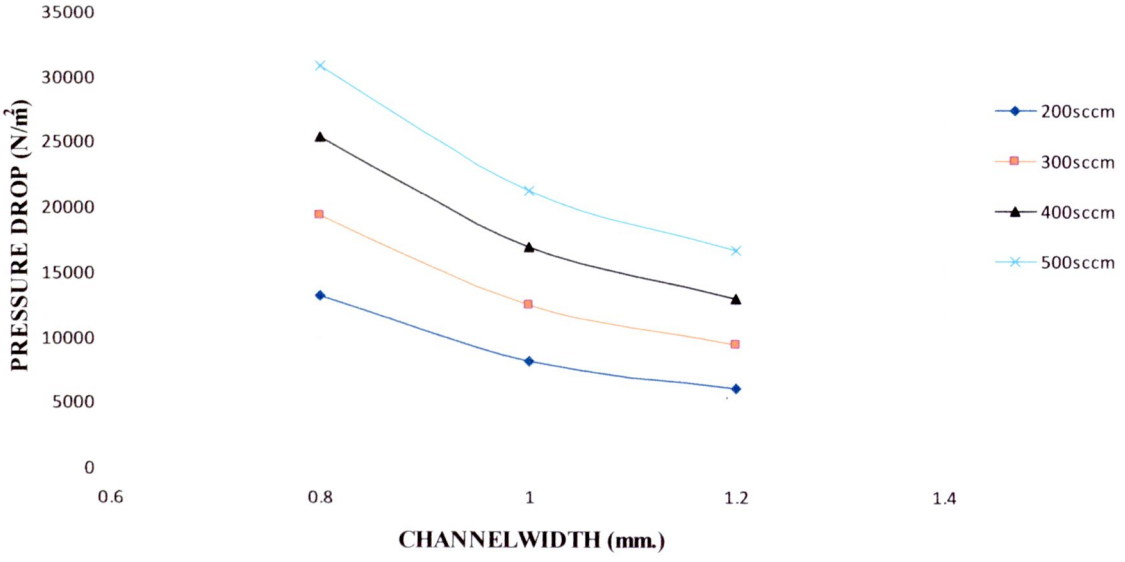

Figure 5.46 Channel width and pressure drop

This figure 5.40-5.43 shows 0.8 and 1.2 width serpentine flow field that pressure drop increase by decrease of width channel. The pressure drop decreased as the cross section area increase because there is low velocity. The velocities and pressure drop distribution in 0.8, 1 and 1.2 width at 300 cm^3/min was 0.8 mm. has velocity about 9 m/s and pressure drop is 1.935×10^4 N/m^2. Gas distribution has uniform in single serpentine pattern. Lower velocities distribution appears at channel curvatures and high velocities distribution at straight channel. The pressure drop has decreases along with length channel. In 1 and 1.2 depth channels have velocity same about 6 m/s, and pressure drop is 1.24×10^4 and 9410 N/m^2, respectively. When vary flow rate between 200-500 cm^3/min then 0.8 width channel has a highest pressure drop and velocity, 1 and 1.2 width channels has lower than pressure and velocity, respectively are show in figures 5.44-5.45. Channel width and pressure drop show in figure 5.46 which describe to trend pressure drop line and channel width from each flow rate.

The 0.8 mm channel width, the rib space area is dependant on the contact resistance and the pressure drop along with the channel length which the contact resistance effect is more significant. Higher contact area (rib area) is reduces the contact resistance more so than little rib width. Moreover, the narrower channel width with the same number of channels results in easier water removal.

The result of effect channel width was show the velocity and pressure drop, which it is depend to changing cross section area of flow channels, it can affect its velocity and mass flow rate. The lower cross section area gives higher than velocity and pressure drop. Moreover, a larger rib area reduces the contact resistance and easier water removal. Therefore, the flow-field width of a PEMFC flow-field is one of the major variables for optimizing the performance of fuel cell.

The results of effect channel length, channel width and channel depth were found pressure drop which this data is come form numerical modeling. It was shown in appendix B.

When it found pressure drop, it could transform data to ratio $\frac{L_e}{D}$ from minor loss in all cases. Example was show calculation of channel radius which it set $\frac{R}{D_H}$ equal 1.5, channel width and depth was 1 mm. and flow rate is 300 cm^3/min.

From equation :

$$\frac{\Delta P}{\rho g} = \text{Minors Loss} = f_t \frac{Le}{D} \cdot \frac{v^2}{2g} \tag{5.3}$$

$$\frac{L_e}{D} = \frac{1}{f_t} \cdot \frac{\Delta P}{\rho} \cdot \frac{2}{v^2} \tag{5.4}$$

When $f_t = \frac{64}{R_e}$ for laminar flow

ΔP = pressure drop from numerical modeling. In this case equal 1.24×10^4 N/m^2

v = velocity in cross-section. In this case equal 5 m/s and R_e equal

Replace all parameters in equation 5.4, it found

$$\frac{L_e}{D} = \frac{1}{f_t} \cdot \frac{\Delta P}{\rho} \cdot \frac{2}{v^2} = \frac{1}{1.29} \cdot \frac{2551.85}{0.089} \cdot \frac{2}{3.33^2}$$

$$= 1772.118$$

Calculation from same method in example again was found $\frac{L_e}{D}$ of all cases which shown in appendix E. For results in this part could do easy in used, therefore it makes to graph in figure 5.47. This model was validated in appendix E for testing can be real using.

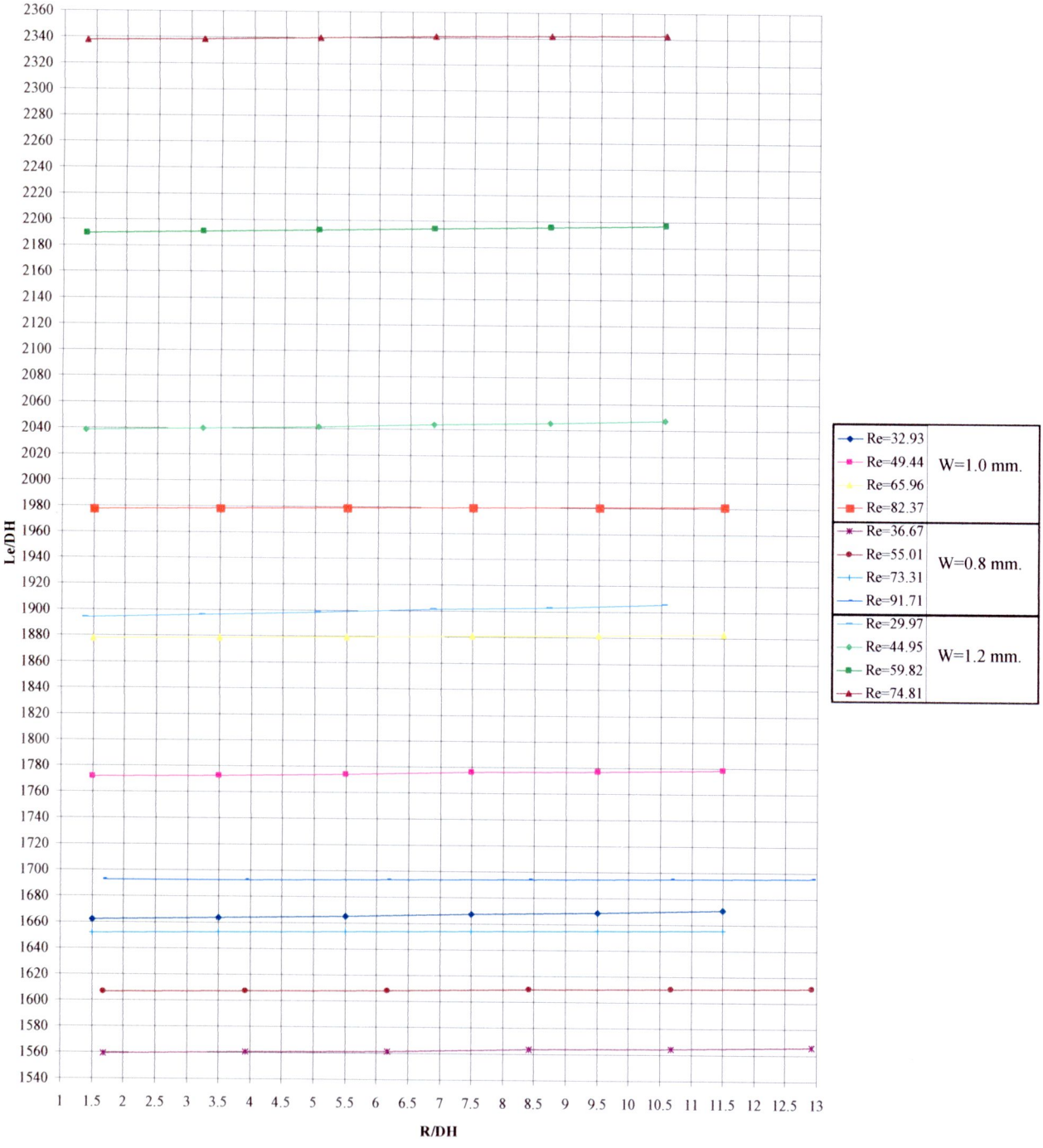

Figure 5.47 Graph of relationship between $\frac{L_e}{D}$, $\frac{R}{D_H}$ and Reynolds Numbers in 6 serpentine channels and 1 mm. channel depth

5.1.4 Effect of Manifold Inlet-Outlet on Flow Field

a) Straight Manifold

For a multi serpentine pattern of PEMFC flow field should be supplied through flow dividing manifold so as to distribute evenly the gas flow. As the number of cells increases, however, flow distribution between then is generally not uniform. Channel with the lowest flow supply determines the low performance. Therefore, manifold has important for gas distribution into flow field.

Effect of manifold inlet-outlet will focus on the 5 different manifolds on 6 different channels. There are 2-channels serpentine, 3-channels serpentine, 4-channels serpentine, 5-channels serpentine and 6-channels serpentine with inlet and outlet manifold at top and bottom flow field, respectively that it is changing length is 5-7 mm. and width 3-11 mm. which it depend by number of channel. The solutions from the model will be shown and analyzed for these different manifold configurations and compare flow field without manifold. The results of flow and pressure drop are effect of straight manifold show in figures 5.48-5.65.

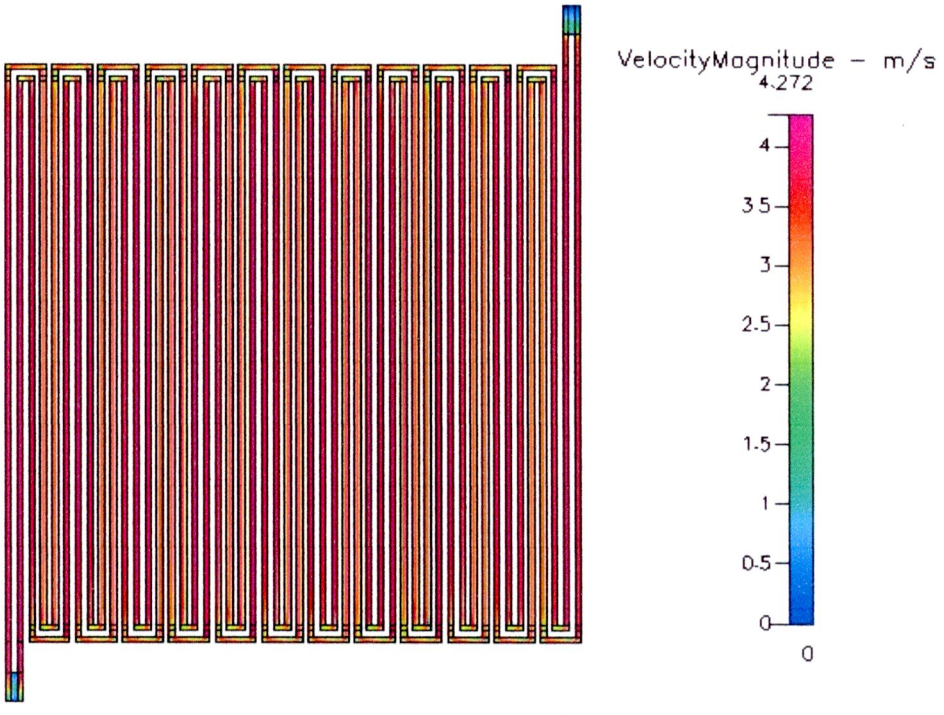

Figure 5.48 Velocity distribution at 300 cm^3/min of manifold 2 channels

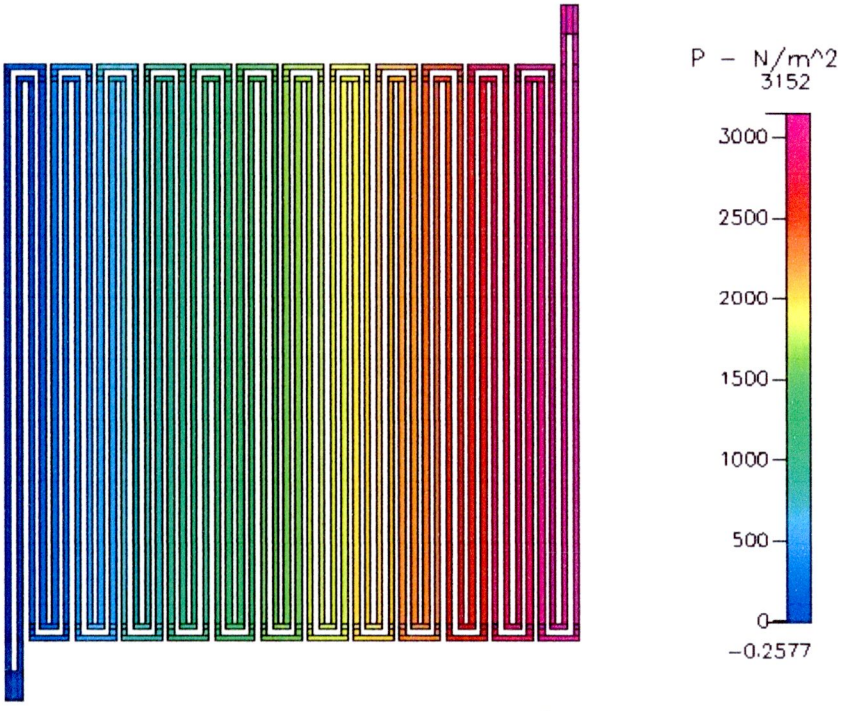

Figure 5.49 Pressure distribution at 300 cm^3/min of manifold 2 channels

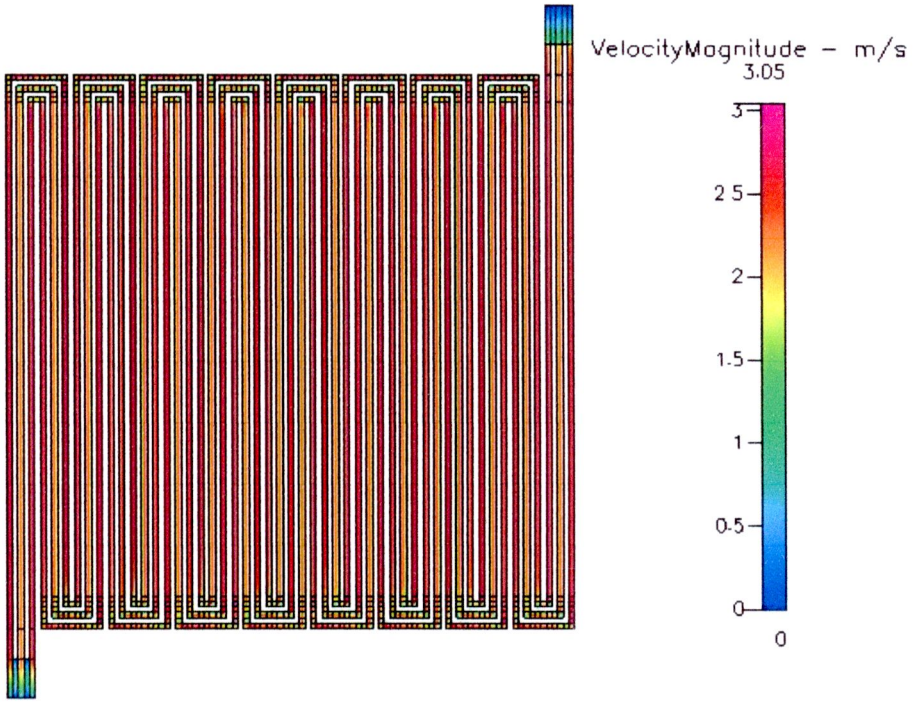

Figure 5.50 Velocity distribution at 300 cm^3/min of manifold 3 channels

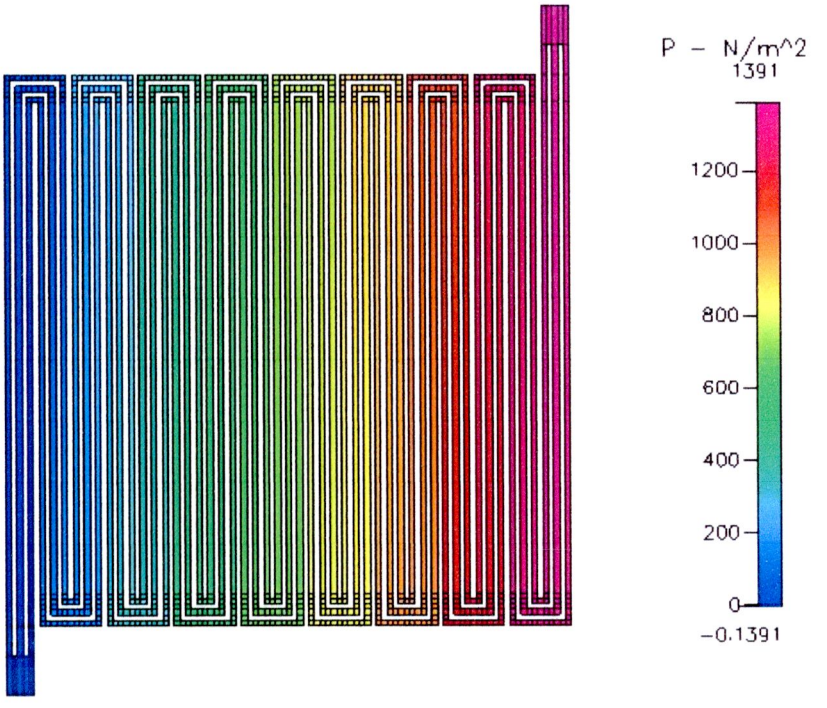

Figure 5.51 Pressure distribution at 300 cm^3/min of manifold 3 channels

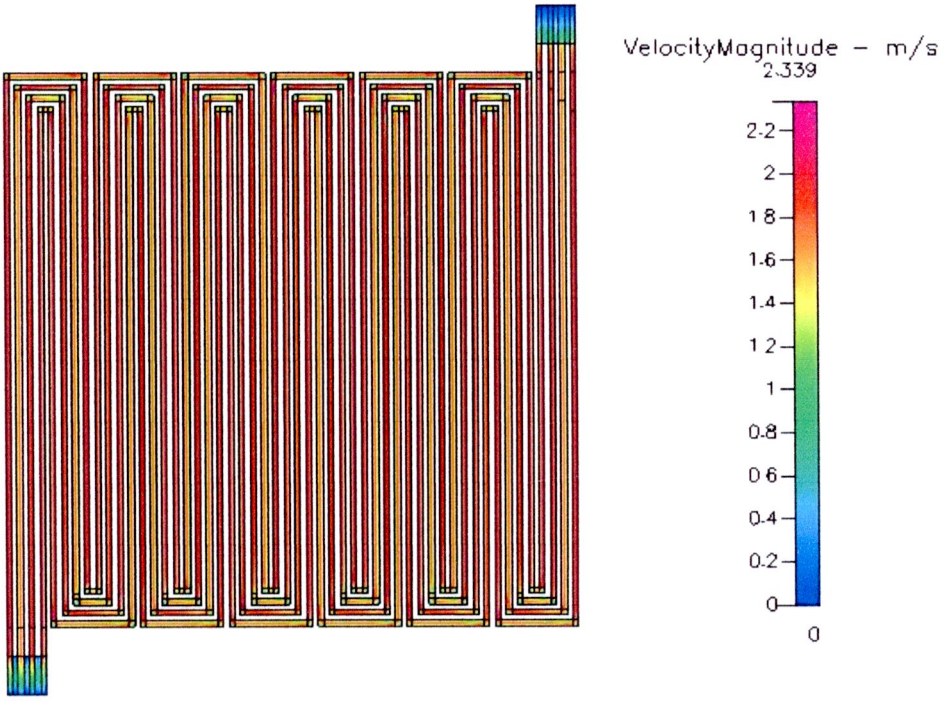

Figure 5.52 Velocity distribution at 300 cm^3/min of manifold 4 channels

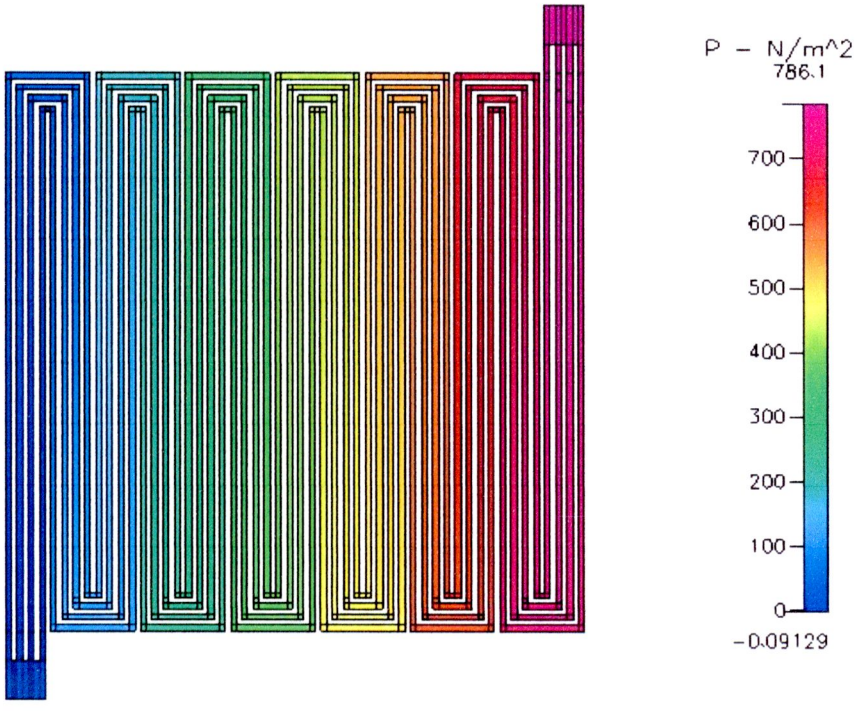

Figure 5.53 Pressure distribution at 300 cm^3/min of manifold 4 channels

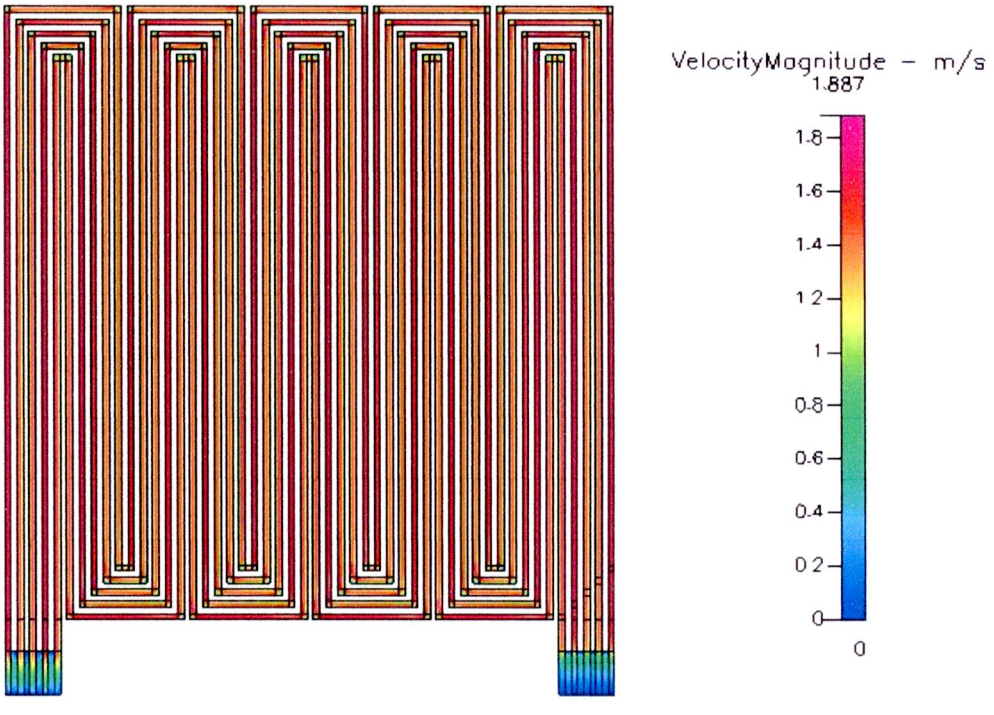

Figure 5.54 Velocity distribution at 300 cm^3/min of manifold 5 channels

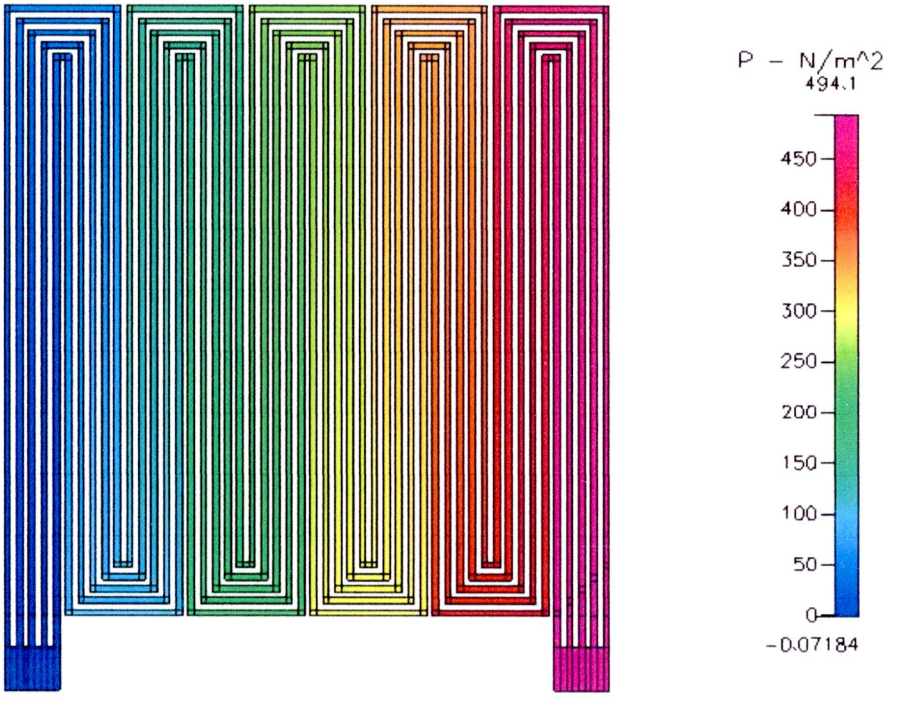

Figure 5.55 Pressure distribution at 300 cm^3/min of manifold 5 channels

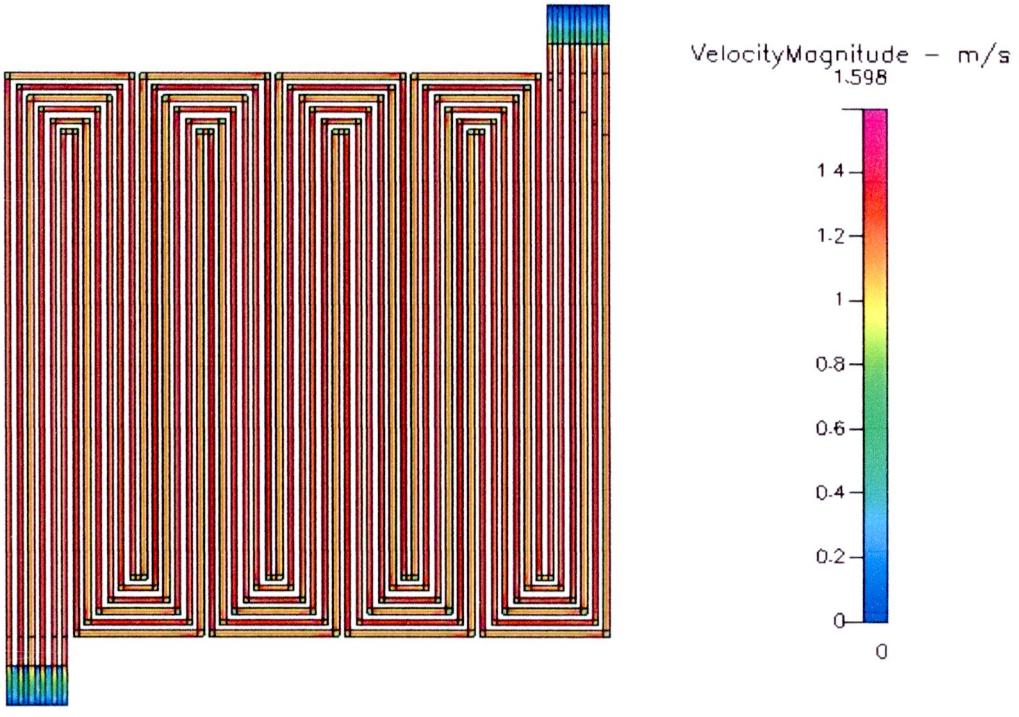

Figure 5.56 Velocity distribution at 300 cm^3/min of manifold 6 channels

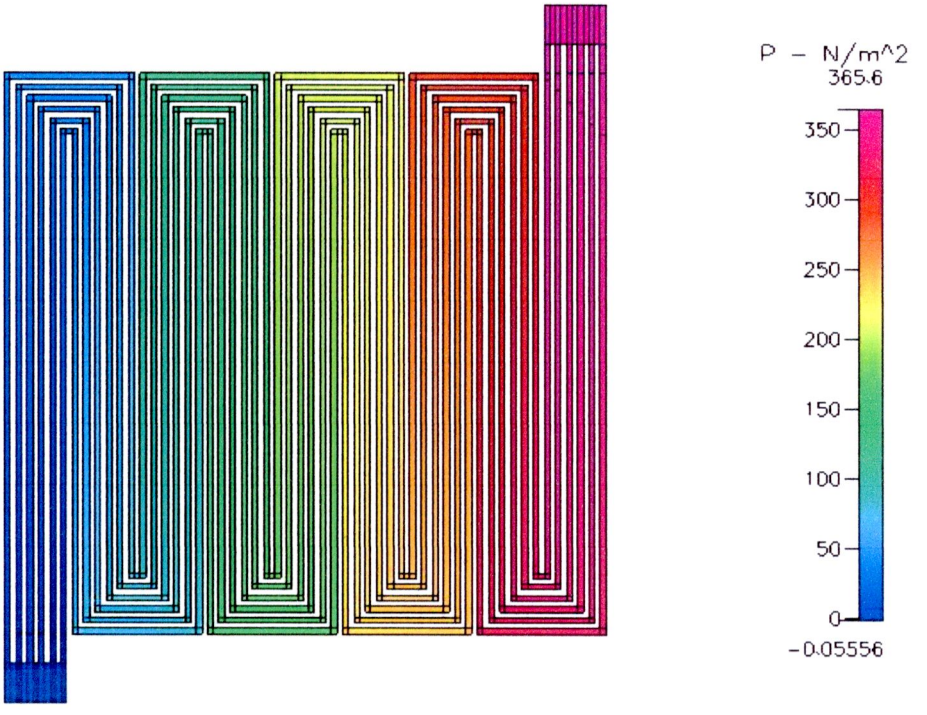

Figure 5.57 Pressure distribution at 300 cm^3/min of manifold 6 channels

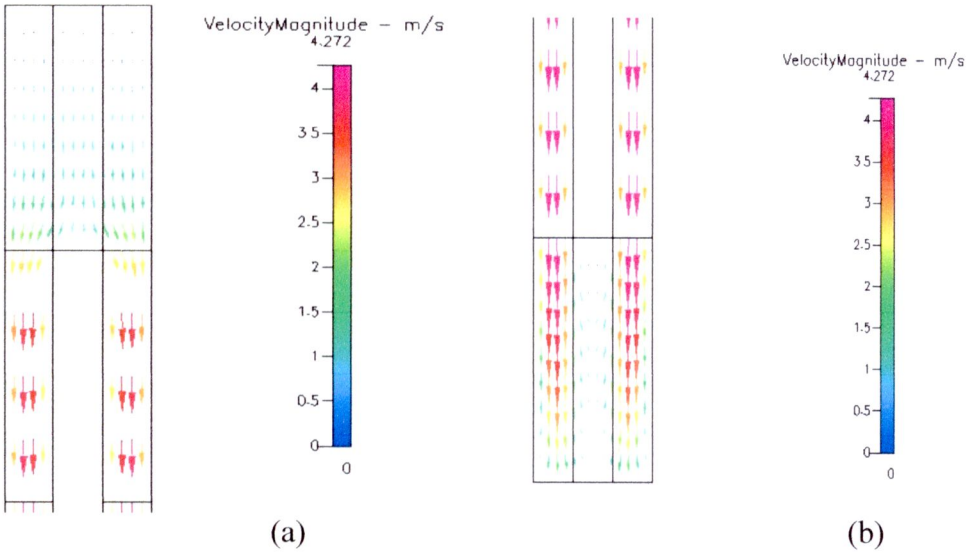

(a) (b)

Figure 5.58 Characteristic of flow at 300 cm^3/min in manifold 2 channels
(a) inlet (b) outlet

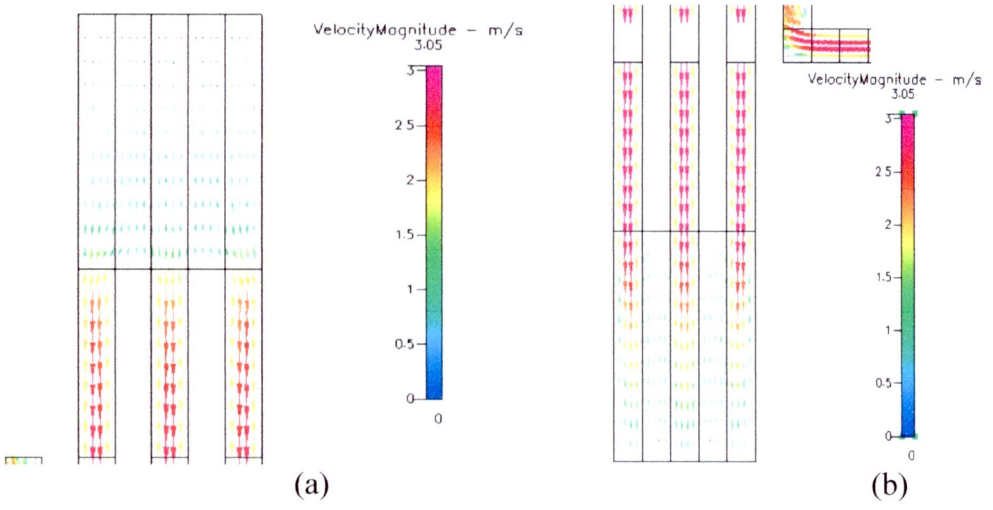

Figure 5.59 Characteristic of flow at 300 cm^3/min in manifold 3 channels (a) inlet (b) outlet

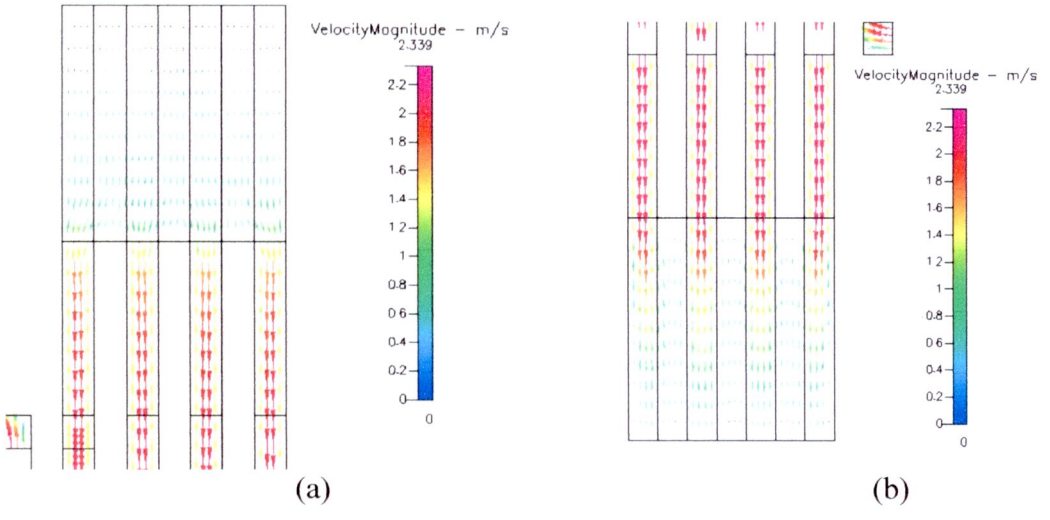

Figure 5.60 Characteristic of flow at 300 cm^3/min in manifold 4 channels (a) inlet (b) outlet

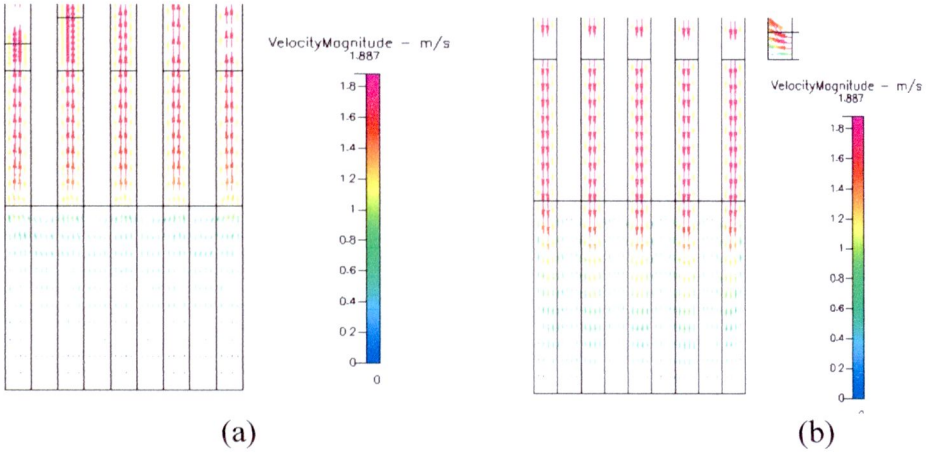

(a) (b)

Figure 5.61 Characteristic of flow at 300 cm^3/min in manifold 5 channels
(a) inlet (b) outlet

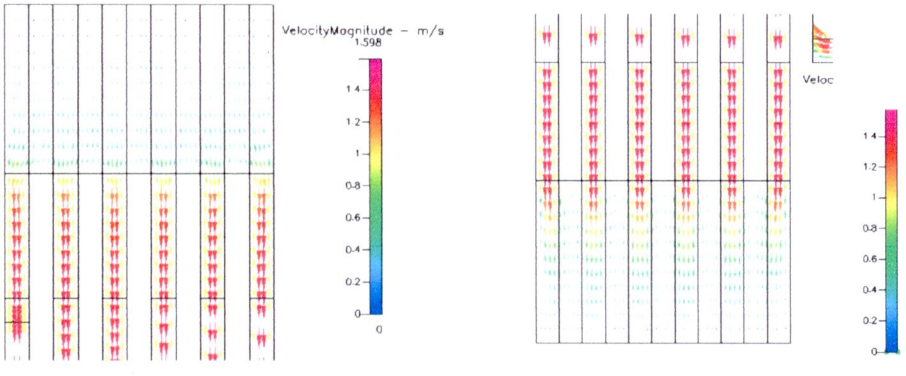

(a) (b)

Figure 5.62 Characteristic of flow at 300 cm^3/min in manifold 6 channels
(a) inlet (b) outlet

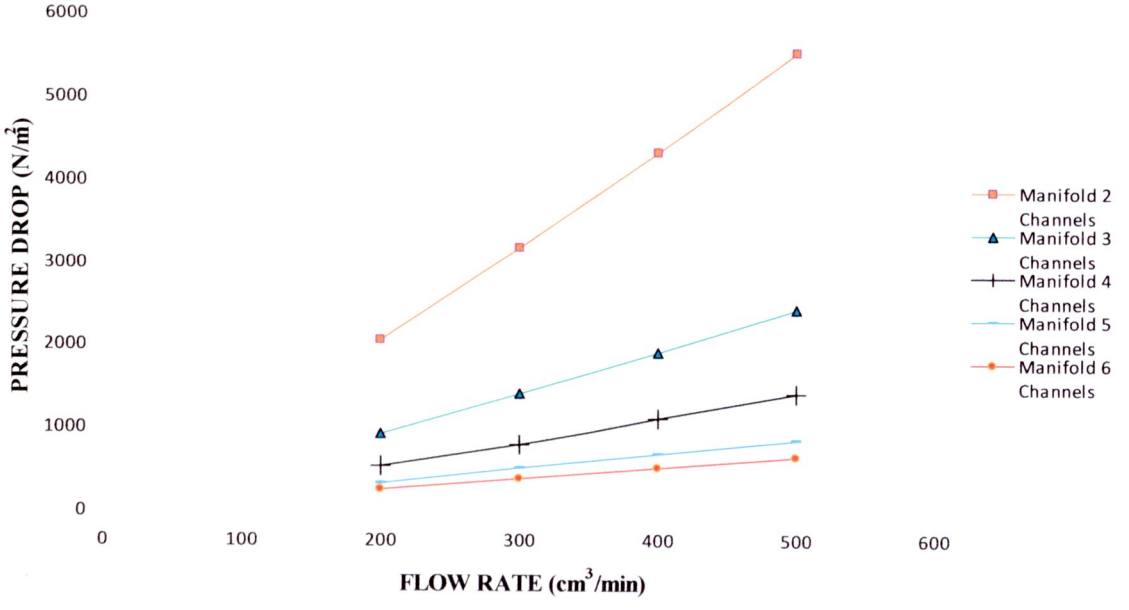

Figure 5.63 Pressure drop and flow rate in different manifold pattern

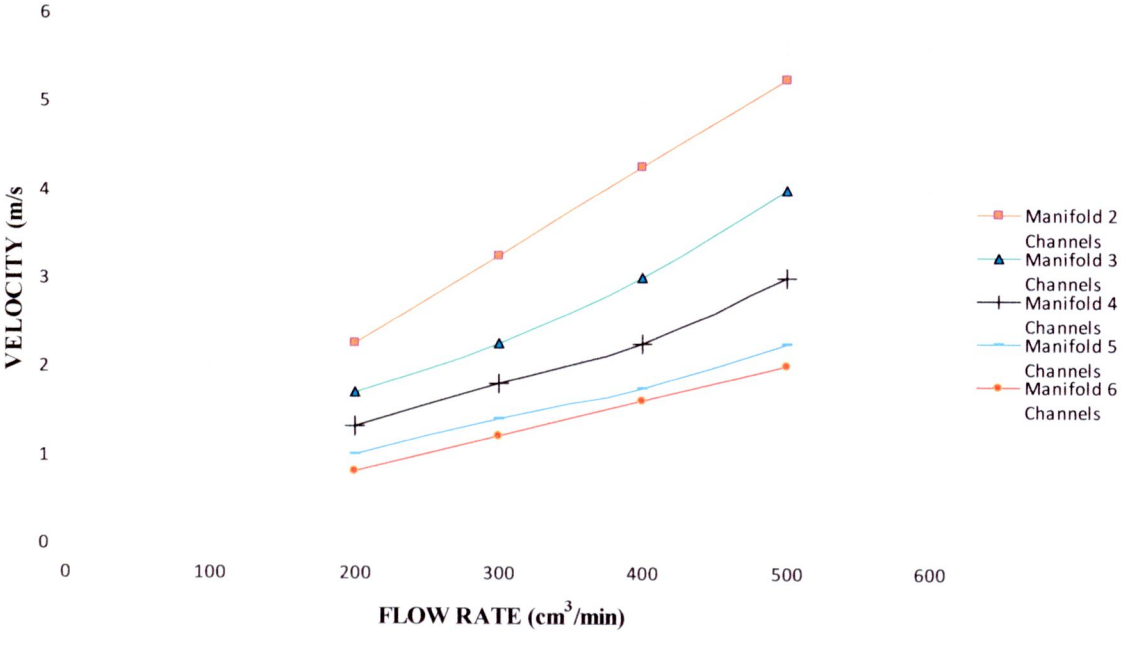

Figure 5.64 Velocity at depth 0.5 mm. and flow rate in different manifold pattern

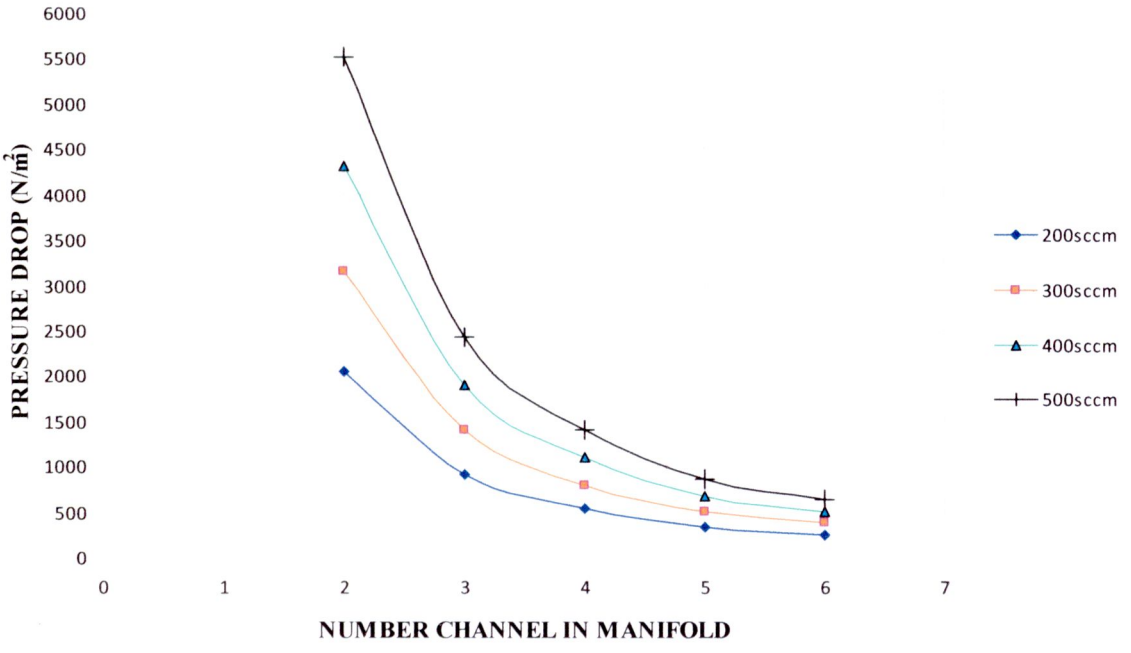

Figure 5.65 Number channels in manifold and pressure drop

In figure 5.48-5.57 shows straight manifold inlet and outlet in 2 to 6 channels which velocity in 2 to 6 channels manifolds at 300 cm^3/min have about 3.25, 2.25, 1.8, 1.4 and 1.2 m/s, and pressure drop is 3,152, 1,391, 786.1, 494.1 and 365.6 N/m^2, respectively. When its compare with flow field without manifold that its have nearby velocity and pressure drop all change channel, it found good gas distribution. Figures 5.58-5.62 are shown the flow separation in each channel. Inlet manifold in 2 to 6 channels manifolds are low velocity in upper manifold and improve velocity along with length manifold. In taking each channel is separate gas flow equilibrium in all channels and improves velocity along with straight channel. Outlet manifold in 2 to 6 channels manifolds are high velocity in upper manifold and decrease along with length outlet manifold. In figures 5.63-5.64 show vary flow rate between 200-500 cm^3/min then 2 channels manifold has a highest pressure and highest velocity, 3 to 6 channels manifolds have lower pressure and velocity, respectively. Figure 5.65 shown number channel in manifold and pressure drop are describe to trend pressure drop line and type manifold from each flow rate.

The result of effect manifold flow-field was shown the velocity, pressure drop and gas distribution in modeling. It is concluded that changing flow-field configuration by varying sizing of manifold can affect its gas distribution go to channel. The manifold gives show velocity distribution in take and out of channel and pressure drop. Therefore, the manifold flow-field is one of the major variables for optimizing the performance of PEMFC.

b) Curve Manifold

The effect of curve manifold configuration on the flow distribution through the 6 channels is presented in figures 5.67-5.82. The computational flow for

various manifold configurations with 45 turn and 90 turn and then passes through 6 channels. There is 4 manifolds in this studied which type 1 inlet and outlet manifold with non-fillet curve and 90 turn and type 2 with inside fillet curve and 90 turn and type 3 with fillet curve and 90 turn and type 4 with fillet curve and 45 turn. Configuration of manifolds curve was shown in figure 5.66.

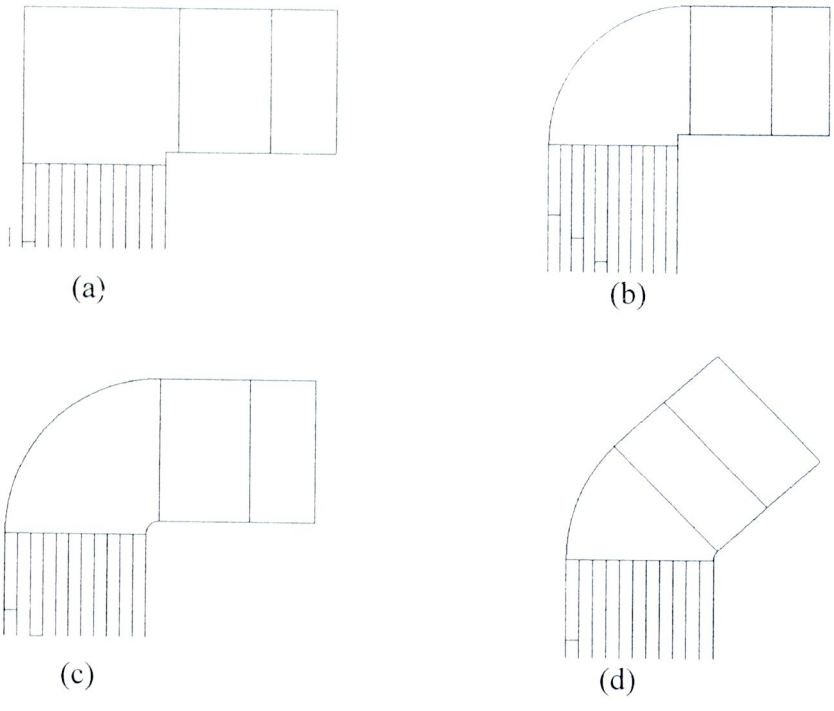

Figure 5.66 Manifolds curvatures (a) 90 turn non-fillet manifold (Type 1) (b) 90 turn outside fillet manifold (Type 2) (c) 90 turn fillet manifold (Type 3) (d) 45 turn manifold (Type 4)

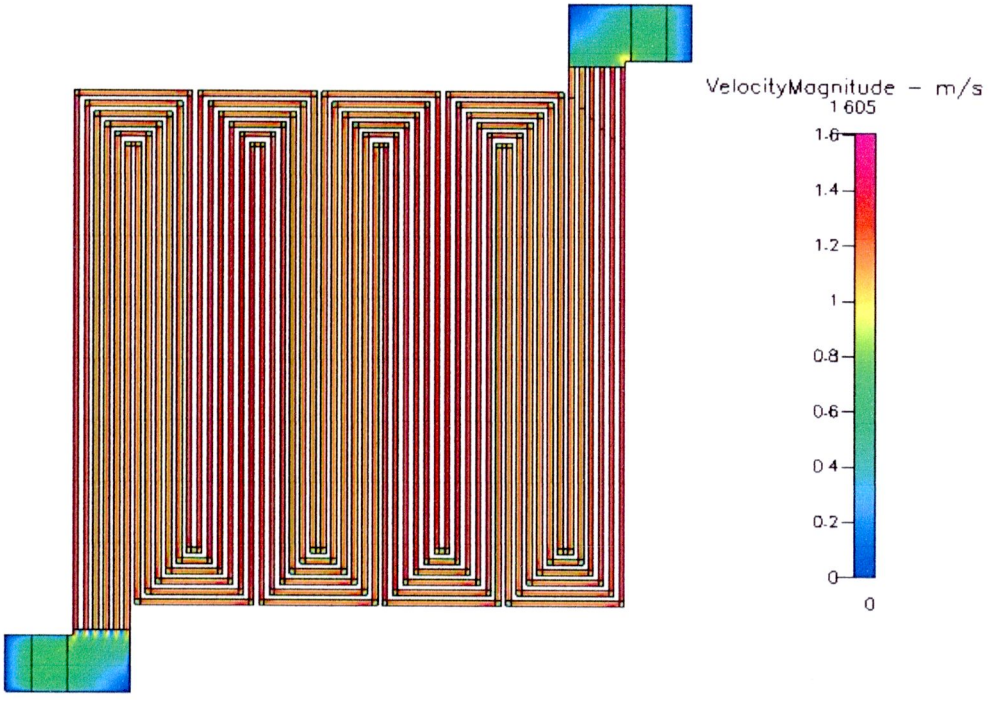

Figure 5.67 Velocity distribution at 300 cm^3/min of type 1 manifold

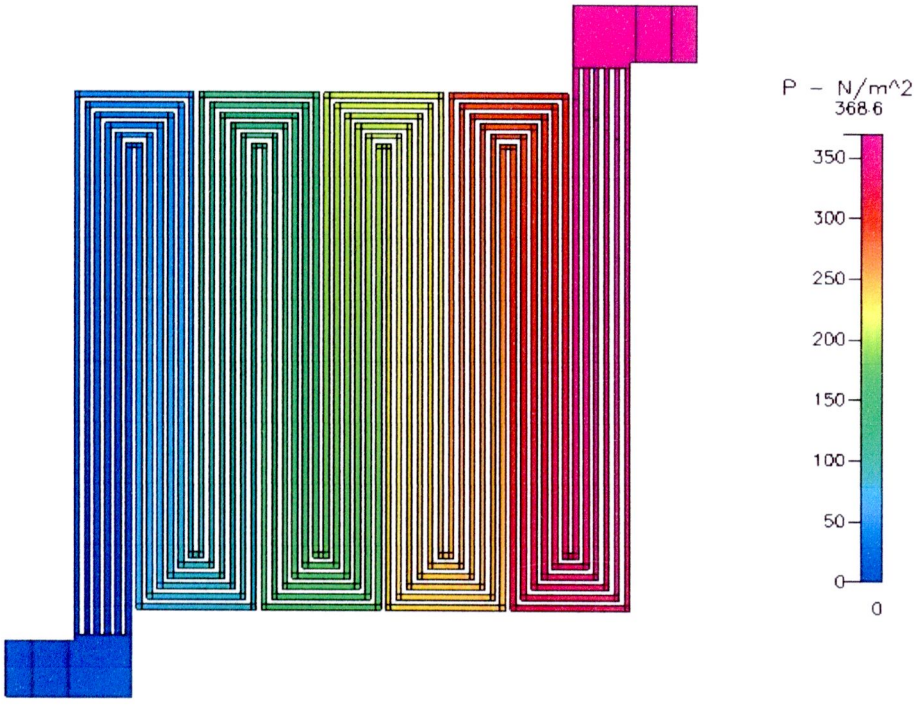

Figure 5.68 Pressure distribution at 300 cm^3/min of type 1 manifold

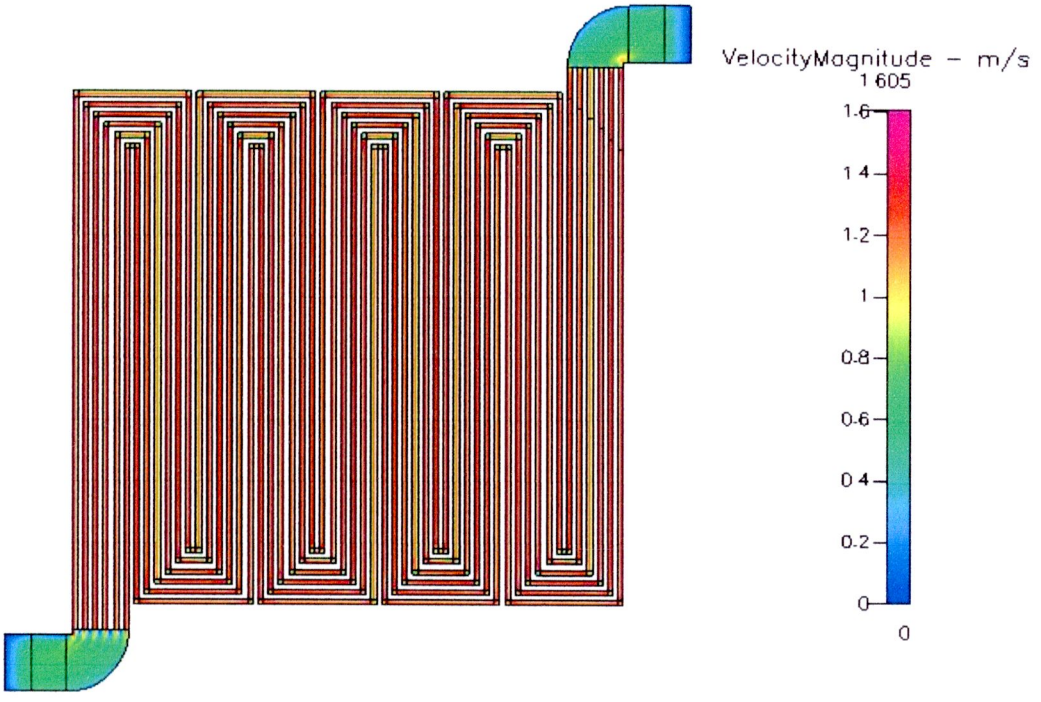

Figure 5.69 Velocity distribution at 300 cm^3/min of type 2 manifold

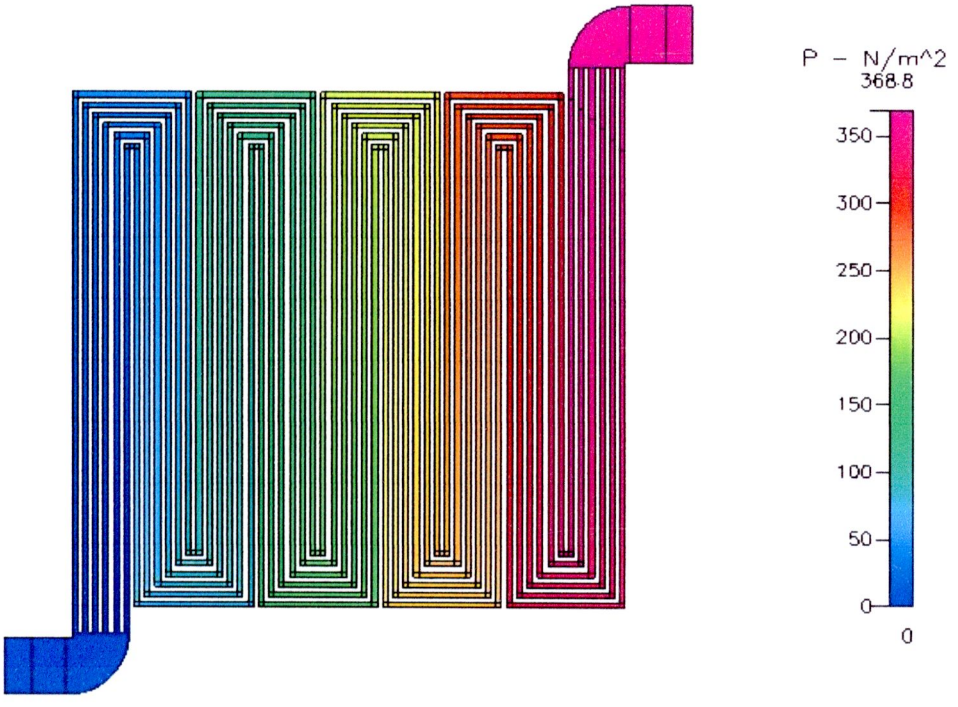

Figure 5.70 Pressure distribution at 300 cm^3/min of type 2 manifold

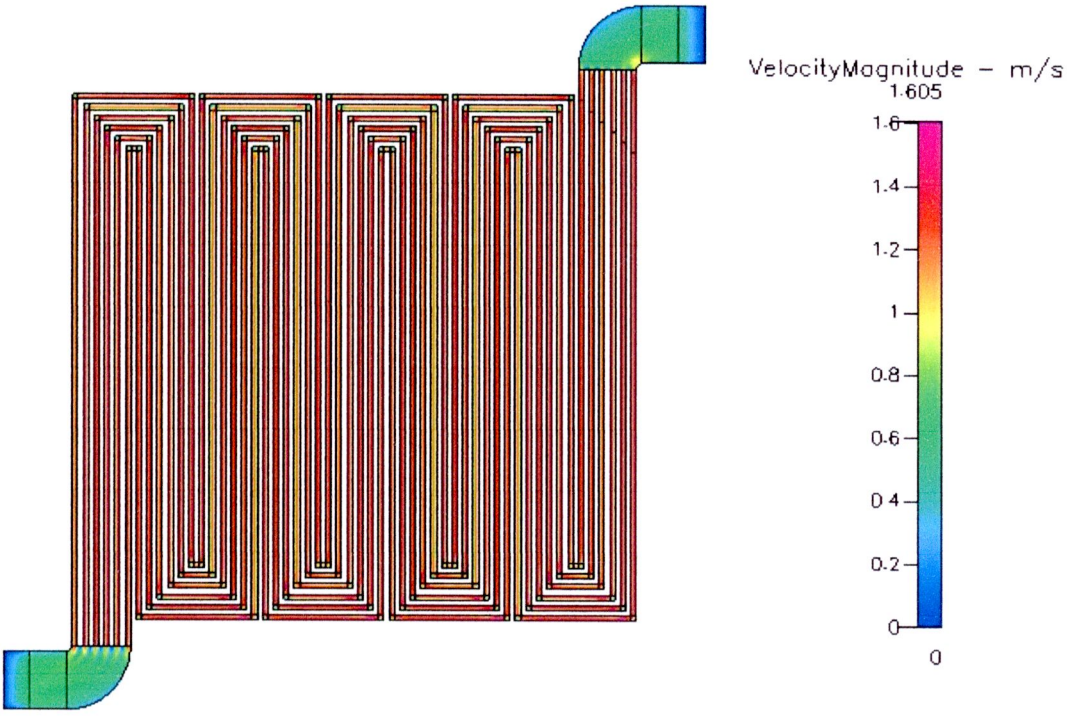

Figure 5.71 Velocity distribution at 300 cm^3/min of type 3 manifold

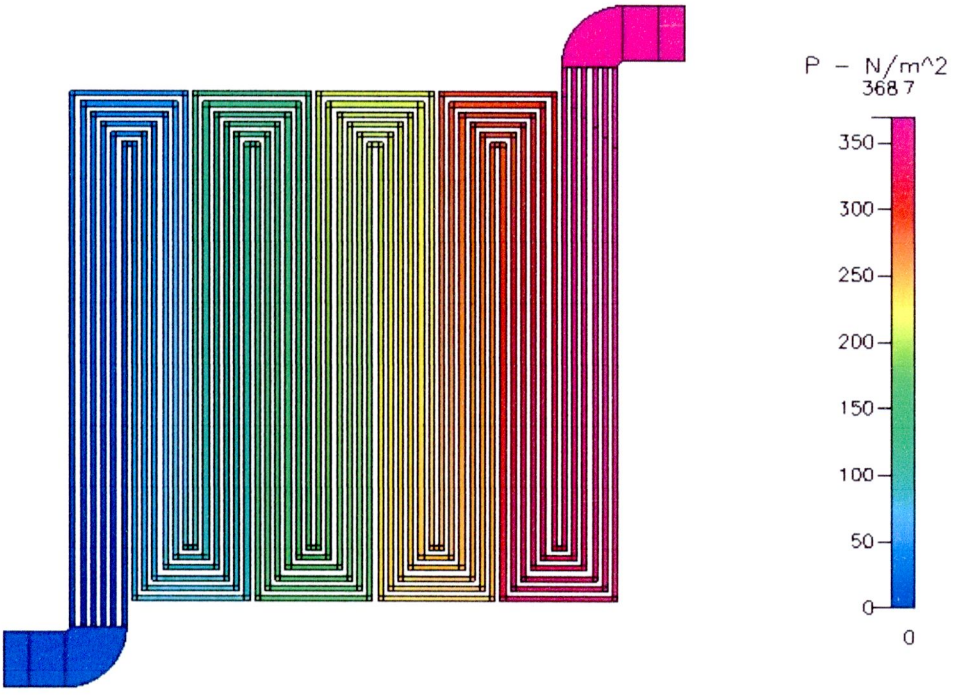

Figure 5.72 Pressure distribution at 300 cm^3/min of type 3 manifold

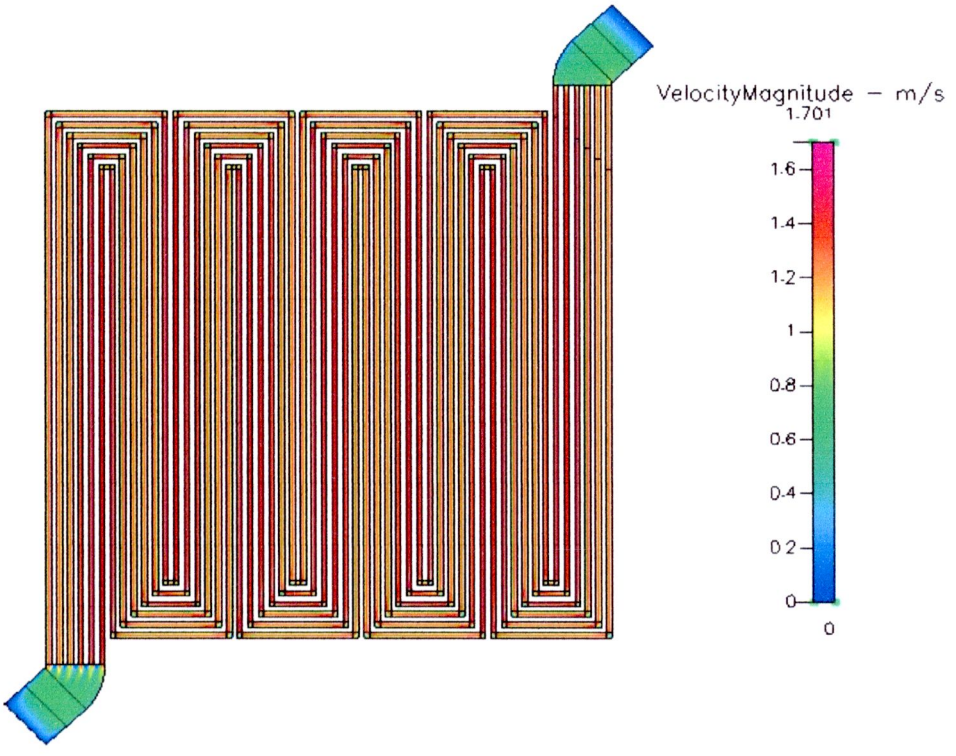

Figure 5.73 velocity distribution at 300 cm^3/min of type 4 manifold

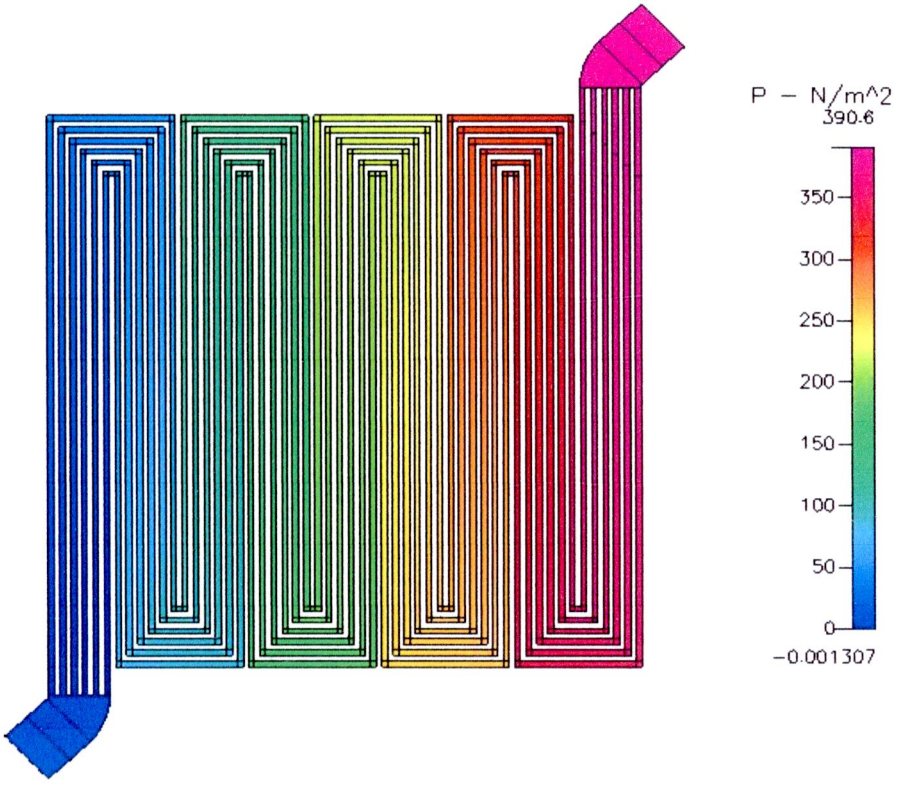

Figure 5.74 Pressure distribution at 300 cm^3/min of type 4 manifold

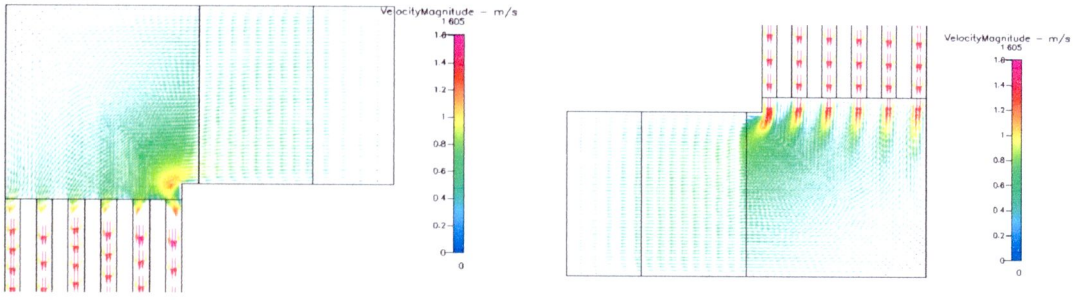

Figure 5.75 Characteristic of flow at 300 cm^3/min in type 1 manifold
(a) inlet (b) outlet

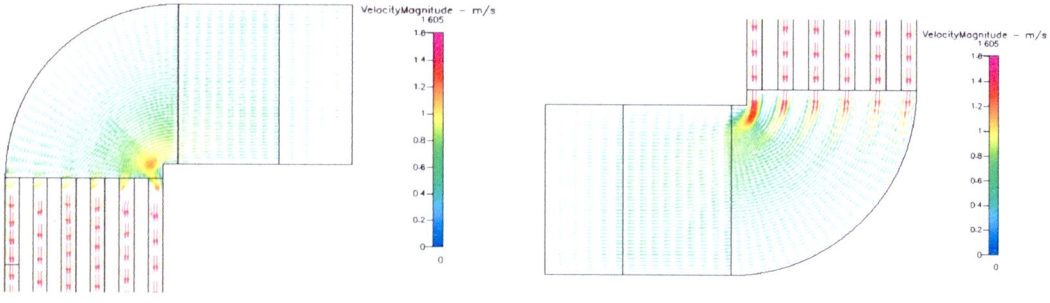

Figure 5.76 Characteristic of flow at 300 cm^3/min in type 2 manifold
(a) inlet (b) outlet

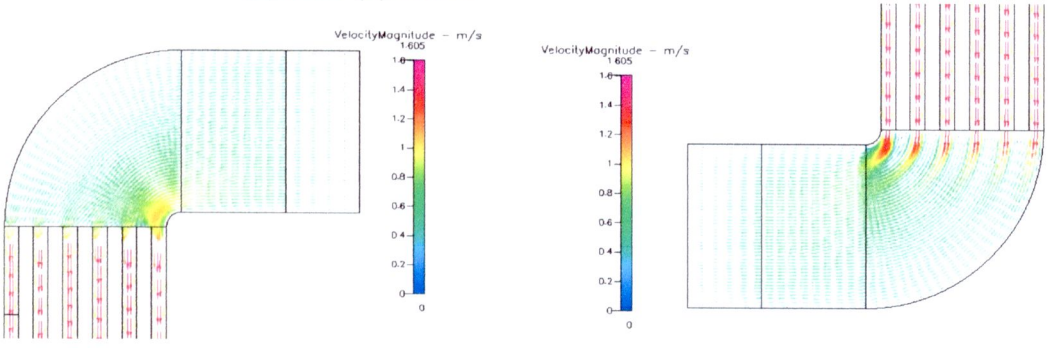

Figure 5.77 Characteristic of flow at 300 cm^3/min in type 3 manifold
(a) inlet (b) outlet

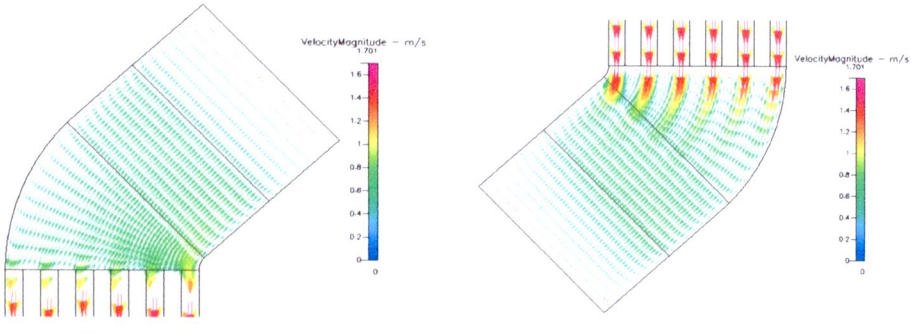

Figure 5.78 Characteristic of flow at 300 cm^3/min in type 4 channels
(a) inlet (b) outlet

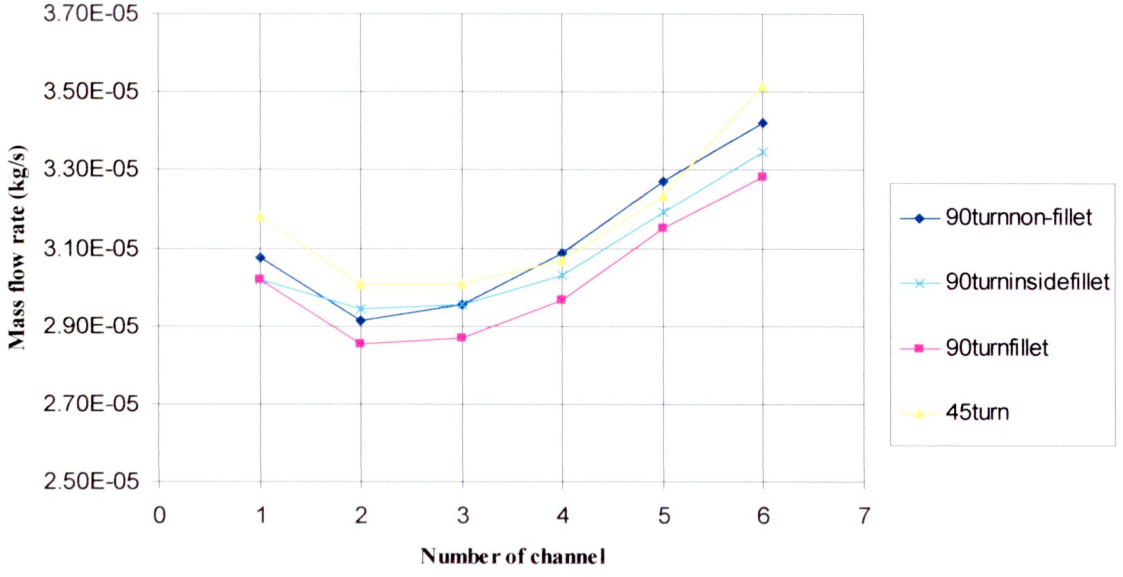

Figure 5.79 mass flow distribution for various inlet manifolds

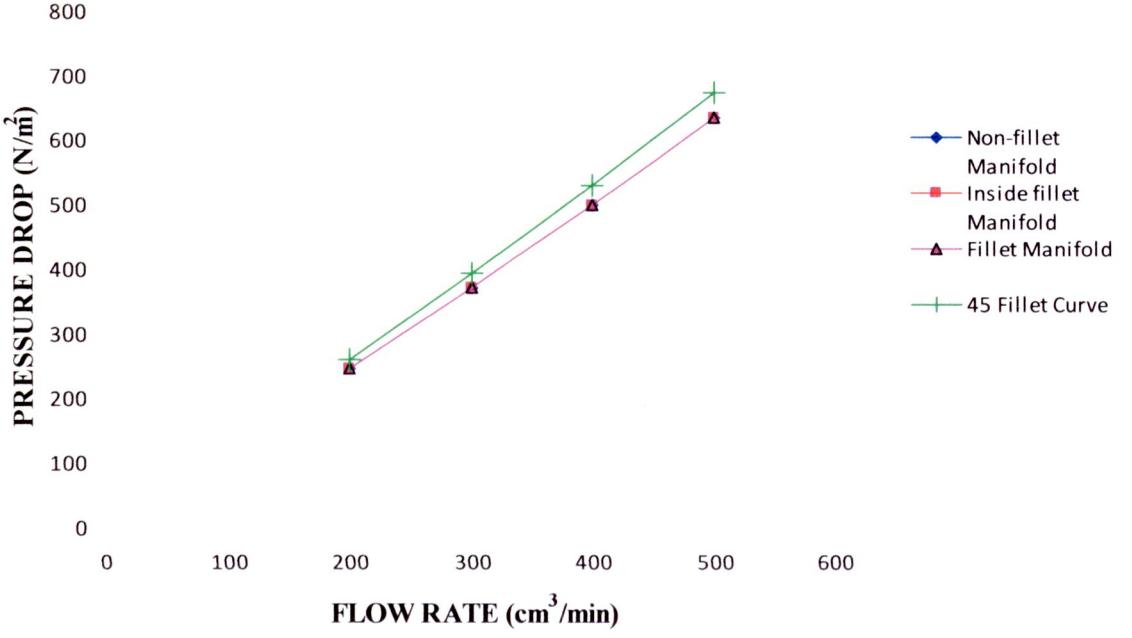

Figure 5.80 Pressure drop and flow rate in different manifold pattern

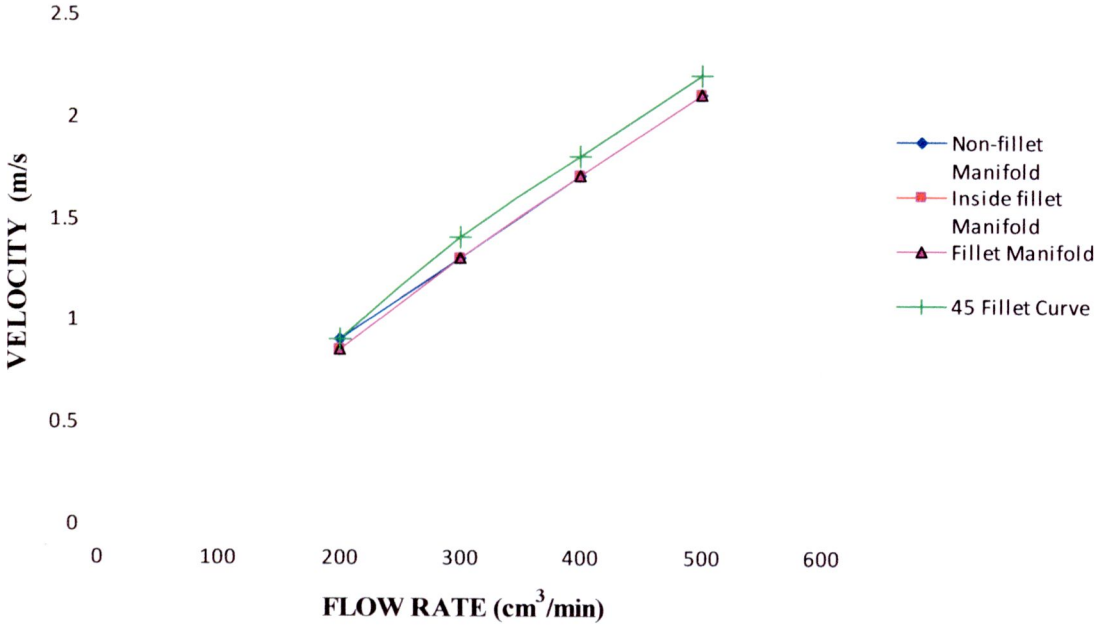

Figure 5.81 Velocity at depth 0.5 mm. and flow rate in different manifold pattern

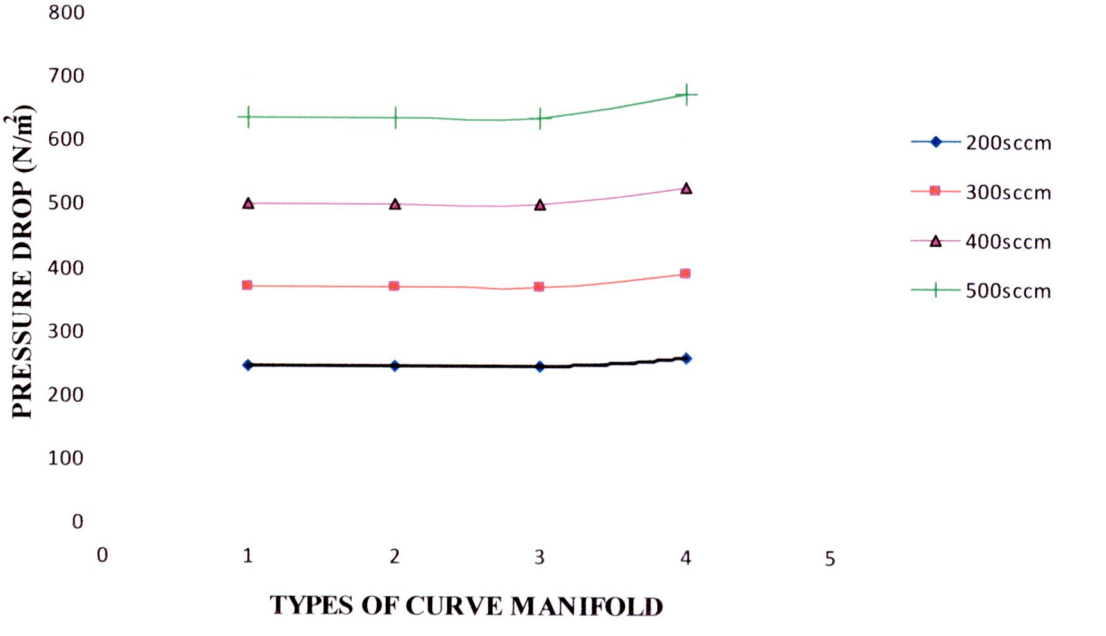

Figure 5.82 Type of curve manifold and pressure drop

In figure 5.67-5.74 shows curve manifold of inlet and outlet in 6 channels which mass flow rate in at 300 cm^3/min have velocity about 1.3 m/s in type 1-3

manifolds and 1.4 m/s in type 4 manifold and pressure drop is 368 in type 1-3 manifolds and 390.6 N/m^2 in type 4 manifold. Figures 5.75-5.79 are shown the flow separation in each channel. Inlet manifold in 6 channels serpentines are low velocity in upper manifold and improve velocity along with length manifold. In taking each channel is separate gas flow, for the Type 1 manifold with 90 turns non-fillet curve, a large flow separation occurs at the inner wall just behind the 90◦ turn inside the manifold. For the Type 2 inlet manifold with a 90 turn and fillet at the outer wall and a non-fillet turn at the inner wall, flow separation still occurs so that the pattern inside the manifold is little improved. When the inner wall is changed to fillet, as displayed in type 3 manifold, the flow separation totally disappears. The flow pattern is more improved for Type 4 manifold with a 45 turn and smooth flow separation more than others. As anticipated, the mass flow rate is the lowest at the second channel for all the manifolds. It is noticeable that type 1 manifold with a round turn only at the outer wall shows no improved flow distribution. This implies that the flow separation still found in the Type 4 manifold has a strong impact on the overall flow distribution. By contrast, the manifold types with a type 4 display a more uniform flow distribution along the cells and an increased mass flow rate at the second channel. Manifolds could be improved configurations provide substantially increased gas flow rates due to the suppression of flow separation at the inner wall. The increase in mass flow at the second channel is very favorable in terms of the overall cell performance because the cell with the lowest gas flow rate limits the overall current. In figures 5.80-5.81 show vary flow rate between 200-500 cm^3/min then type 4 manifold has high pressure drop and velocity at channel depth 0.5 mm.. Other types of manifolds have nearby pressure drop and velocity. Figure 5.82 shown number channel in manifold and pressure drop are describe to trend pressure drop line and type manifold from each flow rate.

The results of effect curve manifolds flow-field were shown the velocity, pressure drop and gas distribution go to each channel. It is concluded that changing flow-field configuration by varying curve and fillet of manifold can affect its gas distribution go to channel. The curve manifold gives show gas distribution in take and out of channel and pressure drop.

5.1.5 Design Flow Field Pattern

The results of all effects design flow field studied can be use to design a new flow field, which should be improve cell performance. The new flow field is concept in good gas distribution and pressure drop. In this study design flow fields is 2 ways multi-serpentine header flow field. Concepts of design are separate gas distribution to 2 ways for increase reaction area in shorter time and decrease channel lengths which depend on pressure drop are not over. Outlet is combines all channels for help pulse the water in storage at this area.

This first design flow field has 6 channels serpentine and divides 2 ways for gas distribution. Position of inlet is top and near center in polar plate and separate 2 ways turn right side and left side of flow field in 3 channels serpentine. All channel turn back to middle of flow filed. 3 channels combine to 6 channels in middle flow field at outlet. Outlet has larger than inlet because it helps for good water management. This configuration is shown in figure 5.83 and results show in figure 5.84- 5.88.

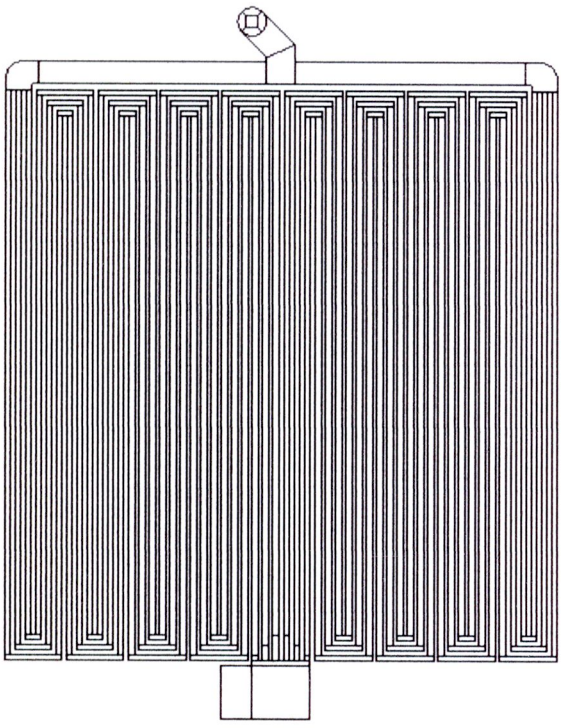

Figure. 5.83 2 ways multi-serpentine header flow field

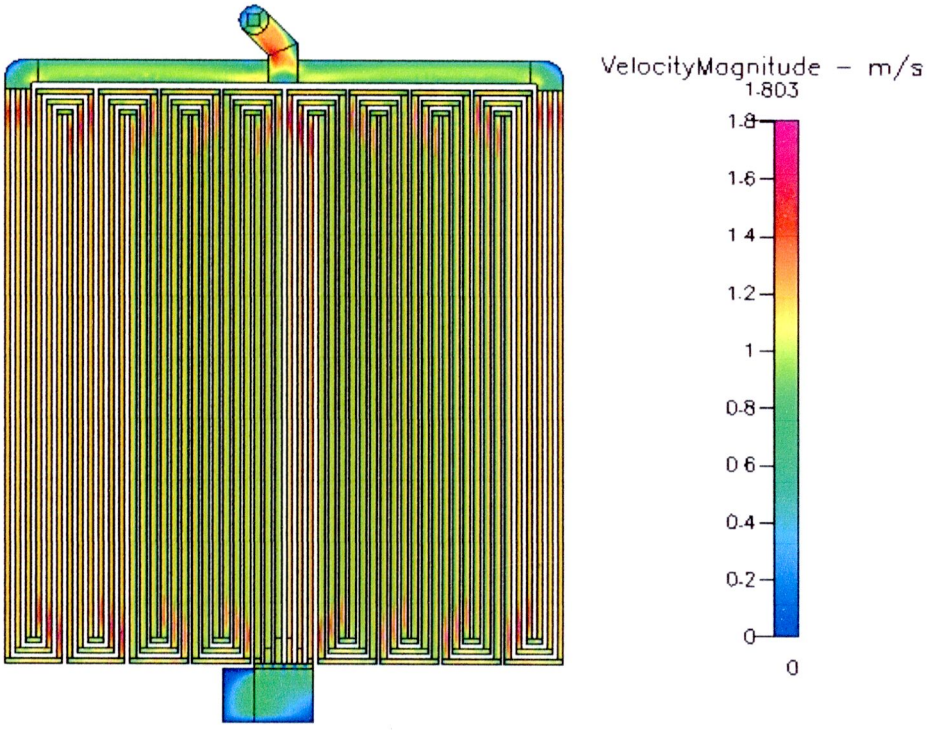

Figure 5.84 Velocity distributions at 300 cm^3/min of first design flow field

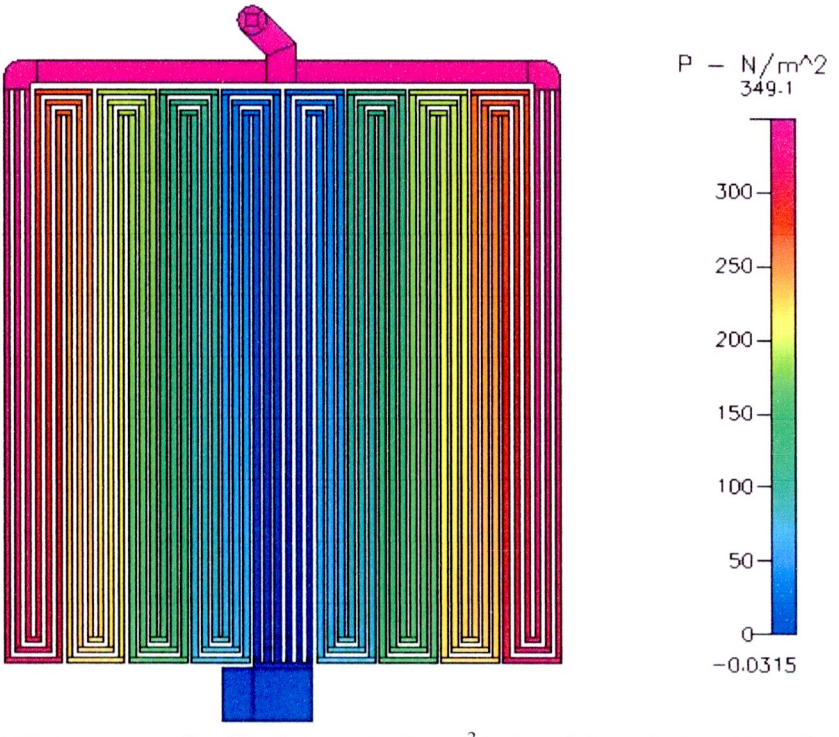

Figure 5.85 Pressure distributions at 300 cm^3/min of first design flow field

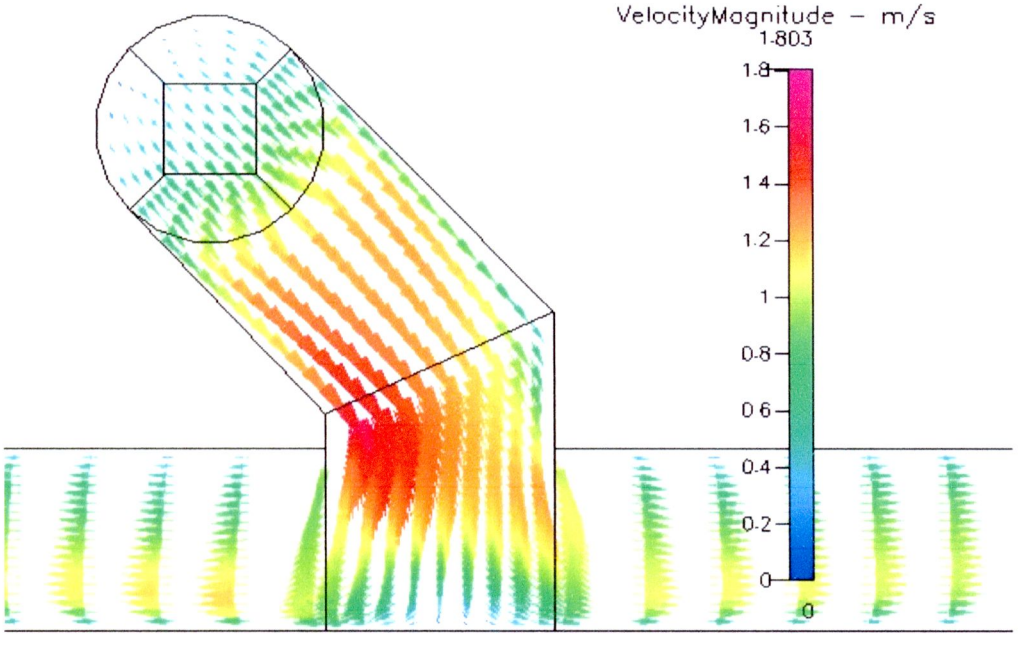

Figure 5.86 Inlet velocity distribution at 300 cm^3/min of first design flow field

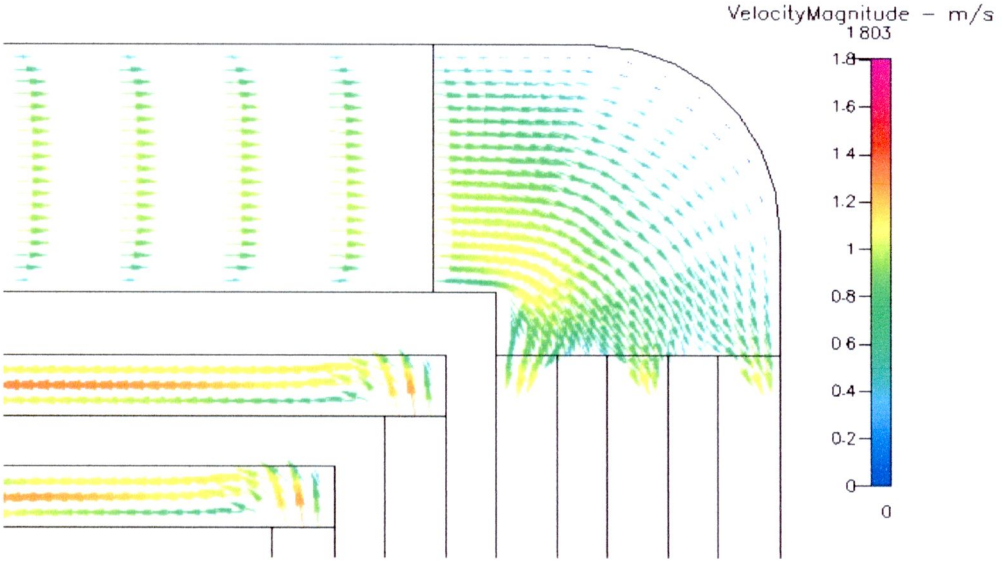

Figure 5.87 Curve velocity distribution at 300 cm^3/min of first design flow field

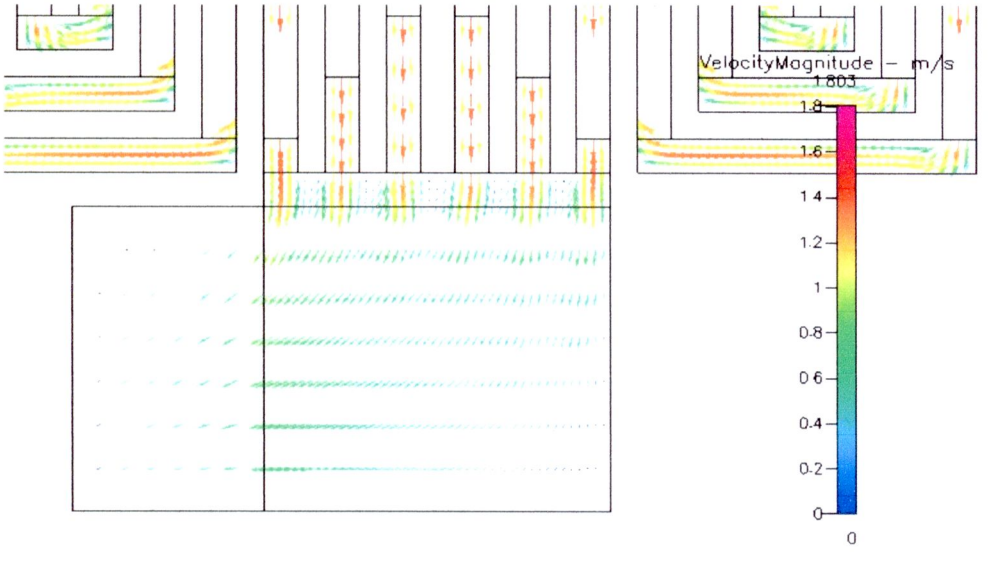

Figure 5.88 Outlet velocity distribution at 300 cm^3/min of first design flow field

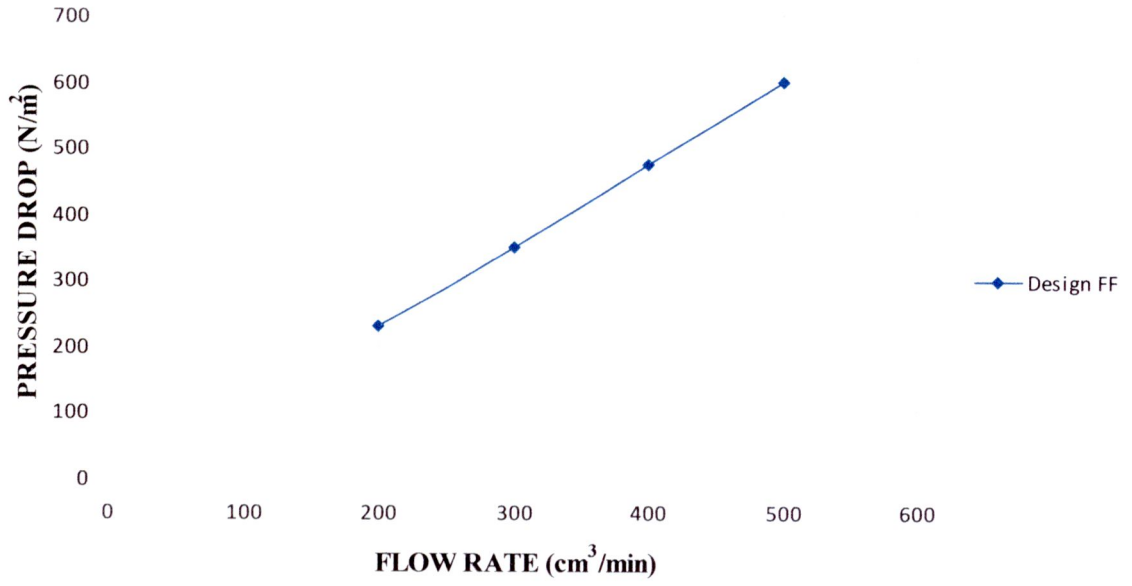

Figure 5.89 Pressure drop and flow rate

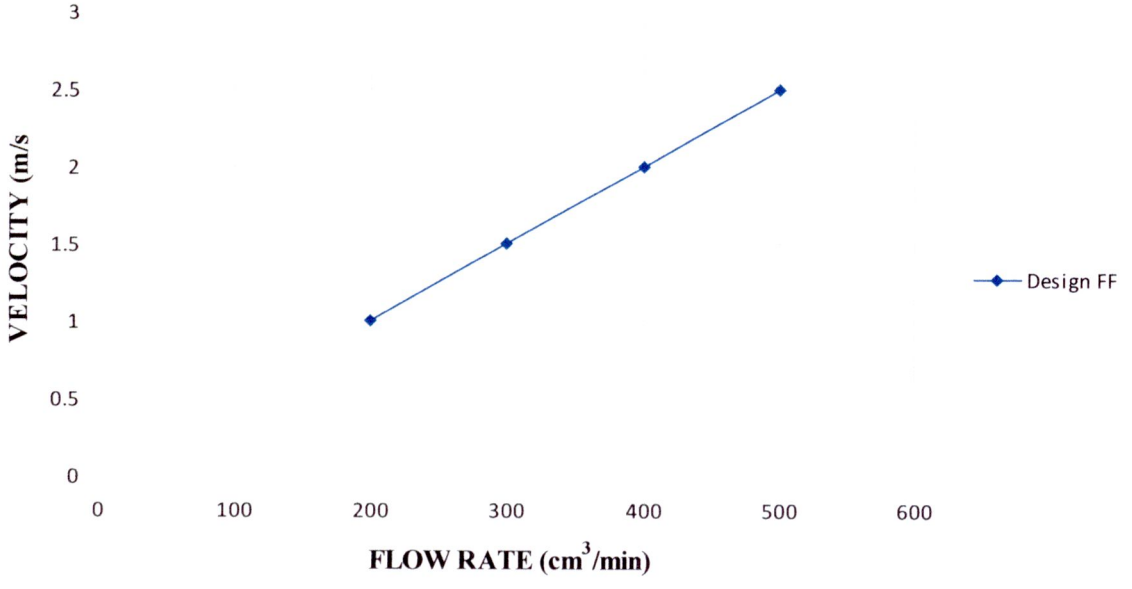

Figure 5.90 velocity at channel depth 0.5 mm. and flow rate

New flow field is 2 ways multi-serpentine header flow field shown effect of gas distribution in figure 5.84-5.88. Velocity at channel depth 0.5 mm. is about 1.5 m/s and pressure drop is 349.1 N/m^2. At inlet, gas flow separate to 2 ways is equilibrium and gas flow in curve is good gas distribution. In curve area, gas flow rate distribute to 3 channels is nearby all channel. Outlet manifold has good gas distribution for pulse water out of cell. This flow field shown it trend better performance more others because it has high flow rate and pressure drop, good gas distribution. In second design flow field was studied in next below this flow field. In figures 5.89-5.90 shown the pressure drop and velocity in 200-500 cm^3/min.

5.1.6 Chemical Reaction in Flow Field Pattern of Fuel Cell

The study of chemical reaction in fuel cell was described to H_2, O_2 and H_20 distribution and current density in design flow field. In this modeling was constant voltage at 0.6 Volt and gas velocity at 500 cm^3/min. It has 6 serpentine channels (old flow field) and 2 ways multi-serpentine with header flow field for compare performance in this model. The results of chemical reaction are shown in figure 5.91-5.100

a) 6 serpentine channels flow field

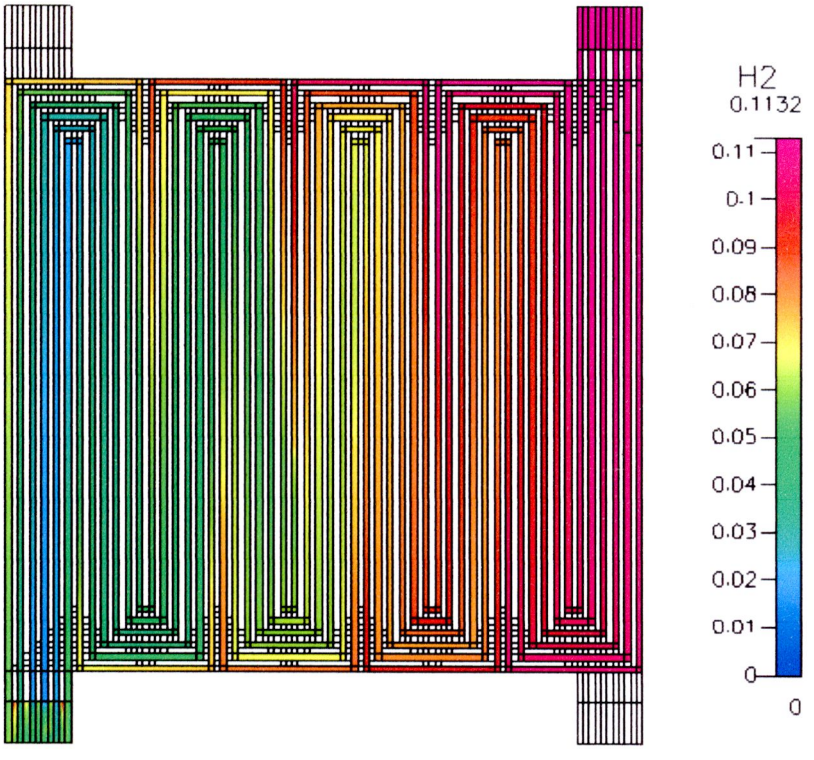

Figure 5.91 H_2 in anode at 500 cm^3/min of 6 serpentine channels

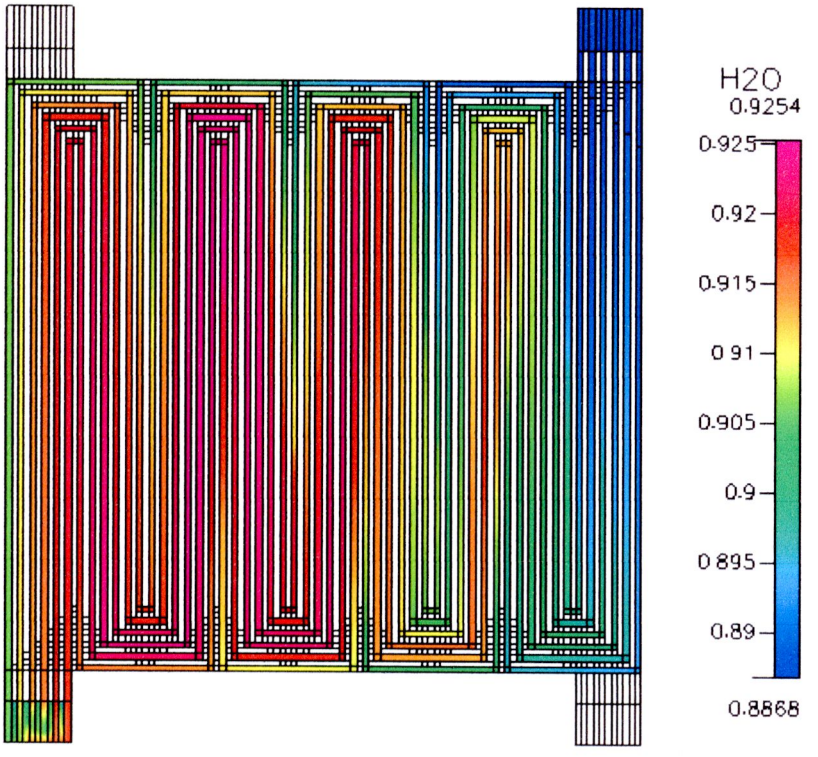

Figure 5.92 H_2O in anode at 500 cm^3/min of 6 serpentine channels

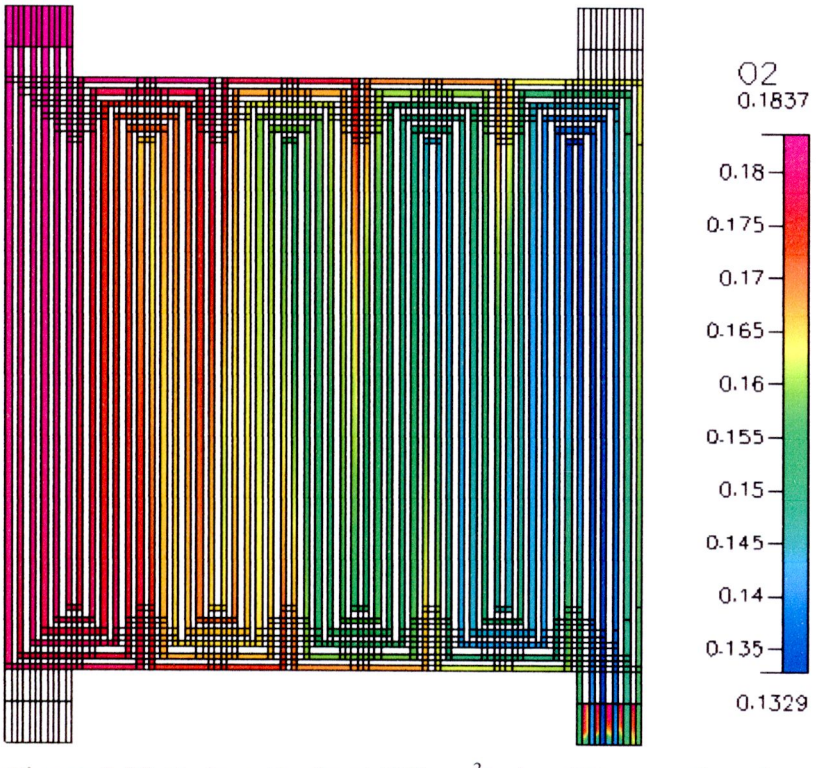

Figure 5.93 O_2 in cathode at 500 cm^3/min of 6 serpentine channels

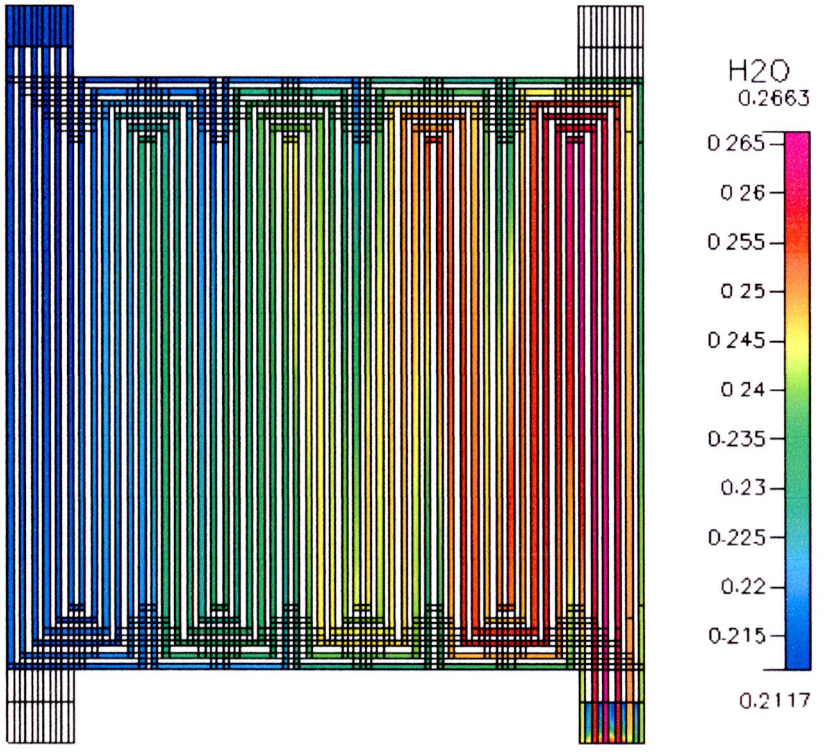

Figure 5.94 H_2O in cathode at 500 cm^3/min of 6 serpentine channels

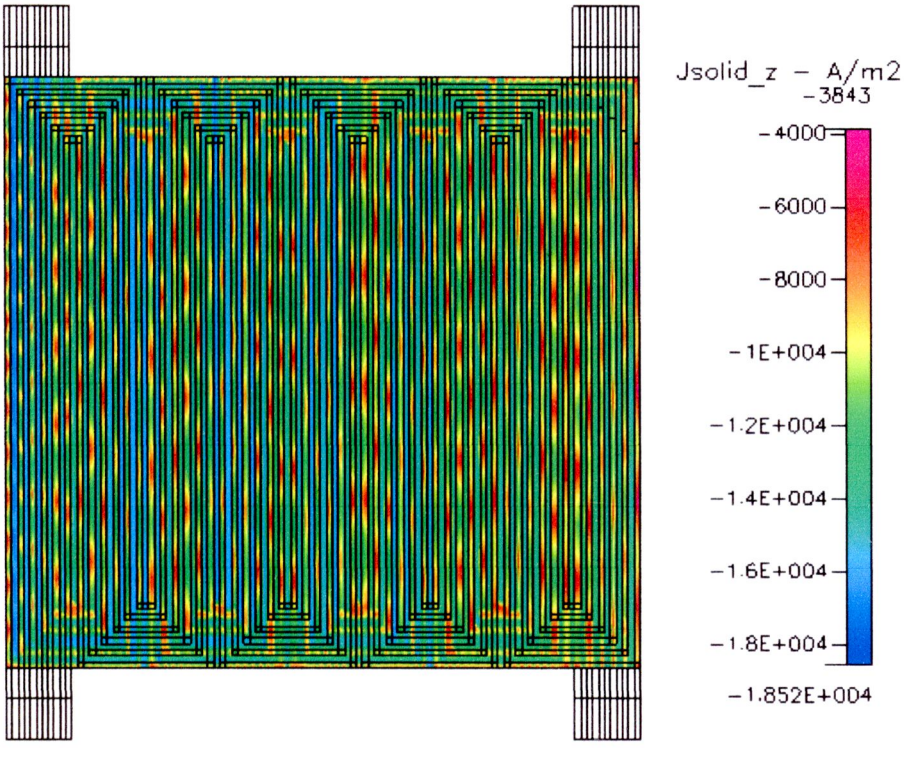

Figure 5.95 Current density in cathode at 500 cm^3/min of 6 serpentine channels

At anode side was found the consumption of hydrogen is fast when go to reaction area. Hydrogen was decreased along with channel. Start, hydrogen gas about 0.1132 and outlet has about 0.055 which used in electro-chemical reaction about 0.0582 by mass fraction. Water in anode side was increased along with channel length until outlet. At cathode side was found the oxygen consumption is constant until fifth turn of serpentine channel and start decreased at this point until outlet. Oxygen is start 0.1839 and used for electro-chemical in reaction area until outlet is 0.14 then oxygen was used about 0.0439 by mass fraction. Water in cathode side was begun increased at middle flow filed until outlet that it increased about 0.533 by mass fraction. The current density has appears in all flow field. It has about 1300 mA/cm^2 and it good distribution on flow field.

b) 2 ways multi-serpentine with header flow field

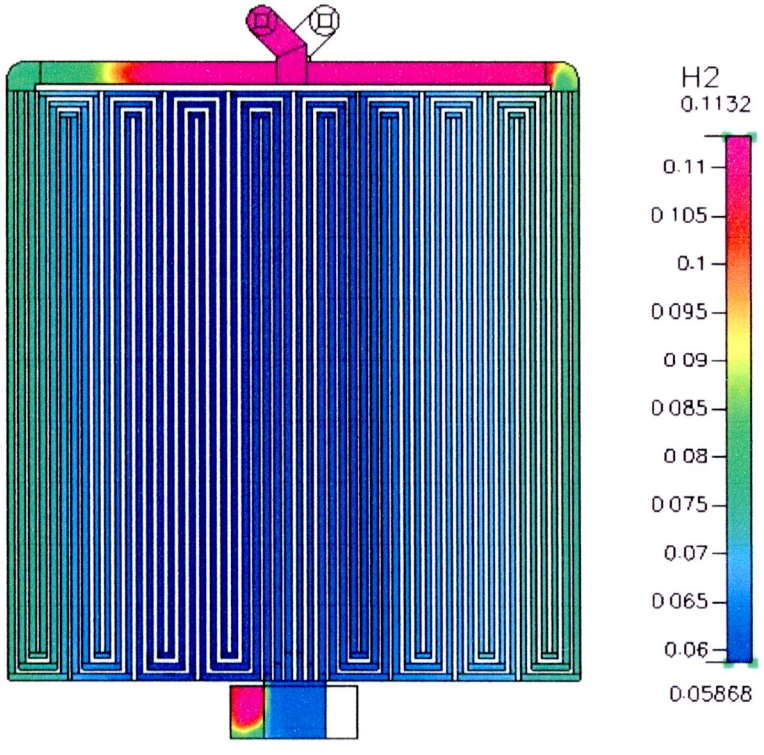

Figure 5.96 H_2 in anode at 500 cm^3/min of 2 ways multi-serpentine with header flow field

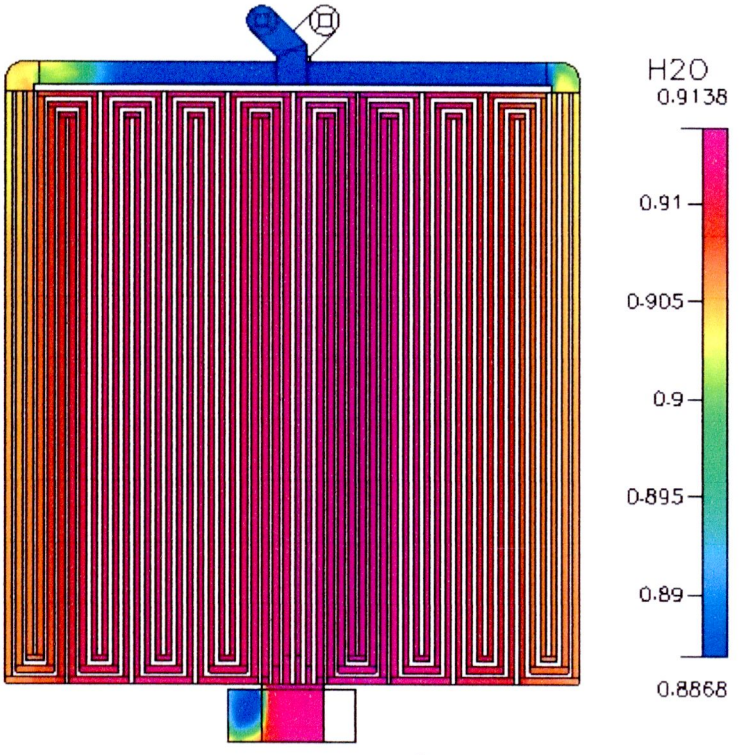

Figure 5.97 H_2O in anode at 500 cm^3/min of 2 ways multi-serpentine with header flow field

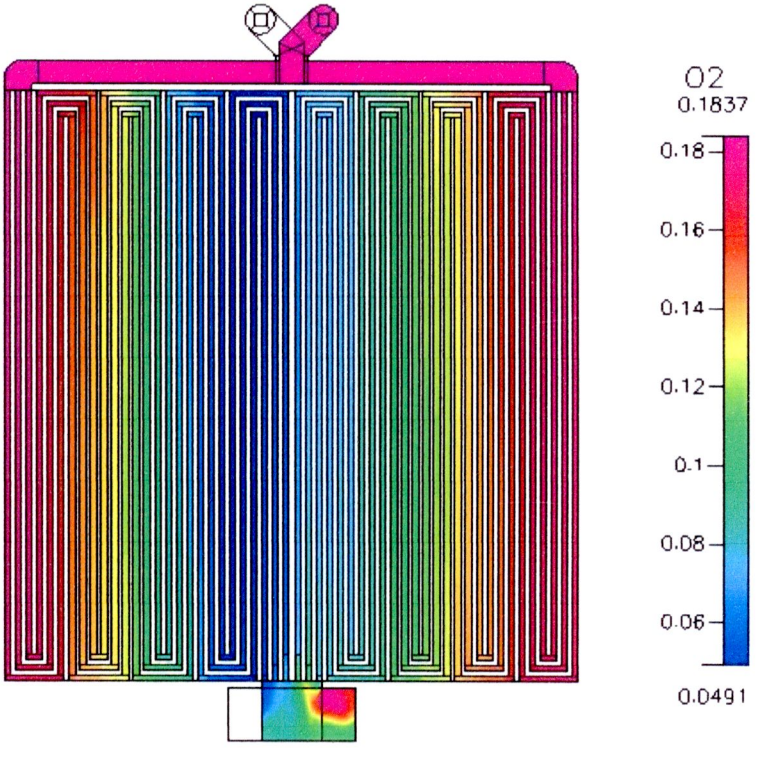

Figure 5.98 O_2 in cathode at 500 cm^3/min of 2 ways multi-serpentine with header flow field

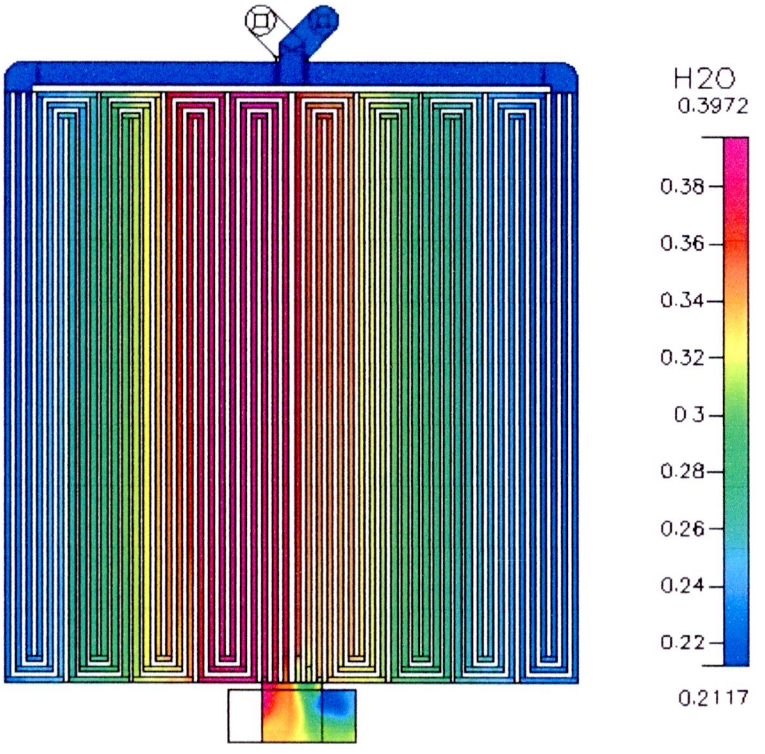

Figure 5.99 H_2O in cathode at 500 cm^3/min of 2 ways multi-serpentine with header flow field

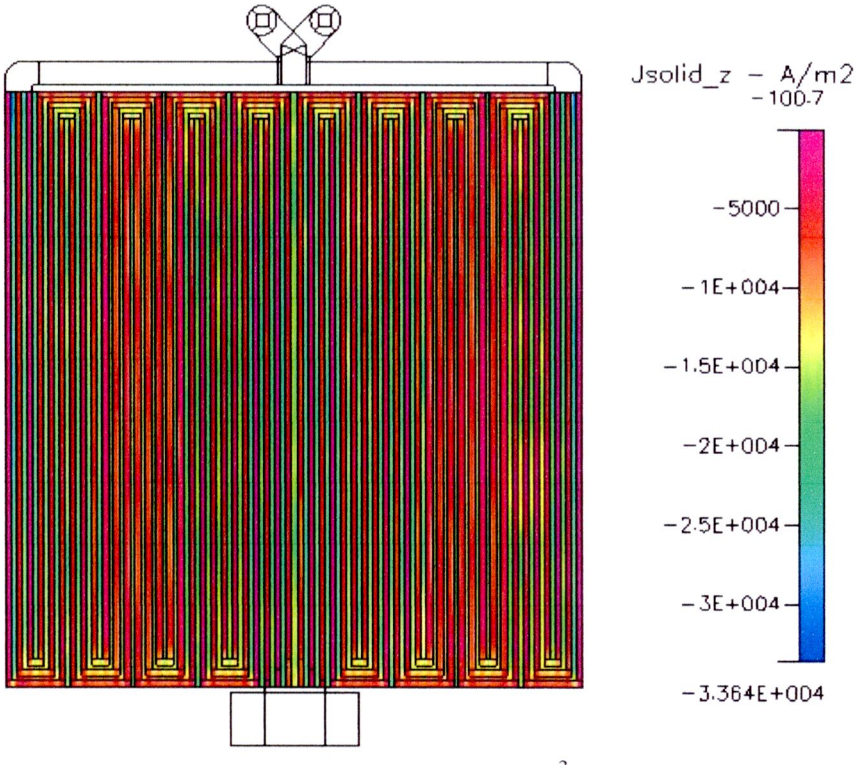

Figure 5.100 Current density in cathode at 500 cm^3/min of 2 ways multi-serpentine with header flow field

Hydrogen in anode side is divide to 2 ways before go to reaction area when hydrogen go to this area was fast consumption and decreased along with channel length. Gas has constant about 0.058 by mass fraction in third turn of serpentine flow field. Hydrogen was used to electro-chemical reaction about 0.058 by mass fraction. Water in anode side, it was increased along with channel length in this side about 0.03 by mass fraction. At cathode side, oxygen was consumption along with the channel length until outlet that it was begin used in second turn of serpentine flow field. The start, oxygen has 0.1837 and outlet has 0.06 then it used about 0.12 by mass fraction. Water in cathode side, it was increased along with channel length which add about 0.17 by mass fraction. Oxygen and water was same increased in second turn. The current density has appears in all flow field. It has about 1600 mA/cm^2 at 0.6 Volt and it good distribution on flow field. IN both side, it was shown the high gas distribution which has good electro-chemical reaction in this flow field. The results of this flow field were used building a prototype of single fuel cell for testing performance experimental.

5.1.7 Model Validation with Experimental

The results were verified with experimental in polarization curve of cell potential versus cell current density for the model is in good agreement with the experimental polarization curve. This over prediction of cell current is due to the one phase nature of the model, i.e. the effect of reduced oxygen transport due to water flooding at the cathode at high current density is not accounted for. In addition to the cathode flooding effect, the anode drying is also a contributing factor to the reduced performance at high current density. Similar to the polarization curve, the model power density curve shows good agreement with the experimental curve in the load region below the mass transport region. At this point, it should be noted that at present time, the polarization curve is the only experimental data that are available in the literature. , therefore polarization curves are commonly used to validate the agreement between model and experiments.

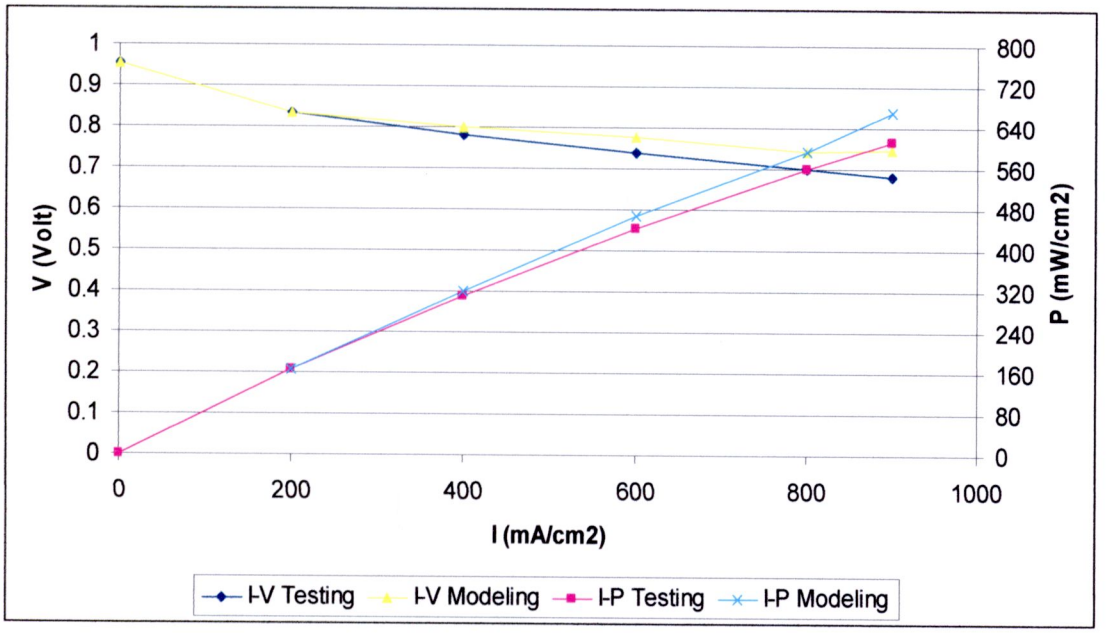

Figure 5.101 Comparison of model and experimental polarization curves.

5.2 Experimental Analysis Results

The performance of fuel cell predict from I-V curve. Experiment test between old fuel test and new choose fuel cell. It has component is MEAs used in this work were a combination of Nafion 117 and catalyst loadings Pt of 6.0 mg/cm^2 in anodes and cathodes, respectively. The GDLs were carbon product. The clamping force used in this work was 50 lbf/bolt. The compression was held constant for all cases in this work so that the contact resistances by compression between the flow field rib and GDL were identical for all types of flow field design. A model RBL488 Series Electronic Loads for fuel cell performance test and collect data with a computer. Digital mass flow controllers, products of MKS, were used to control the flow rates of fuel and oxidant in 500 cm^3/min. Two bubbler-type humidifiers were used to control both the anode and cathode humidification. The humidifications for both the anode fuel and cathode oxidant were controlled by changing the humidifier bottle temperature. The temperatures of the anode and cathode humidifier bottles were 70 and 70 °C, respectively. The cell temperature was 50-70 °C, controlled by heating installed outside the cell, for both the anode and cathode. The polarization curves were achieved by changing the current and waiting for the voltage until it converged to a stable value. The experiment of this studied used 4 types of flow field, which consist of 4 channels serpentine, 6 channels serpentines, 4 part multi-serpentine channels and 2 ways multi-serpentine channel with header. The results of experiment shown in figure 5.102-5.105.

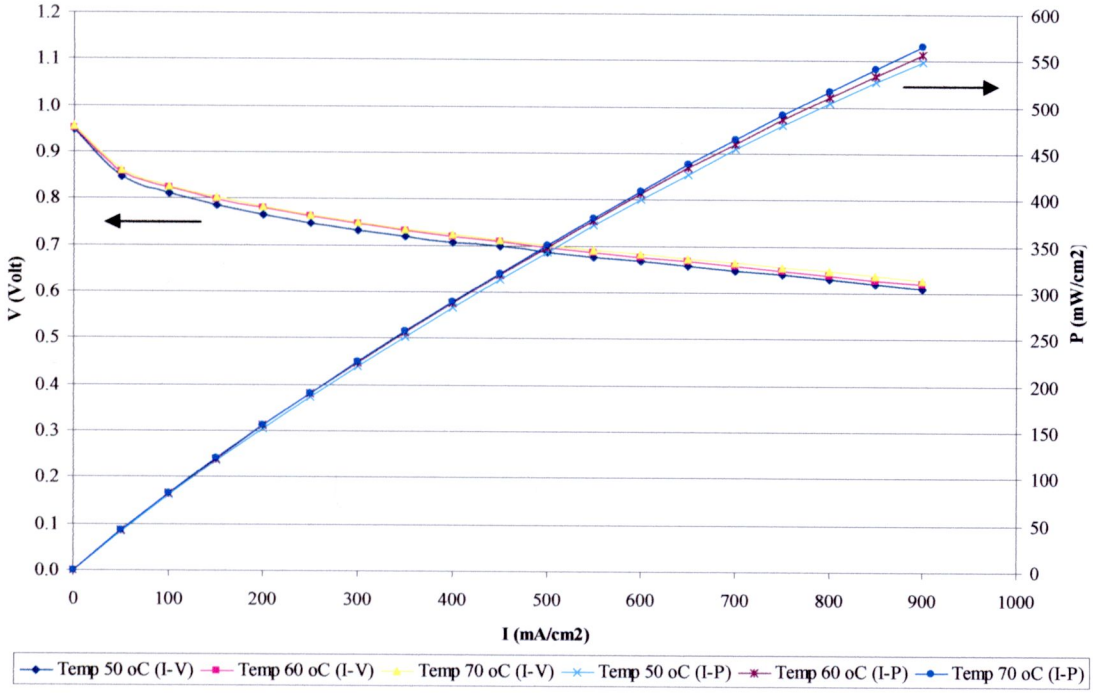

Figure 5.102 Performance curve of 4 serpentine channels fuel cell

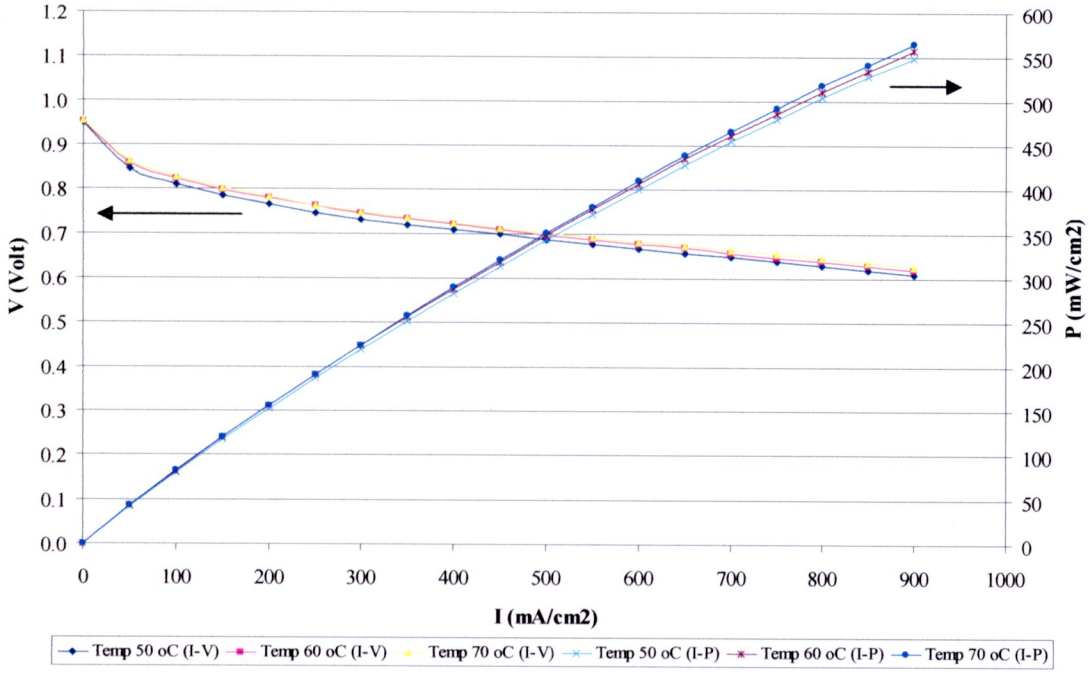

Figure 5.103 Performance curve of 6 serpentine channels fuel cell

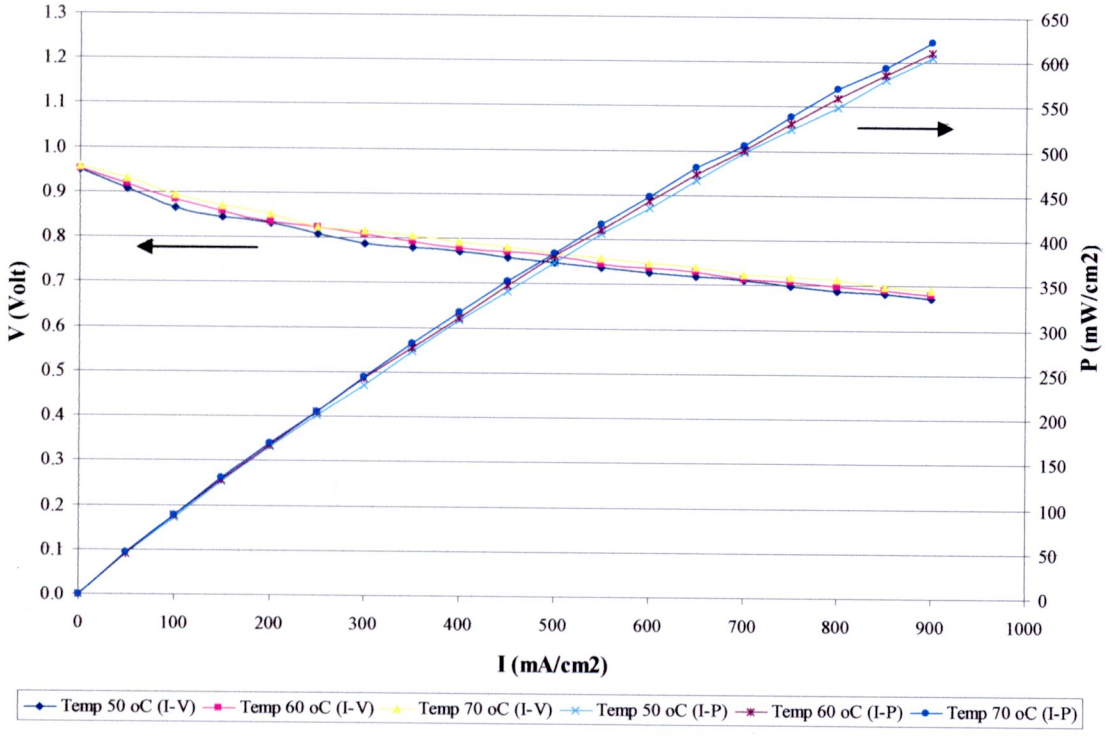

Figure 5.104 Performance curve of 2 ways multi-serpentine channels fuel cell

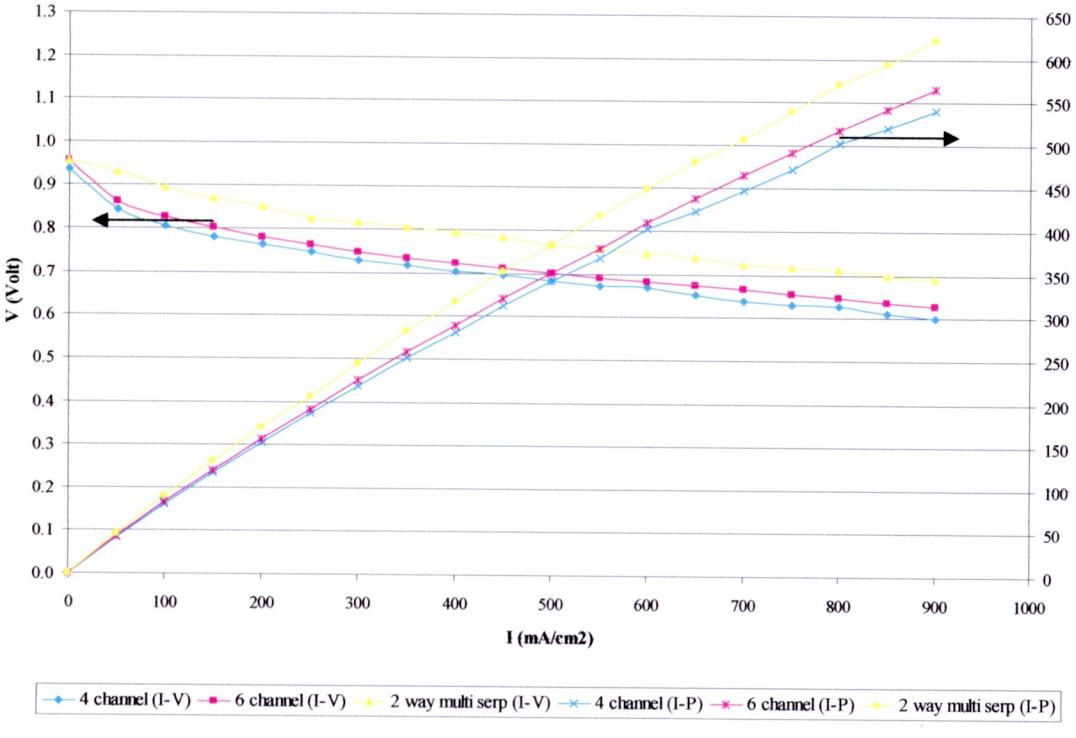

Figure 5.105 Comparisons between the old fuel cell and the new fuel cell at 70 ^{o}C

In figures 5.102-5.105 are show the performance of fuel cell in changing temperature on 3 types of flow field. The performance is nearby in 50-70 °C which 70 °C temperature is best performance in all types. It has better about 3.5% and 2.25% at 60 °C and 50 °C, respectively in new fuel cell, 900 mA/cm^2. In 4 serpentine channels has better about 0.22% and 2.9% and 6 serpentine channels has better about 1.31% and 28% at 60 °C and 50 °C, respectively. The high temperature of fuel cell has low ohmic resistance, and more active electrochemical reaction at upstream of flow channel. Therefore, the limiting current appears at downstream of flow channel. However, the concentration and current density become non-uniform but membrane could not dry in high temperature.

The performance of fuel cell is compare with old fuel cell and new fuel cell when considerate of current density, voltage and power density was found performance of new fuel cell is better than 2 old fuel cells. At 900 mA/cm^2, new fuel cell gave 621.9 mW/cm^2 at 0.691 Volt and 4 and 6 serpentine channels fuel cell gave 541.2 and 565.2 mW/cm^2 at 0.608 and 0.628 Volt, respectively. The new fuel cell has performance of cell better than 6 serpentine channel flow field about 10.03% and 4 serpentine channel flow field about 14.91 % in power density. Therefore, new flow field is optimization with performance of fuel cell more than old fuel cell.

New fuel cell in this research is compare the performance in others research for validated fuel cell. It shown in table 5.2 and performance curve shown in figure 5.106

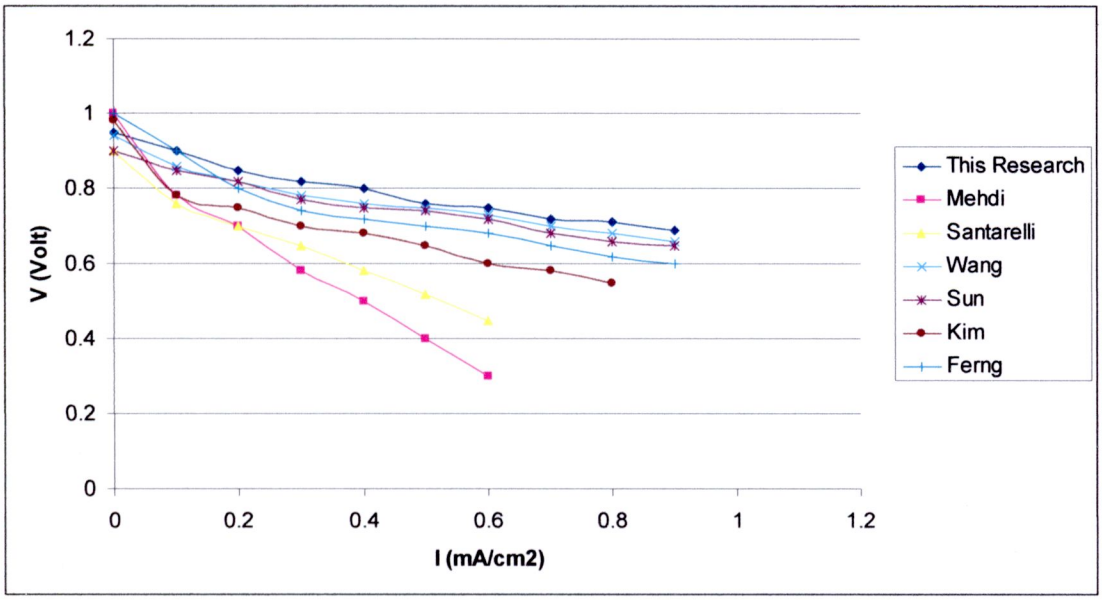

Figure 5.106 The performance was compared between this research and others

Table 5.2 Compare performance of this research and others.

Authors	Years	Methods	Properties Part	Current Density (A/cm^2)	Cell Potential (V)
This Research	2011	Reaction Area = 100 cm^2 T=70 °C	Polar Plate in Graphite and Serpentine flow field Membrane 117	0.85	0.7
Amirinej-ad,M, et. al.	2006	Reaction Area = 5 cm^2 T=70 °C	Single Cell of ElectroChem, FC05-01SP Membrane 117	0.2	0.7
Santarelli, M.G., et.al.	2007	Reaction Area = 25 cm^2 T=70 °C	Single Cell of ElectroChem, EFC25-01SP Membrane 115	0.2	0.7
Wang,L.	2003	Reaction Area = 50 cm^2 T=70 °C	Polar Plate in Graphite and Serpentine flow field Membrane 115	0.7	0.7
Sun,H.	2005	Reaction Area = 5 cm^2 T=70 °C	Polar Plate in Graphite and Serpentine flow field Membrane 117	0.65	0.7
Kim,S.	2007	Reaction Area = 100 cm^2 T=70 °C	Polar Plate in Graphite and Serpentine flow field Membrane 112	0.3	0.7
Ferng,Y. M.	2007	Reaction Area = 100 cm^2 T=70 °C	Polar Plate in Graphite and Serpentine flow field Membrane Gore 5620	0.5	0.7

This data in figure 5.106 and table 5.2 was shown the new fuel cell in research (fuel cell size 10 x 10 cm^2 and nafion 117) has a best performance the others. It has better more than Wang L. about 0.15 A/cm^2 and Amirinej-ad,M, et. al. about 0.65 A/cm^2. When compare with Ferng, Y.M. and Kim,s. , which it was a same fuel cell size, it has a better more than about 0.35 A/cm^2 and 0.55 A/cm^2, respectively.